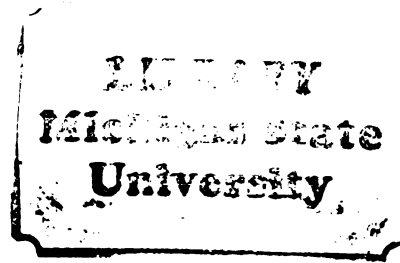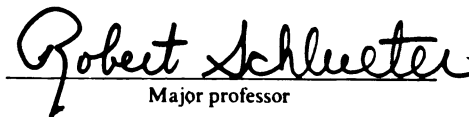This is to certify that the

dissertation entitled

Simulation and Security Analysis Methods

for Transients Due to Loss of Generation Contingencies

presented by

Mohsen Lotfalian

has been accepted towards fulfillment
of the requirements for

Doctoral degree in Systems Science

_____
Major professor

Date September 29, 1982

0-12771

SIMULATION AND·SECURITY ANALYSIS METHODS

FOR TRANSIENTS DUE TO LOSS OF GENERATION CONTINGENCIES

By

Mohsen Lotfalian

A DISSERTATION

Submitted to
Michigan State University
in partial fulfillment of the requirements
for the degree of

DOCTOR OF PHILOSOPHY

Department of Electrical Engineering
and Systems Science

1982

ABSTRACT

SIMULATION AND SECURITY ANALYSIS METHODS
FOR TRANSIENTS DUE TO LOSS OF GENERATION CONTINGENCIES

By

Mohsen Lotfalian

The inertial and governor distribution of mismatch power due to loss of generation contingencies causes stability and security problems on boundaries and lines that are vulnerable to these power flows.

Simulation methods based on load flow techniques are developed to allow direct assessment of stability and security problems associated with the inertial and governor power flows. A set of security measures for detecting the weak boundaries between generation groups which cause the stability and security problems in large networks is defined.

The DC load flow methods for simulating the inertial and governor response of generating units to loss of generation contingencies are compared to the midterm stability simulation of the same contingencies on a 49 bus test system, and the accuracy of the load flow methods is shown to be good. It is also shown that the inertial and governor response of generating units causes different power flows and thus different stability and security problems.

The inertial and governor load flow methods permit simulation of loss of generation contingencies on immense

power system models that could not be handled using the Midterm Stability Program and present techniques.

The security measures for inertial and governor power flows are shown to capture the strict synchronizing coherency (SSC) loss of controllability property for the inertial and governor state models that causes the vulnerable boundaries to inertial and governor power flows. These security measures are shown to be identical to the square of the r.m.s. coherency measure for the probabilistic modal disturbance loss of generation contingencies.

A method is developed to identify and rank the vulnerable boundaries due to inertial and governor power flows from the weakest to the strongest based on the security measures and a commutative grouping algorithm. The method is applied to the 49 bus test system, and the weakest boundary to inertial and governor power flow due to loss of generation contingencies is identified. The identification of the weakest boundary is shown to be accurate, since it is shown that the loss of stability associated with inertial and governor power flows occurs across this boundary.

ACKNOWLEDGMENTS

TABLE OF CONTENTS

LIST OF TABLES

vii

LIST OF FIGURES

CHAPTER 1

INTRODUCTION

The recent series of contracts for interregional power
transfer for the purpose of either oil/gas displacement or
economy will add significant additional stress to the trans-
mission system that delivers power from Quebec, Ontario, and
the Midwest to the Northeast United States. The multiple
large transfers on an existing network will cause short
lines to operate closer to their thermal overload limits,
thus making them more vulnerable to contingencies caused
by line overloads. The transfers will cause long lines to
operate closer to their stability limits, which are approx-
imately the same as or even less than thermal limits if
the line is long enough. Thus, the transfers will make the
system with long lines more vulnerable to stability prob-
lems. Facility additions for coping with these transfers
as well as the imposed transfers themselves may well inval-
idate empiric predictions based on experience of vulnerable
boundaries and lines and the set of critical contingencies.
Present AD-DC load flow and transient stability simulation
techniques and the associated planning methods discussed
later in this chapter can, however, be used to determine
the effects of transfers and facility additions on both

security and stability for a variety of operating condi-
tions for an exhaustive set of line outage contingencies
and for a set of fault contingencies.

The security and stability problems associated with
loss of generation contingencies on the large networks
associated with interregional transfers cannot be:

(1) adequately simulated using present techniques;

(2) handled using present planning methods;

(3) empirically predicted because of (a) these transfers,
     (b) facility additions, and (c) the lack of simula-
     tion techniques, planning methods, and experience with
     the kind of stability and security problems that occur
     for the loss of generation or load contingencies.

The problem that is overlooked in present simulation
techniques and planning methods is that a loss of genera-
tion or load is at different time frames after the contin-
gency distribution on all generation in the interconnection
inertially (proportional to the inertia of each generator)
or distribution on all generation under governor frequency
regulations (proportional to the frequency response charac-
teristic of each generator). Both distributions of the mis-
match will cause inadvertant power flows throughout the
network focusing to the point of the mismatch. Planners
assume that the present planning methods will detect the
security and stability problems associated with the flows,
and that there are large margins between present thermal
current loading and the thermal limits that can handle

these inadvertant flows without security or stability
problems. The large multiple interregional transfers with
the possible addition of long transmission lines may well
eliminate the large thermal margins, cause stability mar-
gins to decrease due to both the transfers and the addi-
tions of long lines with inherently smaller stability mar-
gins, and bring into question whether present simulation
techniques and planning methods can uncover the stability
and security problems associated with the distributions of
loss of generation or load mismatch. The stability and
security problems in the Northwest associated with the
large interregional transfers from the Bonneville Power
Administration (BPA) to California over long transmission
lines for loss of generation contingencies [1] suggest that
such problems actually exist with interregional transfers
on long lines and may likely occur for the large multiple
transfers being contracted in the Northeast for both oil
displacement and economy.

The study of these security and stability problems in
the Northwest was simplified since the transfers were over
one set of lines, and transfers were only in one direction
at any time. The problems for the Northeast are much more
complicated since the transfers are from north to east,
north to west, and west to east simultaneously. Thus, the
lack of simulation techniques for interconnection wide
inertial and governor transient response to loss of gener-
ation or load contingencies and the lack of security

assessment methods for detecting vulnerable boundaries and lines, and the critical loss of generation contingencies becomes an acute problem.

There are two principal contributions in this thesis. The first is the development of load flow based simulation techniques for determining "snapshot" pictures of the system's transient response after a loss of generation contingency. The inertial load flow [2, 3] was developed after the 1965 Northeast blackout to simulate the inertial response of generation after a loss of generation contingency. This inertial load flow is utilized to capture the snapshot of the state of the system transient when the effects of the loss of generation (load) contingency have propagated throughout the system, and the deceleration (acceleration) of the system is identical and constant everywhere but before governors have had an opportunity to respond to arrest the deceleration (acceleration) of system inertia.

A governor load flow is proposed and developed in this research to capture the snapshot of the system transient when the governor response to the drop in frequency is complete, but before automatic generation control or operator action can replace the lost generation or load in the utility that experienced the contingency. These inertial and governor load flows are applied to simulate a loss of generation contingency on a test system and are shown to be quite accurate in capturing system transient response as

compared to midterm transient stability simulations. The results suggest that the inertial and governor responses can be quite different and that each can cause stability problems that are not detected by normal first-swing transient stability simulations, load flow simulations, or line outage studies.

The second major contribution of this thesis is the development of a security assessment methodology that can detect the boundary and line vulnerabilities and could be extended to determine the critical contingencies for the inertial and governor distribution of mismatch for loss of generation or load contingencies. This methodology will be based on a new set of security measures, theoretical understanding of the controllability and observability of the classical transient stability model that causes these vulnerabilities, and methods for using these security measures for detecting the boundaries and lines between generator groups that cause these vulnerabilities for inertial or governor distribution of mismatch for loss of generation or load contingencies. These methods are obviously new in approach and are important in this application because planners have little experience with the security and stability problems associated with inertial and governor distribution of loss of generation mismatch and have no experience with such problems on the large network associated with the transfers being contracted for oil displacement in the Northeast.

The remainder of this chapter is devoted to a review of presently available simulation techniques (section 1.1) and associated planning methods (section 1.2) with a discussion of their limitations in simulating or properly assessing security and stability for the inertial and governor distribution of loss of generation or load mismatch after such contingencies. A review of security measures that have been proposed for security assessment is presented in section 1.3. A review of the research presented in this thesis is then given in section 1.4.

1.1. Review of Present Simulation Techniques

The present planning studies are performed in several steps with a variety of simulation techniques, such as AC and DC load flow programs for steady state analysis of the network and time domain dynamic simulation for analyzing the dynamic performance during the disturbance (transient stability program, midterm stability program, long-term stability program).

To determine the performance of an interregional power transmission system, AC load flows are used to simulate large interregional and subregional power transfers under normal network conditions and single contingency conditions. A few important double contingencies are also analyzed. Linear techniques, such as DC load flow, outage distribution factors (ODF), and transfer distribution factors (TDF), are used to identify critical facilities which

limit the interregional power transfers by the evaluation of an exhaustive set of first and second contingencies. Linear techniques are also used for contingency analysis procedure. Transient stability studies are performed to show the power system is capable of absorbing the first power swing and remaining stable upon the loss of any single transmission element, transformer, or generating unit.

To clarify whether the present methods are able to assess the stability and security problems associated with inertial and governor distribution of loss of generation or load contingencies, a brief description of each technique is necessary.

1.1.1. Load Flows

Load flow solutions provide bus voltage magnitudes and angles and real and reactive power flow on each element (line, transformer) in the transmission system for specified generation and load injections. This information is needed to test the system's ability to transfer power from generation to loads and check for overload limitations in particular lines and voltage violation at buses.

The physical characteristics of generation and load require that the load and generation injection to the load flow be represented in terms of active and reactive power rather than by bus current injections. Therefore, in a load flow study, the electrical condition at a bus is described by P, Q, V, and θ, which are active power

injection, reactive power injection, voltage magnitude, and voltage angle at each bus, respectively. For the generator buses, P and V are specified because these quantities are controllable. For load buses, one generally specifies the real power P and reactive power Q injections. At a bus called a swing bus (slack bus), V and θ are specified. This bus is defined to account for losses in the transmission system which are not known before the load flow solution is obtained. The objective of load flow is to determine the two quantities at each bus that are not specified.

For preliminary evaluation of planning and operating conditions, DC load flows [4] are used without reference to voltage conditions. With this network representation (power-angle relationship), it has become possible to carry out the thousands of load flows that are required for contingency analysis (security assessment) on large scale systems. This method has been able to assess many overload-related system problems.

DC load flow is used for the computation of outage distribution factors (ODF) and transfer distribution factors (TDF). These distribution factors have been used to rapidly compute the change in real line flow with the change in bus power injection and the change in line flows for line outages.

1.1.2. Outage Distribution Factors (ODF)

When a transmission line is opened, the power which
the line was carrying is distributed to other lines
according to the characteristic of the network. Thus, the
ODF [5] represents the percentage of flow on line A trans-
ferred on line B for loss of line A. The ODF's are used to
determine contingency loading under all first and second
contingency line outage conditions.

1.1.3. Transfer Distribution Factor (TDF)

The transfer distribution factor [5] represents the
percentage of the change in generation between two areas
appearing on any specific line. That is, the transfer fac-
tor is the ratio of the increase in loading on a facility
(line, transformer) divided by the increase in power trans-
fer (between two areas) that caused that increased loading.
The TDF's can be used to calculate the power transfer
between A and B that will increase the loading on a given
line to its thermal limit. The TDF's can be applied in
conjunction with ODF's to determine the line outage contin-
gencies and transfers that would cause overloads on the
system or a particular line.

1.1.4. Decoupled Load Flow

To achieve a more accurate result than linearized load
flow and also to be able to study voltage and reactive con-
ditions, decoupled load flows [6] were developed. This

technique can rapidly calculate AC load flow quantites for specified contingencies. This method takes advantage of the weak coupling between (P-δ) and (Q,V) components and solves separately the (P-δ) and (Q,V) equations.

The AC load flow or decoupled load flow outage distribution factors and transfer distribution factors are used to simulate transmission limitations for a planned power transfer, selected outages, and generation participation of different regions involved.

1.1.5. Transient Stability and Midterm Stability Programs

In this method, the network solution is obtained in time step by time step computation of a steady state load flow solution and integration of machine differential equations.

Transient stabiilty programs [7] generally utilize simplified representations of machines. This program is valid only for the study of first power swing after the disturbance. The Midterm Stability Program allows longer simulation intervals and detailed representation of synchronous machines, excitation systems, governor controls, and system loads. The Midterm Stability Program [8] can accurately simulate both the inertial and governor transient response to loss of generation or load contingencies since the generator models include proper governor control models, and the program can simulate over intervals above a few seconds. The program cannot simulate governor response for large

systems because the number of generators that can have
governor controls is very limited, and the cost of simulat-
ing even small system models above twenty seconds becomes
large. Both of these difficulties with the Midterm
Stability Program in simulating inertial and especially
governor response to loss of generation or load contingen-
cies may be overcome in the future as this program under-
goes further development. At present, it is not suitable
for simulating inertial and governor response on the large
data bases associated with the Northeast network involved
in the oil displacement transfers.

1.1.6. <u>Inertial Load Flow</u>

The inertial load flow determines a snapshot picture
of the transient response to a loss of generation or load
contingency at the time instant the effects of the contin-
gency have propagated to every part of the interconnection,
and the rate of change of frequency can be assumed identi-
cal and constant everywhere. The load/generation mismatch
at this time frame has not been compensated by any governor
control action. The mismatch is distributed at this time
frame to each generator by a participation factor that is
the ratio of that generator's inertia over the inertia of
all generators in the interconnection. The load flow
solved for this inertial distribution of the mismatch is
the inertial load flow.

Although inertial load flow programs exist, they are used only by a few utilities to check possible stability and security problems associated with inertial response to loss of generation or load contingencies. These inertial load flows are not utilized to determine security and stability problems for all first and second contingency loss of generation and line outages as done with DC load flow ODF and TDF methods. The utilities that utilize inertial load flows only utilize them as a last step check in the transmission planning process to determine if a specific boundary would be vulnerable to inertial response induced stability or security problems for one or possibly two contingencies of concern.

The inertial load flow simulations that have been performed may not accurately reflect true system responses if the large Multiregional Modeling Group (MMG) data bases were not utilized to produce dynamic equivalents that preserve total system inertia and if the inertia in these MMG data bases is not reduced from maximum generation (summer peak) conditions to actual system generation levels for some base case condition. The only known effort to utilize MMG data bases and reduce system inertia to appropriate levels was a post-mortem study of a 2,000 MW loss of generation at the Nanticocke station in the Ontario hydro system [9].

1.1.7. Long-Term Stability Programs

A long-term stability program [10, 11, 12], which includes network solutions [10], can simulate the network determined stability and security problems associated with inertial, governor, automatic generation control and economic dispatch distribution of mismatch for loss of generation contingencies. Although these programs may be quite powerful, they have not achieved wide usage or industry acceptance. It is not known whether the latest version of this program can be applied to very large data bases and what the relative computational costs for the program are.

It should be noted that inertial and governor response simulations for emergency conditions [13, 14], where tie lines have been lost and large frequency deviations are possible, have recently been developed. These efforts are experimental, have not been utilized by any utility, and are not intended for use when tie lines are present and simulation is required for very large interconnections.

1.2. Review of Present Planning Procedure

For a known operating condition, the planned power transfer is simulated between regions and subregions. This is possible when specific generation dispatches are used. Linear load flows are run for potentially limiting transmission facilities. Transfer distribution factors and outage distribution factors can be used to determine overloads for any line outages and region-to-region transfers.

A simplified load flow program utilizing these factors simulates load flow conditions for all first and second outage contingencies and for all anticipated area transfers. This program also computes the amount of power which can be transferred between two locations in the network under normal conditions and for single and multiple outages. The AC load flows are run to verify the transfer limits and to determine if there are any potential voltage problems. The AC load flows are studied because the use of distribution factors assumes that the network is linear and voltage remains constant. Selective transient stability cases are run and capability of the power system to absorb the ini-initial power swing for different power transfers is checked.

It is important to note that security and stability problems associated with inertial or governor response to loss of generation or load contingencies are not generally assessed by present planning procedures and methods. In these methods, stability is inferred if a comprehensive set of load flows with imposed transfers and all first and second contingency line outages do not exceed transfer limits set by overload considerations, if the network is capable of absorbing the first power swing for a selected set of fault contingencies, and if no voltage problems occur for another selected set of line outage contingencies.

Inertial load flows are sometimes run to check whether particular boundaries or lines are vulnerable for a specific contingency, but the results will not be accurate

unless the dynamic equivalent preserves total system inertia from a MMG data base and unless the system inertia from this data base is reduced to reflect actual operating conditions.

Governor load flow could be run using inertial load flow programs if the participation factors utilized to distribute the power mismatch for loss of generation or load contingencies are the ratio of frequency response characteristic of a particular generation over the frequency response characteristic of all generation in the entire interconnection. No utility has utilized the inertial load flow in this manner because the concept of a governor load flow does not appear in the literature and because many planners [1] assume governor response will be similar or identical to inertial response, which is not necessarily true.

Lack of appropriate simulation techniques for inertial and governor transient response to loss of generation and load contingencies, lack of experience for empiric prediction of boundary and line vulnerabilities to inertial and governor response to such contingencies (due to lack of simulation techniques and the general lack of a need to investigate such vulnerabilities), and the large multiple interregional transfers with associated additions of long transfer lines to accommodate the transfers have together created the need for security assessment methods for inertial and governor response to loss of generation

contingencies. This need is even more apparent, consider-
ing the large multiple transfers being contracted for oil
displacement in the Northeast, the documented stability and
security problems caused by inertial and governor response
in the Northwest, and the additional large interregional
transfer being contemplated in other regions of the
country.

Thus, there is a need to develop a contingency
assessment methodology for identifying weak boundaries
between generating groups in these large transmission net-
works, the vulnerable transmission elements that make such
boundaries vulnerable, and the loss of generation contin-
gencies that cause stability and transfer limit violation
problems across these vulnerabilities. This methodology
will be consistent with present contingency assessment
methods that utilize DC load flow and ODF and TDF pro-
grams.

1.3. Present Status of Security Measures

Security measures (security indices) are considered
as part of operation and security assessment techniques.
The indices are a starting point for more detailed analysis
of limit violations (bus voltages, line and transformer
thermal limitation, angle separation between generators).
The purpose of developing security measures (indices) has
been to express security of a system in terms of a set of
numbers. These indices are supposed to measure different

abnormalities in the system. The security measures developed have been limited for measuring overall relative security of the system for different operating conditions with different contingencies imposed.

At present, there are a variety of security measures for line transformer outages and fault conditions. They are differentiated between steady state and transient measures. In the steady state case, indices are defined for bus voltages and line and transformer MVA flow.

The method used to generate these steady state security measures is the load flow programs described in section 1.1. For a given operating condition represented by a solved base case load flow, the line and transformer outages are simulated using AC load flow, or decoupled AC load flow for bus voltage index and line/transformer MVA flow index calculations. DC or any linearized load flow is also used for line/transformer MVA calculations.

For bus voltage index calculations, the voltage magnitude at each of a specified list of buses in the system is compared with the normal operating limits of the bus (V_{min}, V_{max}); then an index is generated. If the voltage is between the limits (V_{min}, V_{max}), the index is 1. Otherwise, it assumes monotonically decreasing values from 1.0 to 0, based on linear, cubic, or quadratic functions. An overall index is calculated with consideration of a weighting factor for each bus [15]. The line transformer MVA flow index is calculated the same way as the voltage index, except in

this case, the MVA flow is compared with the rating of line and then this index is calculated. In general form, the indices can be written as [15]:

$$\bar{F}_K = \sum_{i=1}^{N} W_{iK} f(X_{iK}) / \sum_{i=1}^{N} W_{iK}$$

where:

i ranges over all relevant components

W_{iK} is weighting factor

f(.) is a function between 0.0 and 1.0

and the overall index for all contingencies is:

$$\bar{I} = \sum_{K=1}^{N} \bar{f}_K / N$$

Hence, $\bar{I}$ is also between 0.0 and 1.0.

A probability of occurrance α_K can be assigned to each contingency; then the index $\bar{I}$ may be written as:

$$\bar{I} = \sum_{K=1}^{N} \bar{f}_K \cdot \alpha_K / \sum_{K=1}^{N} \alpha_K$$

These indices are useful in comparing the overall steady state security levels of different operating states, but they do not identify the specific potential boundary and lines which cause the problems.

Transient security indices are also defined in a manner such that the index is zero if the system would lose synchronism and is 1 if the system remains stable [15].

These measures are proposed as [16]:

(a)   Maximum angle separation index $\hat{\theta}_K$ where:

$$\hat{\theta}_K = \underset{t}{Max}\ \underset{i,j}{Max}\ \theta_{ijK}(t)$$

where $\theta_{ijK}(t)$ is the angular separation between generation bus i and j at time t for fault K, and where the value θ_{Max} varies for small or large systems. A contingency swing factor is defined as:

$$\sigma_K = f(\hat{\theta}_K)$$

where:

$$\sigma_K = 0 \text{ if } \hat{\theta}_K \geq \theta_{Max}$$

$$\sigma_K = 1 \text{ if } \hat{\theta}_K \rightarrow 0$$

and for all faults, the overall transient index is defined as:

$$I = K/\sum_{K=1}^{K} (1/\sigma_K)$$

(b)   Apparent impedance index. This index is calculated from the fact that loss of synchronism in a power system can be a separation of the network by circuit breaker operation when a line protection relay sees an out-of-step condition as an apparent line fault and the circuit breaker acts. Thus, to measure if loss of

synchronism would occur, it should be checked if any relays would trip.

The apparent impedance seen by a relay at the ith terminal of line i,j is given by:

$$Z_{ij} = \frac{V_i}{I_{ij}} = \frac{V_i}{V_i - V_j} \hat{Z}_{ij}$$

or:

$$Z^*_{ij} = \frac{V_i}{V_i - V_j}$$

where $\hat{Z}_{ij}$ is line impedance, and V_i, V_j are terminal voltages.

$$Z^*_{ij} = Z_{ij} / \hat{Z}_{ij}$$

is normalized. Loss of synchronism is assumed if the normalized apparent impedance locus for any transmission line crosses the line segment [0, 1].

A contingency swing factor is also defined for this case as:

$$\sigma_K = g(d_K)$$

where:

$$\sigma_K = 0 \text{ if } d_K = 0$$
$$\sigma_K = 1 \text{ if } d_K \to \infty$$

where d_K is the minimum distance to the line segment
[0,1] from the normalized impedance locus.

The transient security indices described in this sec-
tion are valuable tools for operation and security assess-
ment for fault studies, but they would not be able to
assess the security and stability problems associated with
inertial and governor load flow distributions.

To develop a contingency assessment methodology, a set
of security measures are defined in Chapter 4 of this thesis
for inertial and governor load flow distributions. These
security measures capture dynamic system structure that
causes vulnerable boundaries between strongly bound genera-
tor groups. The security measures developed in this
research are related to but not identical to r.m.s. coher-
ency measures developed in [18, 22] for producing dynamic
equivalents for transient stability studies.

It has been shown [17] that dynamic equivalents pro-
duced by the r.m.s. coherency measure preserve both the
eigenvalues and coherent properties of the unreduced system
and that the r.m.s. coherency measure can be evaluated
based on a probabilistic disturbance, which is computed by
evaluating the coherency measure for a set of determinis-
tic disturbances and summing the coherency measure for each
disturbance. This coherency measure, evaluated for the
probabilistic disturbance, has been shown to [17, 18]:

(1)   produce dynamic equivalents where the eigenvalues with large imaginary values, which are shown to represent intermachine oscillation within the coherent groups, are eliminated; and,

(2)   detect strongly bound coherent groups that are characterized by a tree of n_i-1 stiff interconnections between n_i generators in each group i. These strongly bound groups were shown [18] to be one of five loss of controllability and observability conditions that could be detected by the r.m.s. coherency measure for different types of disturbances. The concept of strongly bound groups (detected by the probabilistic disturbance) would indicate the boundaries of groups are composed of weak interconnections compared to the inertias of the generators in the groups they connect.

It is shown in Chapter 4 that the security measures evaluated for a probabilistic loss of generation disturbance (or alternately summed for an appropriate set of deterministic disturbances) has the coherency measure as a term and can detect the boundaries between weakly connected groups of generators. A ranking table of the security measures between generator pairs from smallest to largest is produced. Groups of generators are formed based on a commutative rule similar to that used for forming coherent groups for producing dynamic equivalents. As one proceeds down this ranking table, individual generators are included in groups and later groups are merged to form larger groups.

As groups are merged, the boundaries between groups should be continuously weaker. When this grouping was carried out on the 49 bus test system, the last group to be lumped into a single system group containing all generators was the group of machines in the external system. This boundary containing lines between the internal and external system was inferred to be the weakest set of lines and the most vulnerable for loss of generation contingencies. This proved to be true, since the loss of generation contingencies run only caused the loss of synchronism across this boundary or set of lines.

It is hypothesized that the second to last group of generators to be aggregated would indicate the second weakest and thus the second most vulnerable boundary, etc. Thus, a ranking of boundaries and hence the associated lines that connect strongly bound groups of generators was formed. Such a ranking and identification of weak boundaries for loss of generation contingencies is extremely helpful in both security assessment and transmission planning for identifying the critical element that bottles up generation, limits transfers, and causes security and stability problems for loss of generation or load mismatch distribution by inertial or governor load flows.

The security measures developed for loss of generation contingencies have a similar form to those developed in [19] for security assessment applications on line outage contingencies. The security measures developed in this

research are much more flexible in that:

(1) They can summarize the effects of a single contingency as in [19, 20] or any set of contingencies.

(2) They can be written for a single transmission element, a set of vulnerable elements, or over-all system elements as in [19].

This flexibility will greatly extend their usefulness in both transmission planning and security assessment applications.

1.4. Summary

The inertial and governor load flow are defined and discussed in Chapter 2. The DC inertial and governor load flow is shown to accurately capture the inertial and governor generator transient response to loss of generation or load contingencies by comparing the angles determined by the inertial and governor load flows for specific contingencies with midterm transient stability simulations of these same contingencies. The results also indicate that the inertial and governor response to a contingency are quite different and that each cause different stability problems that cannot be detected based on a first-swing stability simulation, load flow simulation, or line outage study.

The security measures for the security assessment procedure are defined in Chapter 4. The controllability and observability properties of the classical transient

stability model that cause coherent behavior and that lead
to the boundary and line vulnerabilities for loss of genera-
ation contingencies are discussed. The security measures,
defined in Chapter 4, are then shown to detect these vul-
nerabilities.

Computational results on the 49 bus system using a
security assessment procedure focused on the security meas-
ures and their theoretical capability to detect the con-
trollability property that causes vulnerability to loss of
generation contingencies is presented in Chapter 5. These
results show that boundaries between the generator groups
that lose synchronism based on inertial or governor
response can be determined. It is also shown that a par-
ticular line in the boundary between the groups causes this
vulnerability since the power flows from the entire inter-
connection back to the point of mismatch focus on this one
line that causes the instability.

Conclusions are presented in Chapter 6.

CHAPTER 2

LOAD FLOW METHODS FOR SIMULATING GENERATION RESPONSE TO LOSS OF GENERATION FOR TRANSMISSION PLANNING AND SECURITY ASSESSMENT

Dynamic generation response to loss of generation or load contingencies causes different power flows for synchronizing coefficients, inertial and governor controls, and the automatic generation control/operator distribution of power mismatch. These distributions will stress specific lines and boundaries in the transmission grid that may lead to stability and security problems.

The fundamental hypothesis of this chapter is that each of the power distributions at different time frames is complete before the next distribution of power begins. This hypothesis will allow each of the distributions to be modeled as load flows. One can verify the accuracy and validity of these load flow models for each time frame by simulating the actual state of the system trajectories at different time frames using the EPRI Midterm Stability Program [8], which is the only package available at this time that can be accurate out to the governor response time frame.

The objective of this chapter is to develop load flow models for each of the mismatch power distributions. The

26

load flow problem is stated given the real power injections for all generator losses before the loss of generation or load contingency occur and the magnitude of the mismatch caused by the loss of generation or load contingency. The real power generations are calculated for the inertial generation response, governor response, and the automatic generation control/operator action generation response to a loss of generation contingency. The load flows are then solved given the calculated real power injection at generation buses for a specific distribution of the loss of generation or load mismatch. The bus voltage angles and the real and reactive power flows for each distribution will be the result.

This chapter is composed of two sections. The model for distribution of loss of generation or load mismatch based on synchronizing power coefficients, inertial response, governor response, and automatic generation control (AGC)/operator action will be developed and discussed in section 2.1. The inertial, governor, and AGC/operator load flows for each of these three distributions of loss of generation or load mismatch will then be defined and discussed in section 2.2.

The comparison of the inertial and governor load flows with the simulation results provided by the EPRI Midterm Stability Program will be given in Chapter 3.

2.1. Generation Response to Loss of Generation or Load Contingencies.

Following a loss of generation or load contingency, the power imbalance (PTOT) will first be distributed to the generators according to the synchronizing coefficient or electrical closeness to the disturbed bus. After a short period (0.5 to 2 seconds), when the acceleration at every generator throughout the system becomes equal, the loss of generation mismatch will be redistributed to generators throughout the interconnection in proportion to the inertia of each generator as a percent of total inertia. Next, assuming the system is still stable after the inertia distribution, the loss of generation or load power mismatch will be distributed according to governor control based on the roughly uniform frequency deviation throughout the interconnection. The power distribution at this point would be according to the governor frequency response characteristic of each generator. This third redistribution by governor action begins at approximately six seconds when the inertial distribution is complete. The governor distribution requires twenty seconds to several minutes to complete depending on the magnitude of the mismatch and the response rate capability of all the generation in the interconnection. Finally, if the system remains stable after governor action redistributed the power mismatch, the automatic generation control or the operator of the utility experiencing the loss of generation will distribute this mismatch power in an attempt to reset frequency and interchange to

schedule. This action starts at 1 minute and can be complete in 10 minutes to several hours, depending on the size of the mismatch and the reserve available.

2.1.1. <u>Power Mismatch Distribution According to Synchronizing Power Coefficients</u>.

Suppose that a loss of generation or load (P_{TOT}) occurs at an arbitrary point in the network (bus k). This disturbance will cause a voltage angle change $\Delta\theta_k$ at bus k, and by this means, the power mismatch will be transferred to the various generators. Now if the synchronizing power coefficient of the equivalent lines connecting the disturbed bus k to various generators i are $P_{S_{ik}}$, the individual power change for each generator will be:

$$\Delta P_{ik}(1) = P_{S_{ik}} \Delta\theta_k$$

and:

$$P_{TOT} = \sum_i \Delta P_{ik}(1) = \Delta\theta_k \sum_i P_{S_{ik}}$$

i.e.:

$$P_{ik}(1) = \frac{P_{S_{ik}}}{\sum_i P_{S_{ik}}} P_{TOT} \tag{2-1}$$

where:

$\Delta P_{ik}(1)$ = power changes for generator i for initial distributions of generator mismatch at bus k.

$$P_{S_{ik}} = \frac{E_i V_k}{X_{ik}} \cos \theta_{ik}$$

E_i = voltage magnitude at internal generator bus i

V_k = voltage magnitude at bus k

θ_{ik} = angle across equivalent lines connecting bus i to bus k.

X_{ik} = reactance of equivalent lines connecting bus i to bus k.

The loss of load or generation power mismatch is immediately shared by the generators according to their synchronizing power coefficient with respect to the disturbed bus. The generators electrically close to the point of disturbance will pick up the greater share of the mismatch power regardless of their size.

2.1.2. Inertial Distribution of Mismatch (P_{TOT})

After initial response $\Delta P_{ik}(1)$, every generator will be accelerated (retarded). This acceleration is:

$$a_i = \frac{\Delta P_{ik}}{M_i} \tag{2-2}$$

The synchronizing forces pull all the generators toward a mean acceleration (retardation). At this point, the disturbance has propagated from the disturbed bus, and the acceleration at every generator throughout the system is approximately equal to the system mean acceleration (deceleration).

$$a_m = \frac{P_{TOT}}{\sum_i M_i} \tag{2-3}$$

where M_i is inertia constant of generator i.

The propagation is like the ripple caused when a rock is thrown into a calm pond. The propagation first affects generation directly connected to disturbed bus k as indicated above. As these generators accelerate, they affect generators connected to them that in turn accelerate, affecting generators even further electrically from the disturbance. This propagation is already under way at .025 seconds and is complete at .5 seconds to several seconds depending on the size of the network.

The synchronizing power flows in the entire interconnection will at this time keep the acceleration of each generator close to the system mean acceleration. A transient can accompany this redistribution of mismatch power from generators directly connected to the disturbed bus to all generators in the interconnection by inertial distribution if the mismatch is very large. This transient is observed in synchronizing oscillation of bus angles around the values dictated by the inertial distribution of mismatch power. The mean acceleration at all generators distributes the mismatch P_{TOT} at bus k to each generator in the interconnection by accelerating or retarding its inertia. The power drawn from (or sent to) generator i for a loss of generation (load) contingency for the inertial distribution of power mismatch at bus k is:

$$\Delta P_{ik}(2) = M_i \cdot a_m = \frac{M_i \ P_{TOT}}{\sum\limits_i M_i}$$

The power drawn from or sent to the generators in the interconnection flows over the network. These flows can cause security or stability problems if the flows exceed steady state stability or overload limits on the lines that carry these flows.

2.1.3. Governor Distribution of Mismatch (P_{TOT})

After inertial distribution of mismatch power, each generator is controlled by its governor. A loss of generation (load) contingency causes frequency deviation. Governor frequency regulation on each generator in the interconnection work together to arrest the change in frequency. This frequency regulation begins approximately six seconds after the disturbance occurs. When the governor frequency regulation is complete, frequency is constant at a deviation $\Delta\omega_0$ above nominal system frequency throughout the interconnection. The deviation of power at each generator from the basic analysis of governor response from Figure 2-1 is:

$$P_{ik}(3) = \frac{CAP_i}{R} \Delta\omega_i$$

$$\Delta\omega_i = \Delta\omega_0 \text{ for all the generators}$$

then:

$$P_{ik}(3) = \frac{CAP_i}{R} \Delta\omega_0 = \beta_i \Delta\omega_0 \qquad (2-5)$$
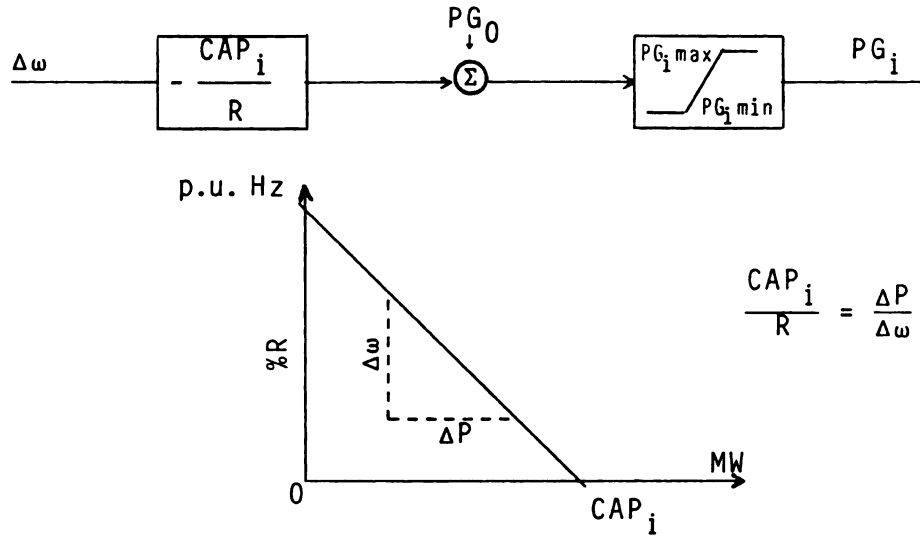
Figure 2-1. Linear Relation of Generation Change to Frequency Deviation by Governor.

where:

CAP_i is megawatt capacity of generator i

R is system regulation coefficient

β_i is frequency response characteristic of generator i

The total mismatch P_{TOT} is the sum of all the power changes. Since the $\Delta\omega_i$ of all the generators are equal to $\Delta\omega_0$, one obtains:

$$P_{TOT} = \sum_i \beta_i \, \Delta\omega_i - \Delta\omega_0 \sum_i \beta_i$$

$$\Delta\omega_0 = \frac{P_{TOT}}{\sum_i \beta_i} \quad \text{p.u. Hz} \tag{2-6}$$

and from (2-5) and (2-6):

$$\Delta P_{ik}(3) = \frac{\beta_i P_{TOT}}{\sum_i \beta_i}$$

β_i is approximately equal to MW capacity of generator
(CAP_i) divided by system regulation coefficient (R). The
other factors involved in governor response are generator
and turbine damping and load dependence on frequency, but
the dominant component is CAP_i/R.

This model of governor action that linearly relates
generation change to frequency deviation is idealized. The
governor deadband causes a generator to be insensitive to
frequency deviation less than .036 Hz; if the frequency
deviation sensed by a generator is greater than .036 Hz,
the generator may still not respond to governor command
if the unit is operating at a valve set point.

The effects of governor deadband and valve set points
have the effect of reducing the frequency response charac-
teristics β_i of generators electrically distant from the
point of mismatch (bus k). The effects of the loss of gen-
eration on both the frequency and acceleration of genera-
tors electrically close to bus k are larger than at
generators distant to bus k, as the effects of disturbance
ripple out and ultimately achieve an inertial distribution.
The larger initial frequency deviations close to disturbed
bus k will overcome governor deadband and valve set point
nonlinearities, making the generator's actual change in
generation at least $\beta_i \Delta\omega_0$. The generators far from the
disturbance do not feel the large initial frequency devia-
tions but only the ripple of that disturbance, and thus the
governor deadband and valve set point nonlinearities may

have the effect of reducing β_i for these generators, even though the same steady state frequency deviation is ultimately experienced.

PJM [21] increased (R in per unit) in the external system from 5% to 16% to compensate for a lower measured frequency response for the external system than predicted when R (per unit) is 5% in both the external and internal system. The measured β for the external system were determined from loss of generation tests in the PJM utility. The reduction of β_i for external system generation from those predicted by [21], when R is the same for internal and external systems, will not only increase the steady state frequency deviation after governor action is complete but will also reduce the percentage of the mismatch taken by the external system.

The power flows caused by the governor mismatch distribution will be different from the inertial distribution and cause quite different power flows back to the point of mismatch. The governor power distribution ($\beta_i/\Sigma\beta_i$) is different from the inertia distribution ($M_i/\Sigma M_i$) since:

(1) M_i is not proportional to CAP_i for generators of different size and type.

(2) The effective β_i is reduced on generation far from the disturbed bus k due to governor deadband and valve set point nonlinearities.

(3) Some types of units may not have governor regulations
     or sharply reduced regulation participation as on
     nuclear units.

(4) Some utilities' automatic generation control dispatch
     is proportional to area control error as well as the
     integral of area control error. When AGC has propor-
     tional control, the effective β_i on generators under
     AGC is increased.

If the governor distribution of power $(\beta_i/\beta\Sigma_i)$ mis-
match is different than for inertial distribution, the
power flows from the external system are channeled to the
point of mismatch over different transmission lines. If
these line flows exceed steady state stability or overload
transfer limits, then stability or security problems result.

The governor action is complete in 20 seconds to sev-
eral minutes depending on the magnitude of the lost genera-
tion or load and the response rate capability of all the
generations in the internal and external system under
governor regulation.

2.1.4. AGC/Operator Distribution of Mismatch P_{TOT}

The final distribution of power imbalance is by the
automatic generation control according to generator partic-
ipation factors or operator action of the utility experi-
encing the lost generation. The operator or the AGC
distributes the mismatch power among generators under control

by means of participation factors γ_i to reset the frequency. The redistribution in the utility for generator i is:

$$\Delta P_{ik}(4) = \gamma_i \; P_{TOT} \qquad\qquad (2\text{-}8)$$

where γ_i is the participation factor for generator i and $\sum\limits_i \gamma_i = 1$.

2.2. Formulation of Inertial, Governor, AGC/Operator Load Flow Problems.

In section 2.1, the distribution of power mismatch over time due to loss of generation contingencies was discussed. Synchronizing power coefficient distribution that happens at the instant of the disturbance causes significant rate of frequency change and power change. The study of this distribution is similar to transient stability studies for fault disturbances because a severe three-phase fault at the generator terminal causes an acceleration similar to loss of generation. The fault is more severe due to voltage changes that effectively weaken the transmission network connected to that generator. The transient stability studies for faults are widely done by the utilities, and the problems that may arise because of synchronizing power coefficient distribution would be less severe and are considered in these studies. Thus, there is no need to develop a load flow for this synchronizing distribution of mismatch.

The distribution of power mismatch based on AGC/operator participation factors for the utility experiencing the disturbance and the stability and security problems associated with this distribution are investigated by present load flow studies on all types of contingencies. These studies, discussed in Chapter 1, establish the overload and transfer limit violation conditions for the utility of concern. Since the AGC/operator load flow is in common use as options in present load flow programs, it will be developed for completeness but will not be investigated further.

The inertial and governor distribution of loss of generation power mismatch can cause large power transfer to the region affected by the loss of generation. The power flows associated with these two distributions of mismatch power are quite different and place unique stress on the transmission grid that can lead to stability and security problems.

Present planning techniques overlook the stability problems that may occur due to these generation responses to loss of generation or load contingencies, and the methods for assessing the stability problem are indirect, as indicated in Chapter 1.

The objective of this section is to formulate inertial, governor, and AGC/operator load flow methods based on the description of section 2.1. This will permit direct assessment of the stability and security problems due to loss of generation or load contingencies. The load flow

methods will also be used for calculating inertial and governor security measures that will be defined in Chapter 4.

2.2.1. <u>Load Flow Formulation</u>

Load flow solutions provide bus vultage angles and power flows in the transmission system for specified generation and load conditions.

To study the affect of generation response to loss of generation or load contingency for inertial, governor, and AGC/operator distribution, the real electrical power to be delivered into the network for each distribution must be specified, and load flow equations must then be solved for unknown, wanted variables.

The load flow equations can be written as:

$$PG_i(K) - PD_i = \sum_{j \in A_i} P_{ij}$$

$$QG_i - QD_i = \sum_{j \in A_i} Q_{ij}$$

(2-9)

$$P_{ij} = V_i^2 Y_{ij} \sin \alpha_{ij} + V_i V_j Y_{ij} \sin (\delta_i - \delta_j - \alpha_{ij})$$

$$Q_{ij} = V_i^2 (Y_{ij} \cos \alpha_{ij} - \tfrac{1}{2} B_{ij}) - V_i V_j Y_{ij} \cos (\delta_i - \delta_j - \alpha_{ij})$$

where:

A_i = set of buses connected to bus i

$PD_i + JQD_i$ = complex power load at bus i

$$\delta_i = \text{phase angle of voltage } V_i$$

$$PG_i(K)+jQG_i = \text{complex power from generation at bus i}$$

$$\alpha_{ij} = (90° - \text{the impedance angle of line ij})$$

$$\beta_{ij} = \text{the total charging susceptance of the line i}$$

$$QG_{i_{Min}} \leq QG_i \leq QG_{i_{Max}} \text{ for regulated buses}$$

$$QG_i = \text{reactive power generated by generator i}$$

These AC load flow equations can be solved given $PD_i + jQD_i$ at load buses, $|V_i|$ and δ_i at the swing bus, and $PG_i(K)$ and $|V_i|$ at generator buses. The variables calculated by solving the load flow equations are $|V_i|$ and δ_i at load buses, losses at swing bus, and QG_i and δ_i at generator buses. The load flow is calculated under the constraint:

$$QG_{i_{Min}} \leq QG_i \leq QG_{i_{Max}}$$

at generator buses where voltage is held to specified levels.

The inertial, governor, and AGC/operator load flows differ based on the generator injection $PG_i(K)$ for inertial (K = 1), governor (K = 2), and AGC/operator distributions described in section 2.1. Before deriving the formulas for $PG_i(K)$ for inertial, governor, and AGC/operator load flows, the equations similar to (2-9) for DC inertial, governor, and AGC/operator load flows are given.

The DC load flow considers only the real power equation and ignores the reactive power equations since reactive power and voltage are assumed to remain unchanged from

base case values for any contingency. Resistance is neglected in almost all cases due to the assumption for large X/R ratios. Thus, equation (2-9) becomes:

$$PG_i(K) - PD_i = \sum_{j \in A_i} P_{ij}$$

$$P_{ij} = |V_i| \, |V_j| \, Y_{ij} \sin(\delta_i - \delta_j - \alpha_{ij})$$

and neglecting the line resistance:

$$Y_{ij} = g_{ij} + jb_{ij} = jb_{ij}$$

which leads to:

$$P_{ij} = |V_i| \, |V_j| \, b_{ij} \sin(\delta_i - \delta_j)$$

For linearization, assume $\delta_i - \delta_j$ is small so that:

$$PG_i(K) - PD_i = \sum_{j \in A_i} |V_i| \, |V_j| \, b_{ij} (\delta_i - \delta_j)$$

and define:

$$P_i(K) = PG_i(K) - PD_i$$

$$P_i(K) = \delta_i \sum_{j \in A_i} |V_i| \, |V_j| \, b_{ij} - \sum_{j \in A_i} |V_i| \, |V_j| \, b_{ij} \, \delta_j$$

or in matrix form:

$$\underline{P}(K) = \underline{J} \, \underline{\delta} \qquad\qquad (2\text{-}10)$$

where $\underline{P}(K)$ is the vector of real power injections at every bus for inertial (K=1), governor (K=2), and AGC/operator load flow (K=3), and $\underline{\delta}$ is the vector of voltage angles at every bus. The matrix $\underline{J}$ is defined as:

$$\{J\}_{ij} = \begin{cases} \Sigma |V_i||V_j|b_{ij} & j = i \\ -|V_i||V_j|b_{ij} & i \neq j \end{cases}$$

For the base case, it is clear that:

$$\underline{P}^\circ = \underline{J}\ \underline{\delta}^\circ \quad , \quad \underline{\delta}^\circ = \underline{J}^{-1}\ \underline{P}^\circ$$

For any loss of generation or load disturbance that produces injections $\Delta\underline{P}(k)$, based on inertial, governor, or AGC/operator distribution, the change in angle $\Delta\delta$ satisfies:

$$\underline{P}^\circ + \Delta\underline{P}(K) = \underline{J}\ (\underline{\delta}^\circ + \Delta\underline{\delta})$$

$$\Delta\underline{P}(K) = \underline{J}\ \Delta\underline{\delta}$$

$$\Delta\underline{\delta} = \underline{J}^{-1}\ \Delta\underline{P}(K)$$

The DC load flow is of course less accurate than the AC load flow. The DC inertial, governor, and AGC/operator load flows may be accurate enough to determine vulnerabilities of elements to overload or stability problems. Even if this DC load flow may not be extremely accurate, it has the significant advantage of being able to be computed for all first and second loss of generation and line outage contingencies at reasonable cost and computer time.

The formulas for calculating the injections $PG_i(K)$ for all generators for inertial ($K=1$), governor ($K=2$), and AGC/operator ($K=3$) distributions of loss of generation or load mismatch are now presented.

The value of $\{PG_i(1)\}_{i=1}^{N}$ for the inertial load flow assumes that the acceleration of every generator is constant $d\omega_i/dt = d\omega_0/dt$, and thus:

$$PG_i(1) = PM_i - M_i \frac{d\omega_0}{dt} \qquad (2\text{-}11a)$$

where:

$$\frac{d\omega_0}{dt} = \frac{\displaystyle\sum_{i=1}^{N}(PM_i - PG_i(0))}{\displaystyle\sum_{i=1}^{N} M_i} \qquad (2\text{-}11b)$$

where:

$PG_i(0)$ = real electrical power delivered to the network
      before loss of generation by generator i

PM_i = $PG_i(0) - \Delta PM_i$ = mechanical power sent to the gen-
      erator after loss of generation ΔPM_i

$$\Delta PM_i = \begin{cases} PG_i(0) & i = j \\ 0 & i \neq j \end{cases} \text{ and } j \text{ is the lost generator}$$

$PG_i(1)$ = real electrical power delivered into the network
      by generator i after loss of generation for
      inertial distribution of mismatch power

The value $\{PG_i(2)\}_{i=1}^{N}$ for the governor load flow assumes that the governor action is complete and that fre-quency is constant everywhere $\omega_i = \omega_0$ so that:

$$PG_i(2) = PM_i - \beta_i \, \omega_0 \qquad\qquad (2\text{-}12a)$$

where:

$$\omega_0 = \frac{\sum\limits_{i=1}^{N} (PM_i - PG_i(0))}{\sum\limits_{i=1}^{N} \beta_i}$$

$PG_i(2)$ = the real electrical power delivered into the network by generator i when governor frequency regulation is complete

β_i = frequency response characteristic of generator i

For the final distribution of power by the AGC/operator $PG_i(K)$ for (K=3) satisfies:

$$PG_i(3) = PM_i - \gamma_i \, P_{TOT} \qquad\qquad (2\text{-}13a)$$

where:

$$\sum_i \gamma_i = 1$$

$$P_{TOT} = \sum_i (PM_i - PG_i(0)) \qquad\qquad (2\text{-}13b)$$

$PG_i(3)$ = real power delivered to the network by generator i after operator or AGC action is complete

γ_i = AGC/operator participation factor

The load flow equations (2-9) or (2-10) are solved for bus voltage angles and power flow across the lines, given the values of $PG_i(K)$ from (2-11), (2-12), and (2-13) for the inertial, governor, and AGC/operator load flows, respectively.

In this set of load flow techniques, the mismatch
power is appropriately distributed among generators based
on inertial, governor, and AGC/operator generation
responses. The AGC/operator distribution is local within
the utility experiencing the mismatch and thus places no
stress on the transmission external to the utility. The
inertial and governor distributions are over all generators
in the interconnection back to the utility experiencing the
mismatch. Severe stability and transfer limit violations
may arise out of the power flows from inertia and governor
generation reponse throughout the interconnection. These
problems are even more severe when long distance power
transfers are planned and when long transmission lines are
utilized to carry these transfers, as discussed in
Chapter 1.

The long distance power transfers, as experienced in
the BPA [1] system or planned from Canada and the Midwest
to replace oil generation in the Northeast, utilize certain
transmission corridors and bring loading much closer to
their thermal overload limits. A loss of generation con-
tingency in the area receiving the transfer causes large
inadvertant transfers over the same corridors providing the
large planned transfers. These inadvertant transfers are
due to inertial or governor distribution of the mismatch
from the loss of generation contingency and can be concen-
trated on just one corridor. The planned transfers can be
distributed among several corridors by establishing the

proper operating practice for each of the utilities in the
interconnection where the transfers are planned. The inad-
vertant transfers cannot be distributed among the various
corridor options but are dictated solely by the inertial or
governor responses of generation in the interconnection and
thus can be concentrated in just one corridor. The combin-
ation of the large planned transfers and the uncontrollable
inadvertant transfers will be shown via simulation in the
next chapter to cause thermal overload limit violations and
steady state stability problems, even when the capacity of
all possible corridors far exceeds the combined transfer
requirements.

Thermal overload can cause loss of equipment life and
sagging of lines that can lead to faults and other contin-
gencies that ultimately can cause cascading outages and
islanding. Stability problems may not be as likely or as
severe a problem for systems with short lines carrying
these long distance transfers because thermal overload
limits, and thus normal operations, are far from the sta-
bility limits. The results in the next section show that
even in this case stability problems can occur. The use of
long lines to carry these long distance transfers, such as
for the BPA system and contemplated for some transfers to
the Northeast from Canada, will possibly cause more severe
stability problems because thermal overload limits on long
lines do not restrict normal operation loads on these
lines to be far below stability limits, and thus such lines

are heavily loaded. Therefore, the inadvertant transfers by inertial or governor distribution can more easily cause stability problems on long lines.

Almost every major blackout and islanding problem can be associated with the interconnection wide power flows. An example of this type has been experienced in [1]. This problem is in great part associated with inertia or governor generation response.

The load flow methods developed in this chapter allow direct assessment of stability and security problems due to generation response to loss of generation contingencies. The development of load flow models leads to a better understanding of the different power transfers associated with inertial and governor load flow time scales. The effects of these power flows on transmission grids were also an objective.

Lack of understanding of different power mismatch distributions in present planning methods, in some cases, caused improper use of inertia load flow that was developed after the 1965 blackout when records of the power flow experienced did not agree with existing load flow analysis. The present planning methods have been considering the power flows due to generation response to loss of generation almost equal for inertial and governor distribution of mismatch power. Conventional load flow is not able to address the stability and security problems associated with inertial load flow and governor load flow. The

present load flow techniques generally distribute the mis-
match power to a large swing generator. This is not what
will happen in a real power system, and the accuracy of
this approximation to inertial or governor distribution
will depend heavily on the representation of the system and
the choice of the swing bus.

The stability problems associated with generation
response to loss of generation are related to system struc-
tural weakness and generation response of synchronizing
generators throughout the interconnection. The vulnerabil-
ity of the lines and stability problems associated with
them cannot be assessed by line outages or any fault
studies.

The recently developed Midterm Stability Package [8]
could be used to assess the stability problems associated
with dynamic generation response of generators, but this
package cannot handle very large data bases required to
analyze large interconnected networks associated with long
distance power transfers where all the generators must have
governor turbine representation. Even if it is upgraded,
it would be very computationally expensive to run for the
simulation time interval needed (> 20 seconds) to analyze
governor action distribution.

For assessing the stability problems associated with
generator response to loss of generation or load contingen-
cies, the load flow methods that were introduced in this
chapter are superior and inexpensive for very large data

bases, compared with the solution time of several hundreds to thousands of differential equations that have to be solved in the Midterm Stability Package, especially for governor action response.

The accuracy and validity of the inertial and governor load flow is shown in Chapter 3 by comparing these load flow results for specific contingencies with the Midterm Stability simulations of the same contingency. The results show that the DC inertial and DC governor load flows are reasonably accurate; that the inertial and governor load flows are quite different for the same contingency; that a separate stability problem can exist for each of these distributions; and finally, that conventional load flow and line outage studies would not have detected these inertial and governor load flow stability problems.

CHAPTER 3

APPLICATION OF THE INERTIAL AND GOVERNOR LOAD FLOW
FOR ASSESSMENT OF STABILITY AND SECURITY
ON A 49 BUS TEST SYSTEM

To demonstrate the performance of the inertial and
the governor load flow methods developed in Chapter 2,
loss of generation contingencies were simulated using the
inertial and governor load flow programs on the 49 bus
Electric Power Research Institute (EPRI) test system. A
schematic of this system is shown in Figure 3.1. The 49
bus test system was chosen since it was used and tested
to validate the Midterm Stability Program, and the governor
models for midterm stability studies were available for
this system. Generator data, governor models, and base
case load flow data used in this study are available
through the EPRI Midterm Stability Package [8] and there-
fore are not reproduced here.

The inertial and the governor load flow results were
compared with the Midterm Stability Program's results of
the same contingencies to verify the inertial and the gov-
ernor load flows.

The following contingencies were simulated on the 49
bus test system to:
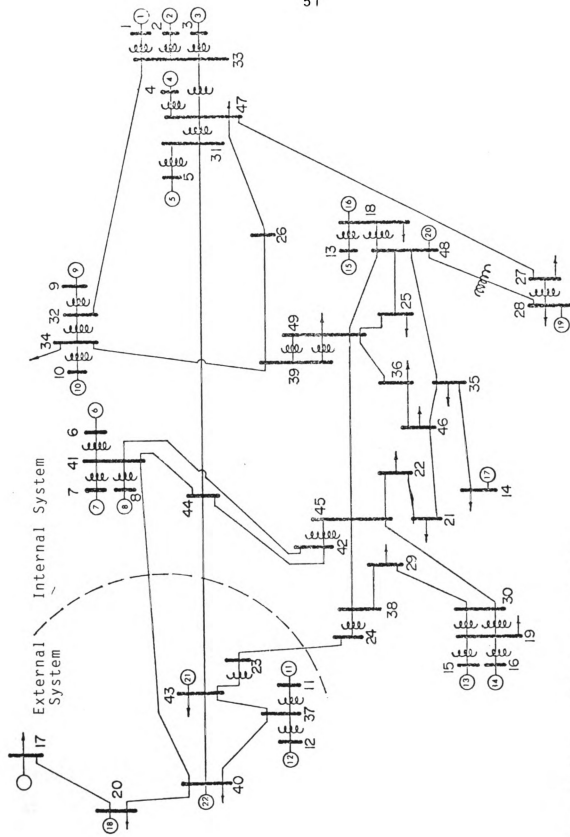
Figure 3.1. 49 Bus Test System.

(a) establish accuracy of inertial and governor load flows
against the midterm stability simulation results.

(b) investigate possible existence of stability and secur-
ity problems associated with inertial and governor
power flows.

(c) show the stability and security problems associated
with inertial and governor load flow cannot be pre-
dicted by present load flow methods and line outage
studies.

3.1. 490 MW Loss of Generation in the External System

The 49 bus test system was operating at the point
given by the base case data with total generation of
24868.32 MW and maximum capacity of 28236 MW. At this
operating point, the external system was importing power
(1381 MW) through the three lines (43, 44), (40, 41), and
(23, 24), with a combined steady state capacity of 3916 MW.

A 490 MW loss of generation was simulated on the 49
bus system for 50 seconds using the Midterm Stability
Program to see the effects of both the inertial and gover-
nor response of generators to a loss of generation contin-
gency on the system. The power flow on the three lines
connecting the internal and external system is shown in
Figure 3.2. The result shows that the internal system par-
ticipates in supplying the mismatch after only 1 second
through the reduction in frequency and thus loss of kinetic
energy in internal system generation. The percentage of
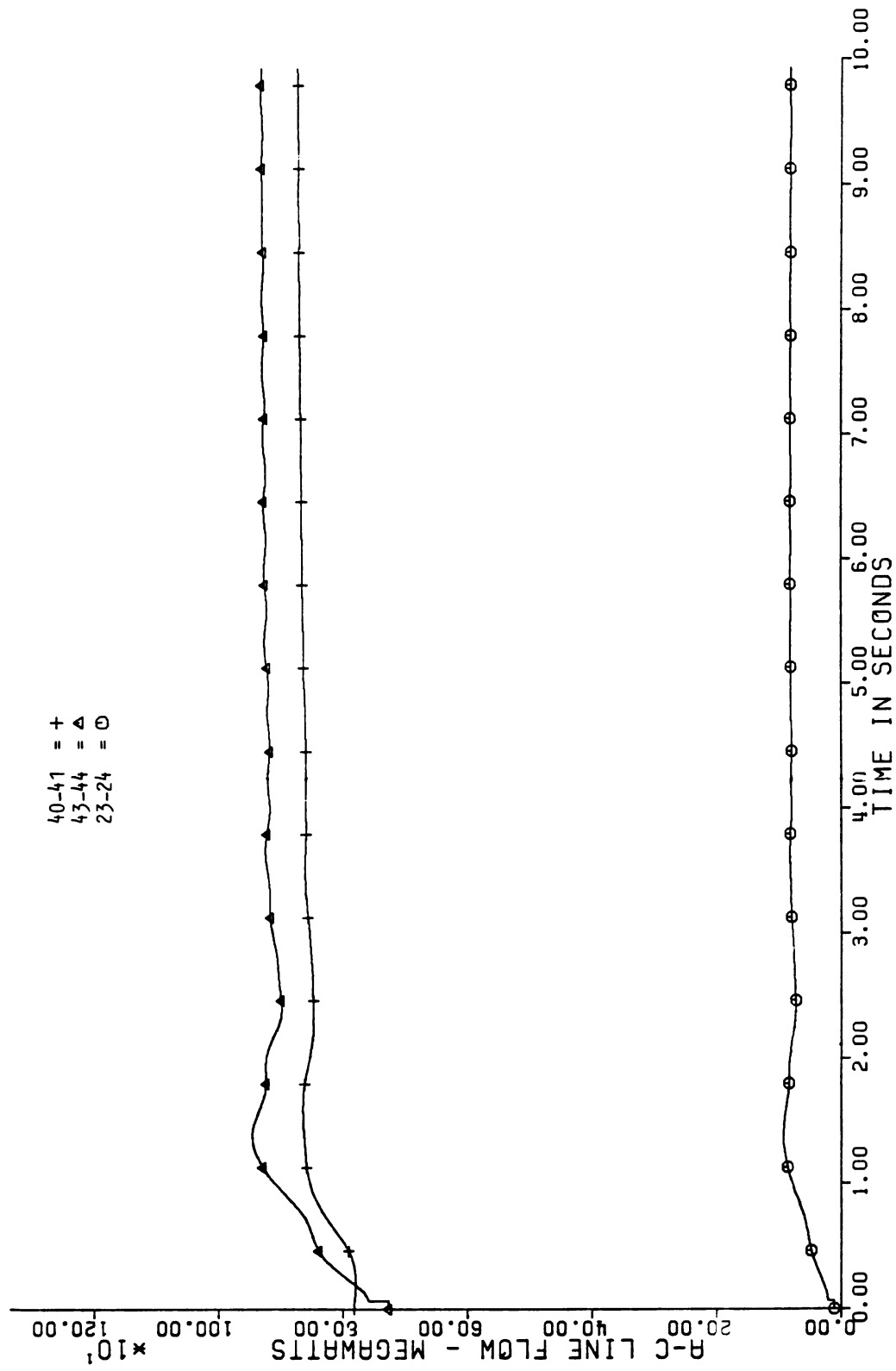
Figure 3.2. Power Flow of Lines Connecting the Internal and External System
After 490 MW Loss of Generation

the MW power transferred from the internal system via these lines (40, 41), (43, 44), (23, 24) is proportional to the ratio of the inertia of the internal system to the inertia of the entire system ($\frac{M_{internal}}{M_{system}}$). The figure also shows that the governor power flow is 24 MW larger than the inertial power flow on line (40, 41) and 12.6 for line (43, 44). That is, for this disturbance, the response of internal generators by governor action is more than the internal response since a larger majority of the generation with governors is in the internal system and thus $\frac{internal}{system}$ $\frac{M_{internal}}{M_{system}}$. It is also shown that line (40, 41) picks up the larger share of the power flow, which is due to its location in the transmission system connecting the internal and external system generation.

Figure 3.3 shows a plot of the frequency deviation at different buses in the system. It can be seen that the generators in the external system decelerate more rapidly since the loss of generation is in the external system. This difference in frequency sets up the changes in the angles that govern the system response during the inertial response time frame and are captured by the inertial load flow. The inertial time frame starts at approximately 1 second when the deceleration of all generators is equal. After 5 seconds, the change in frequency has been arrested, and frequency is constant. This indicates that the governor regulation is complete for this loss of generation.
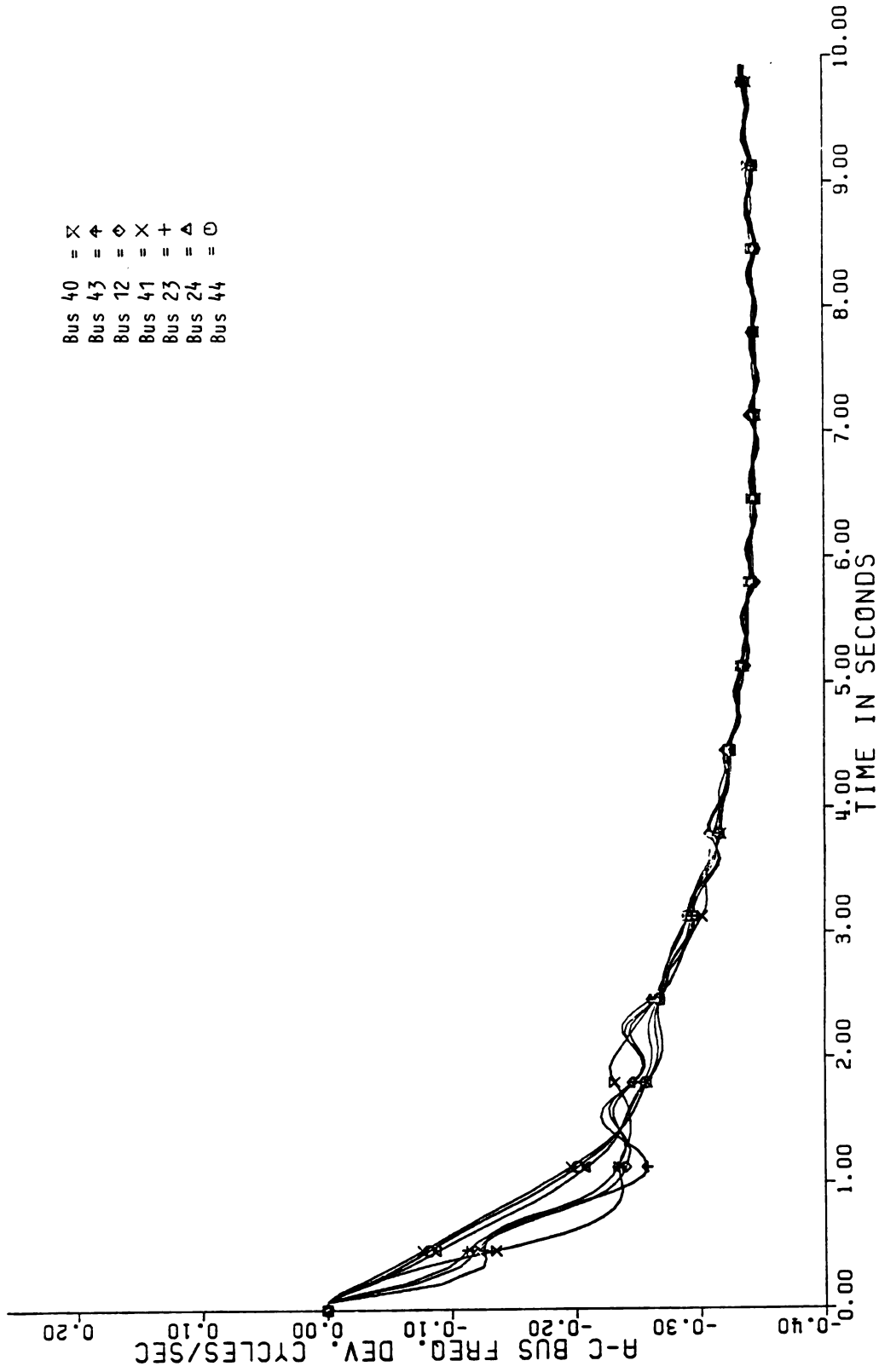
Figure 3.3. Frequency Deviation at Different Buses After 490 MW Loss of Generation.

The DC inertial and governor load flows were run with
490 MW loss of generation contingency at generator 11.
The deviation in generator angles due to inertial and gov-
ernor response were added to generator angles at the
operating point before loss of generation. The resulting
angles were then compared with those of the Midterm
Stability Program. The midterm stability results are
illustrated by straight solid and dotted lines for inertial
and governor responses respectively for some of the genera-
tors in Figures 3.4 to 3.7. The lines reflect the average
angles during the inertial time frame and the steady state
angles after the governor response is completed.

The final results are presented in Tables 3.1 and 3.2,
which compare the midterm stability simulation results with
those of the inertial load flow and the governor load flow
respectively. Tables 3.1 and 3.2 show that:

(1) The inertial and the governor angles are different
     and cause different power flows as they did in tie
     lines connecting the internal and external system.

(2) The DC inertial and governor load flows can predict
     the inertial and the governor angles and thus capture
     the dynamics of the distribution of power mismatch
     with reasonable accuracy expected with a DC linear-
     ized model (15% error). The accuracy of the results
     is indicated by: (a) the agreement of angle differ-
     ences in both cases between the DC load flow and the
     Midterm Stability Program results, and (b) the changes
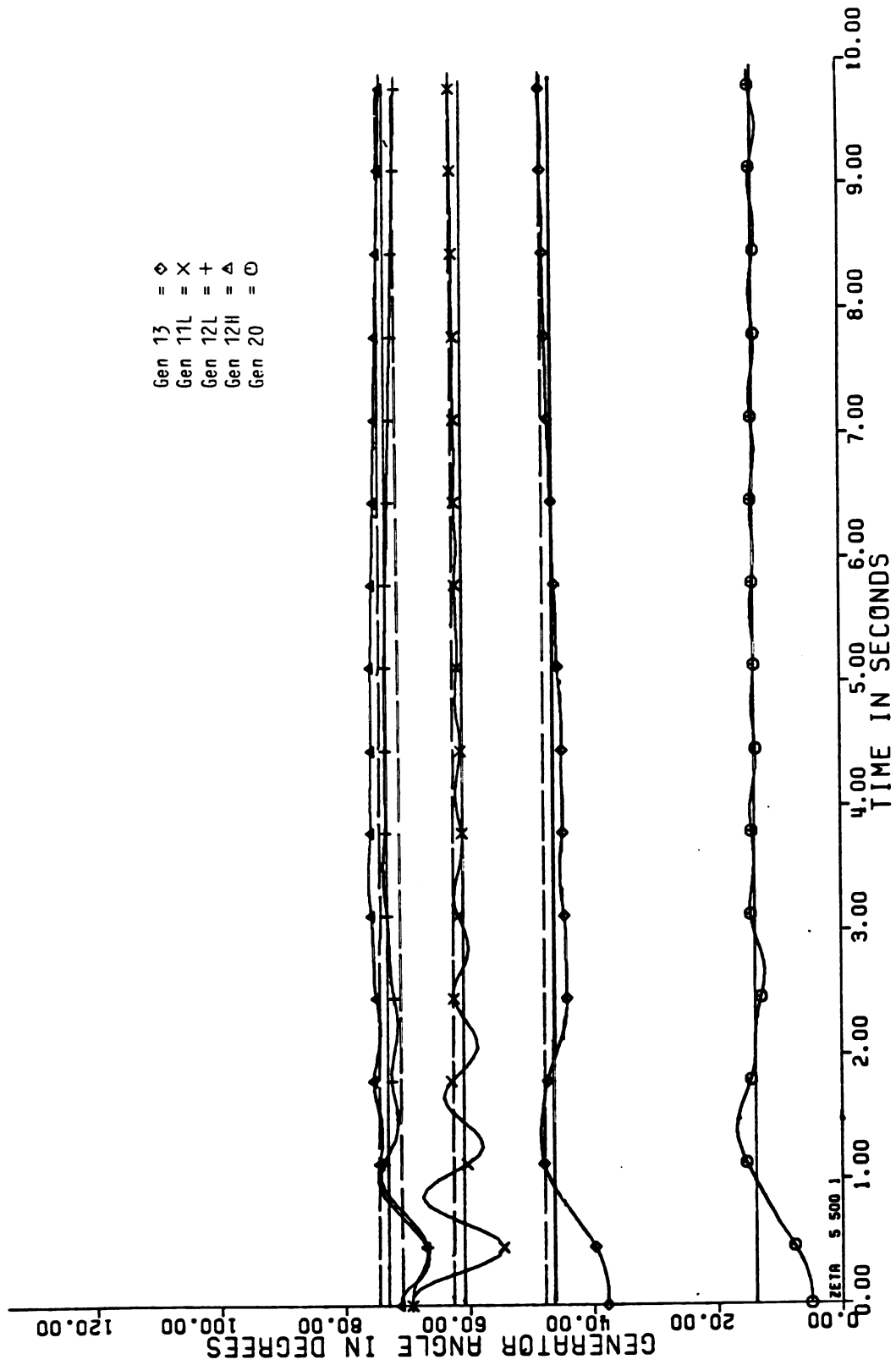
Figure 3.4.   Generator Angles After 490 MW Loss of Generation.

Figure 3.5. Generator Angles After 490 MW Loss of Generation.

59

Figure 3.6.   Generator Angles After 490 MW Loss of Generation.

Figure 3.7. Generator Angles After 490 MW Loss of Generation.

Table 3.1. Comparison of the Inertial Response Generator Angles Obtained from the Inertial Load Flow and the Midterm Stability Program for 490 MW Loss of Generation at Generator Bus 11.

Generator Bus Number	Angle (Degree) at t=0	Inertial Angle (Degree) Midterm Stability	Inertial Angle (Degree) Inertial Load Flow
1	83.98	94.82	88.38
3	86.5	95.25	90.91
4	97.69	111.5	102.24
5	100.18	117.2	103.87
8	89.51	102.5	93.83
10	75.29	86.76	80.05
12	69.26	73.55	75.29
15	55.49	62.37	60.26
17	28.71	39.5	32.83
13	37.77	46.2	32.26
14	27.9	35.52	31.34
16	26.66	35.92	32.77
19	49.91	66.25	55.42
21	34.6	36.12	32.6
20	5.05	13.70	11.02

Table 3.2.   Comparison of the Governor Response Generator Angles Obtained from the Governor Load Flow and the Midterm Stability Program for 490 MW Loss of Generation at Generator Bus 11.

Generator Bus Number	Angle (Degree) at t=0	Governor Angle (Degree) Midterm Stability	Governor Angle (Degree) Governor Load Flow
1	83.98	95.16	102.69
3	86.5	96.23	105
4	97.69	112.25	116.4
5	100.18	110.78	118.16
8	89.51	97.13	104.5
10	75.29	87.75	96.19
12	69.26	71.60	67.47
15	55.49	64.75	74.33
17	28.71	37.57	45.09
13	37.77	48.85	56.4
14	27.9	38.26	46.27
16	26.66	37.40	42.9
19	49.91	62.50	70.9
21	34.6	36.12	34.64
20	5.05	13.70	19.56

observed between simulation results in inertial and
governor time frames are observed in the differences
in the inertial and governor load flows.

Table 3.2 shows that the governor time frame angles
predicted by the DC governor load flow are larger than
those obtained from the Midterm Stability Program. This
overprediction of the angles is in part due to a decrease
in load that is caused by the coupling between active power
and voltage in the Midterm Stability Program which is
omitted in the DC governor load flow. The reduction in
load will reduce the mismatch that must be made up by the
governor response of generators in the Midterm Stability
Program, and thus reduces the angles at the internal gener-
ator buses in the results of the Midterm Stability Program.

A second reason why the angles at the internal genera-
tor buses for the Midterm Stability Program are smaller
than the DC governor load flow is that the generator with
the lost generation is not dropped and thus participates in
the governor response in the Midterm Stability Program but
is dropped in the DC governor load flow. Thus, the remain-
ing generators are required to pick up less generation in
the Midterm Stability Program and hence have smaller angles.

A third reason why the Midterm Stability results would
have smaller angles is the reduction of transmission losses
with the loss of generation. This effect is similar to the
reduction of load with the loss of generation. The genera-
tion changes observed in the Midterm Stability Program show

that the generating units picked up 42 MW less than the
total lost generation at the governor time frame due to the
reasons given above which resulted in smaller internal gen-
erator angles. The modification of Consumer Power Company's
fast decoupled load flow to be able to compute power flows
for inertial and governor response to synchronous generators
has been proposed to EPRI, which would reduce the errors in
both the inertial and governor load flows.

3.2. 790 MW Loss of Generation at Bus Number 12

The second contingency simulated on the 49 bus system
was loss of 790 MW generation at bus number 12 in the
external system. This disturbance was again simulated by
running the inertial and governor DC load flows and the
Midterm Stability Program. The results given in Table 3.3
compare the inertial angles obtained from inertial load
flow and the Midterm Stability Program. The overshoot was
factored in for this case since the contingency was large.
Table 3.3 shows that the inertial angles were predicted
fairly accurately by the DC inertial load flow program
(10%-15% error), with again good agreement in angle differ-
ences. No angle across any line exceeded 90 degrees. That
is, no loss of stability is predicted by inertial load
flow.

Table 3.4 shows the inertial angles across the tie
lines connecting the internal and external system. The
angle across the line (40, 41) is the largest angle

Table 3.3. Comparison of the Inertial Response Generator Angles Obtained from the Inertial Load Flow and the Midterm Stability Program for 790 MW Loss of Generation at Generator Bus 12.

Generator Bus Number	Angle (Degree) at t=0	Inertial Angle (Degree) Midterm Stability	Inertial Angle (Degree) Inertial Load Flow
1	83.98	108.5	103.65
4	97.69	128.0	117.37
5	100.18	124.8	119.07
6	89.51	112.5	105.26
8	89.51	108.25	105.26
17	28.71	57.2	45.92
13	37.77	69.8	57.08
16	26.66	52.6	44.78
21	34.6	57.2	52.00

Table 3.4. Inertial Angles Across the Tie Lines Connecting
            the Internal and External System After 790 MW
            Loss of Generation.

Line	Inertial Angles Across Lines
(41, 40)	71.22
(44, 43)	32.21
(24, 23)	10.1

Table 3.5. Governor Angles Across the Tie Lines Connecting
            the Internal and External System After 790 MW
            Loss of Generation.

Line	Governor Angles Across Lines
(41, 40)	148.2
(44, 43)	128.3
(24, 23)	12.1

observed by inertial load flow, which shows this line was significantly stressed for inertial power flows due to 790 MW loss of generation in the external system.

The governor load flow predicted a loss of stability across the tie lines connecting the internal and external system by showing very large angles across this boundary (angles >> 90°). This is shown in Table 3.5. This was further confirmed by the midterm stability results, where Figure 3.8 shows that the line (40, 41) exceeded its stability limit at 5.35 seconds after the loss of generation and caused line (43, 44) and line (23, 24) to consecutively exceed their stability limits, leading to separation of the internal and external system.

This can also be observed in Figure 3.9, where the frequency at a group of buses in the internal system oscillates with increasing magnitude against the frequency at the external buses, which leads to separation of two groups. The magnitude of this oscillation increases after 1 second, which is the inertial time frame indicating the stability is due to governor generation response rather than inertial generation response.

The separation of the internal and external system caused a very large swing in generator angles. These angles are shown in Figures 3.10 to 3.12. Figure 3.12 shows that after this swing, generators 16 and 17 lost synchronism. This indicates that the stability problems
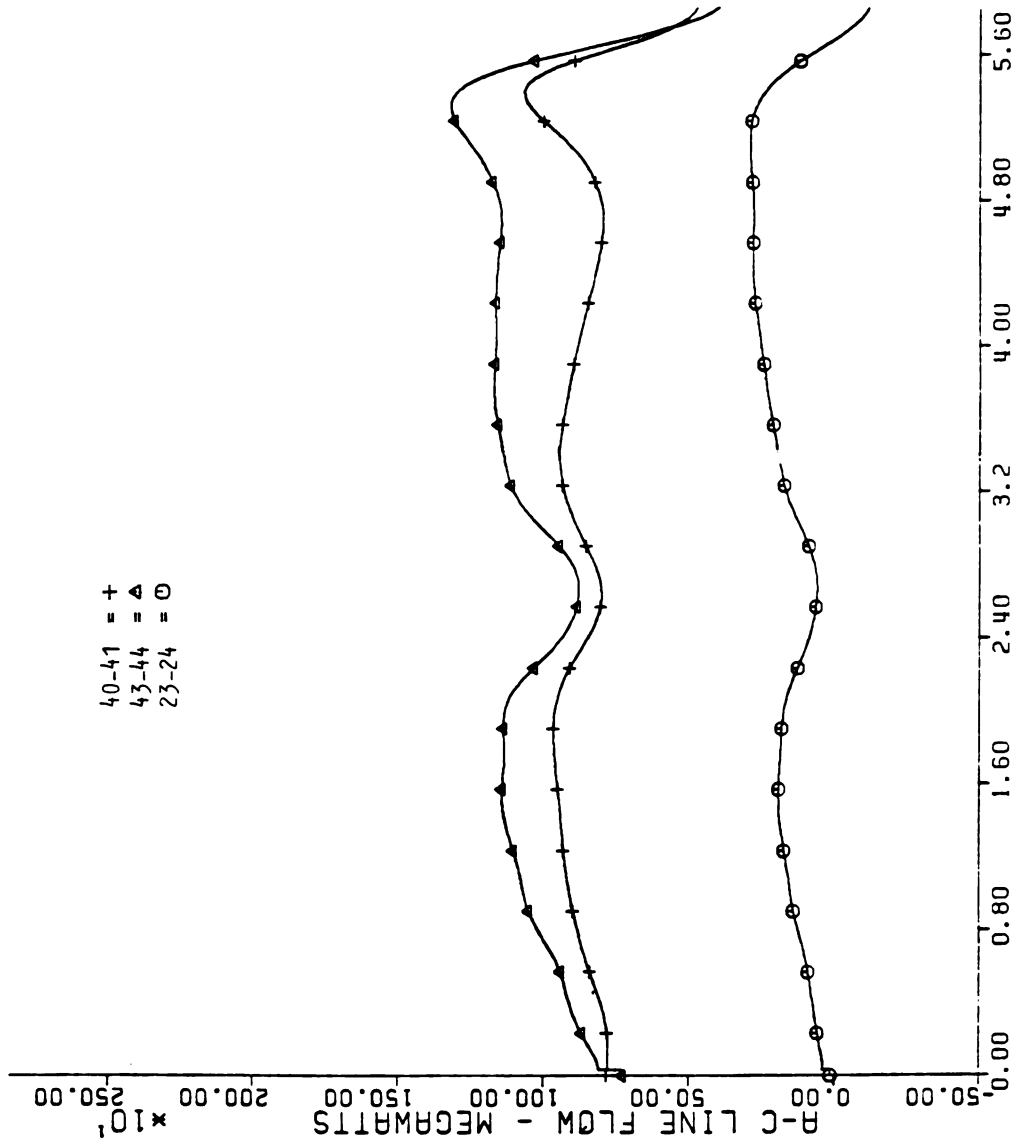
Figure 3.8. Power Flow of Lines Connecting Internal and External System After 790 Loss of Generation.
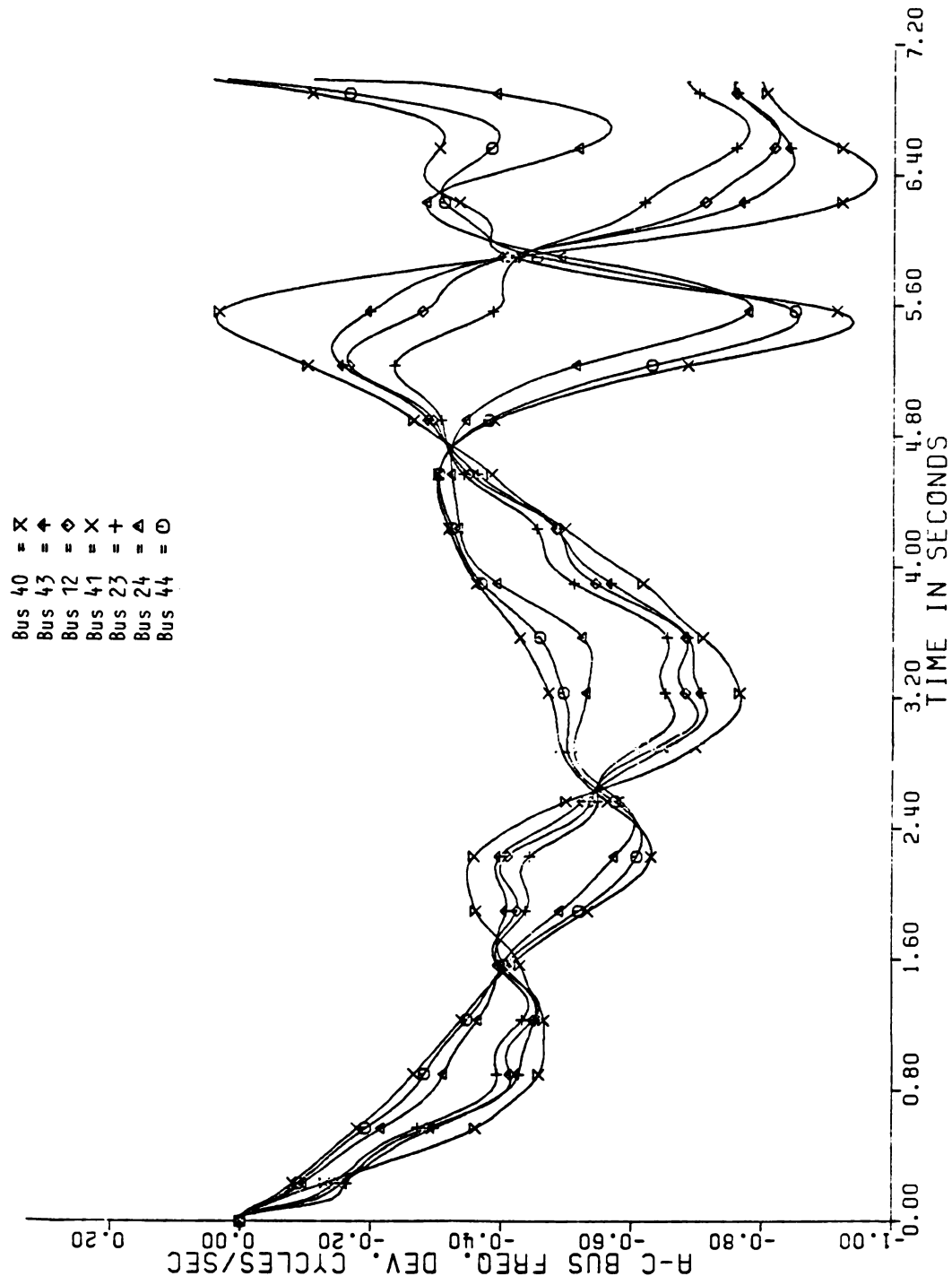
Figure 3.9. Frequency Deviation at the Internal and External Buses After 790 MW Loss of Generation.
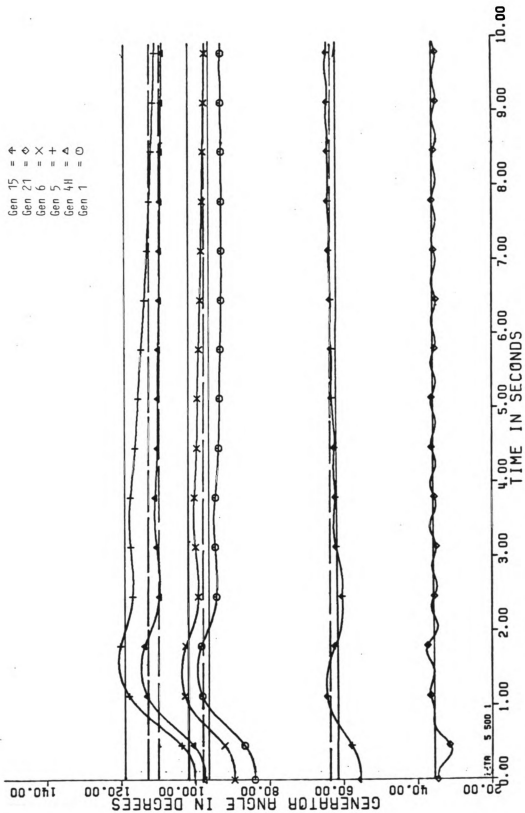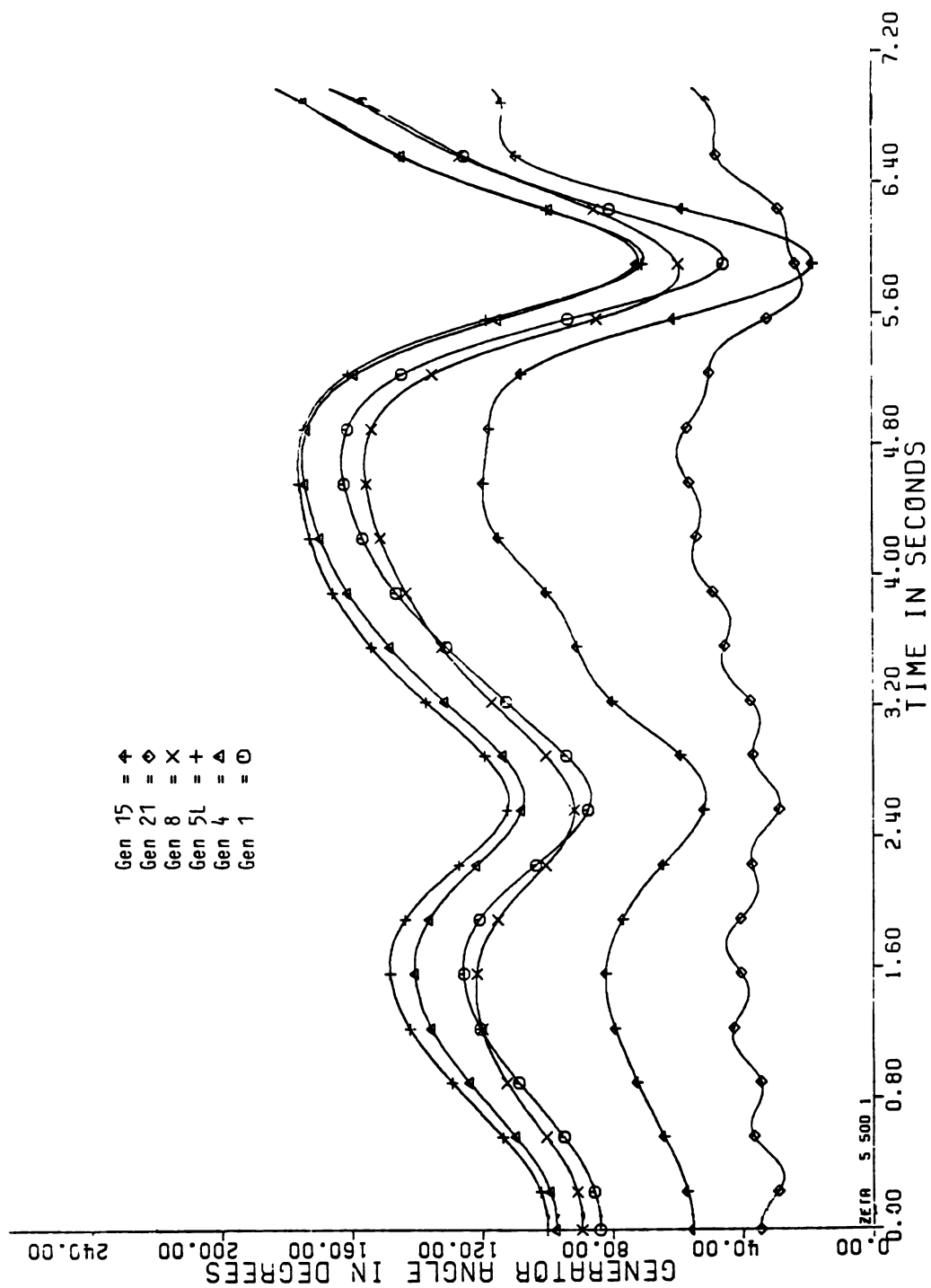
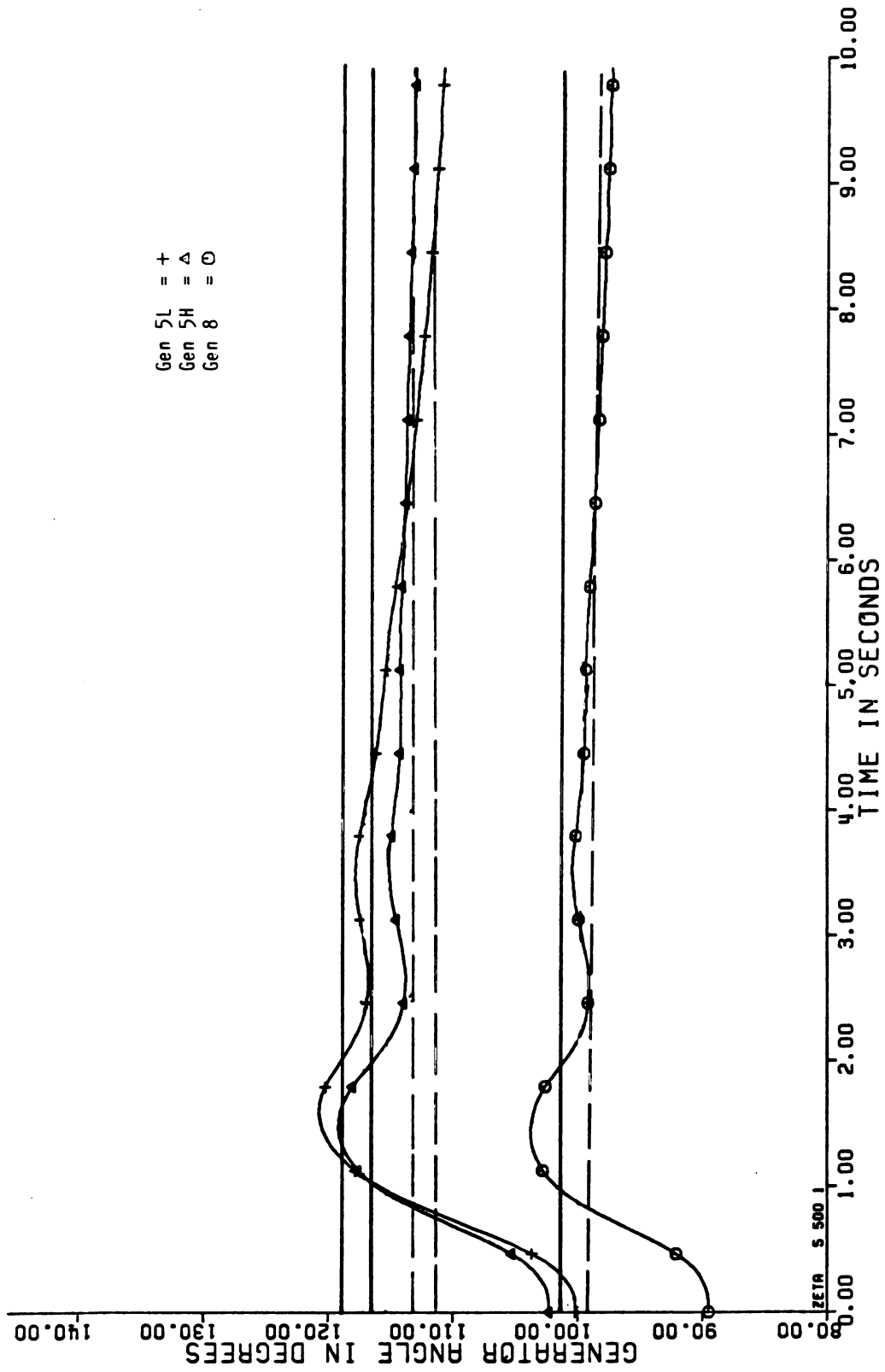Figure 3.10. Generator Angles After 790 MW Loss of Generation.

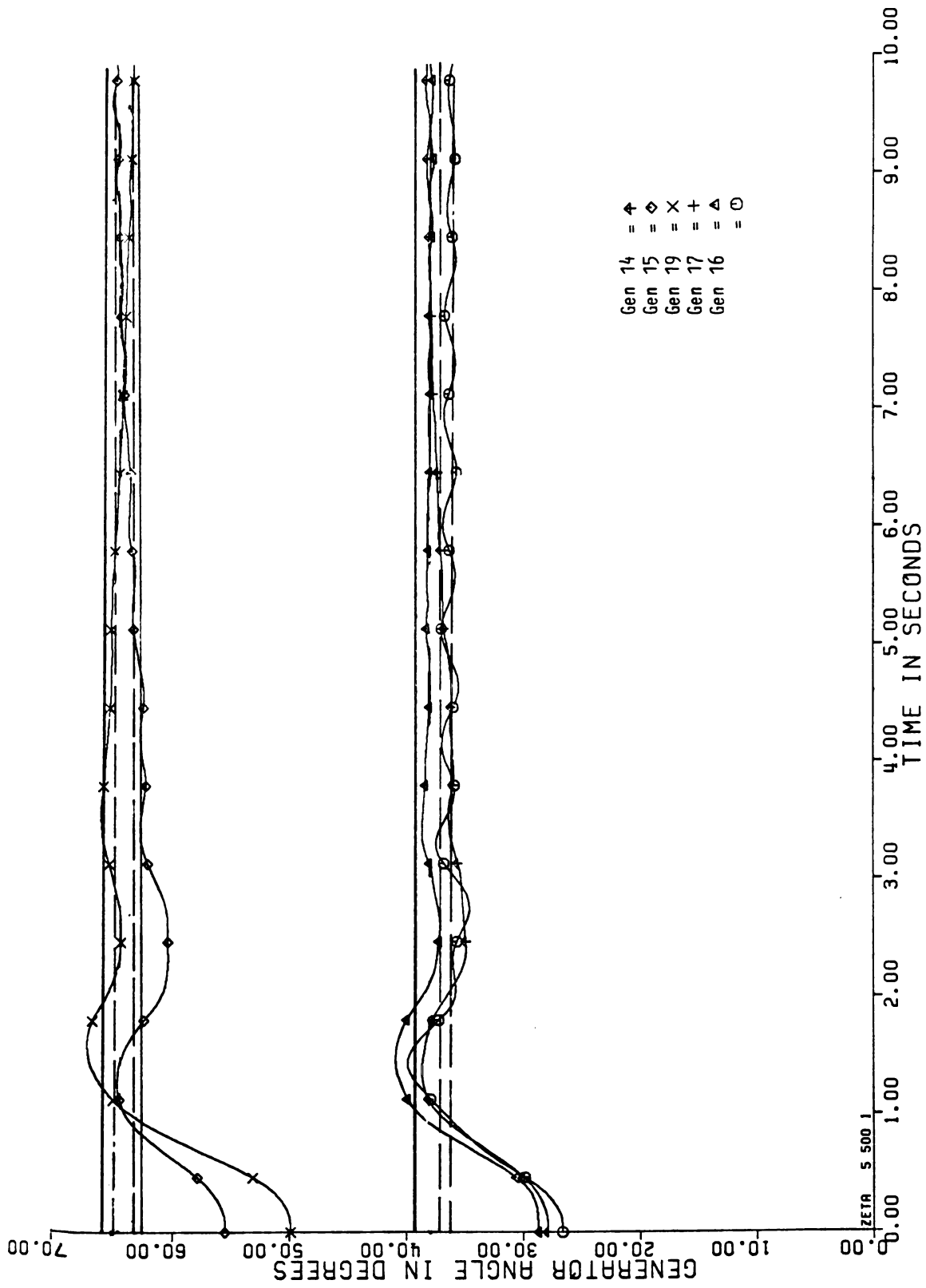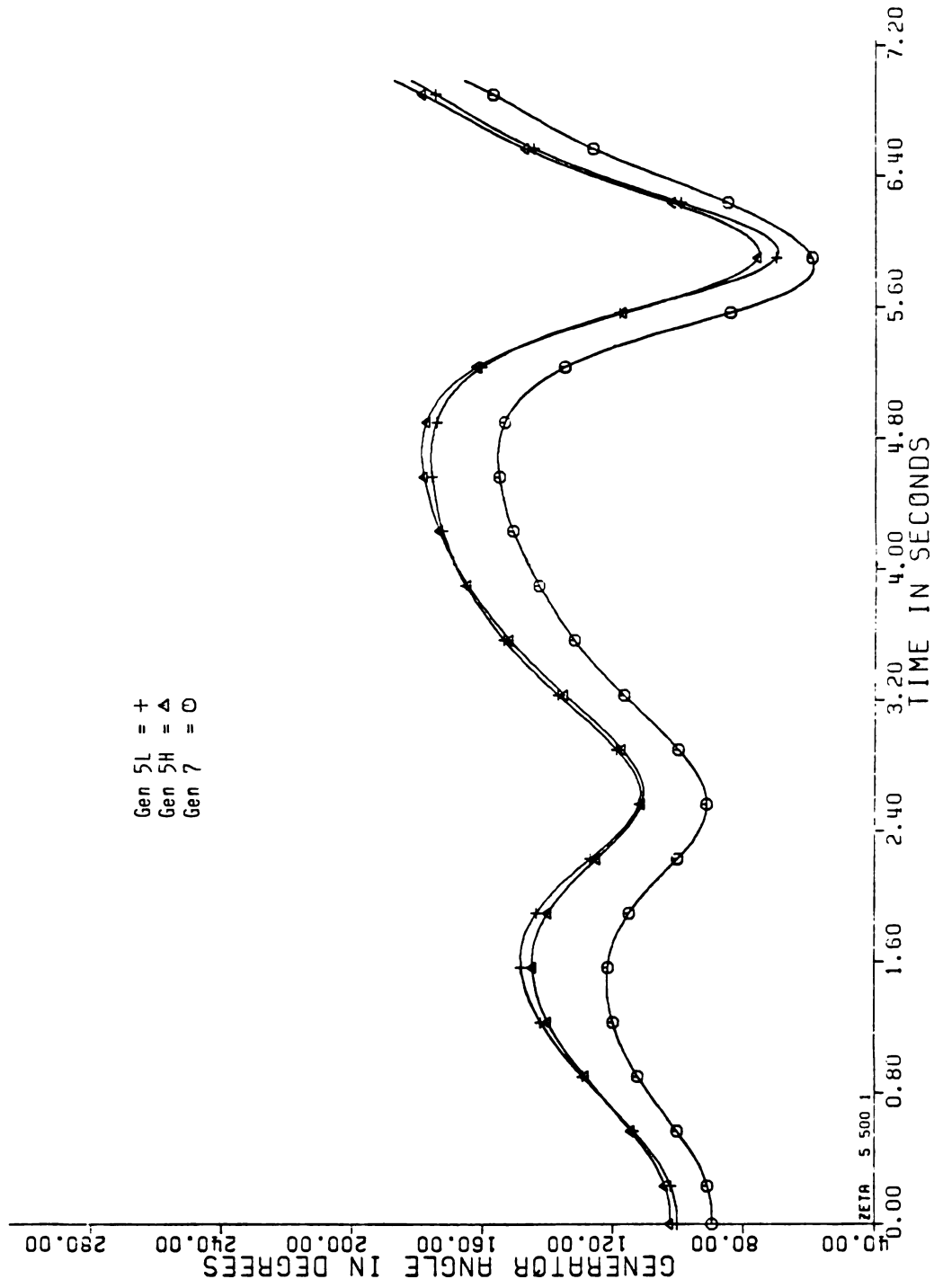Figure 3.11. Generator Angles After 790 MW Loss of Generation.
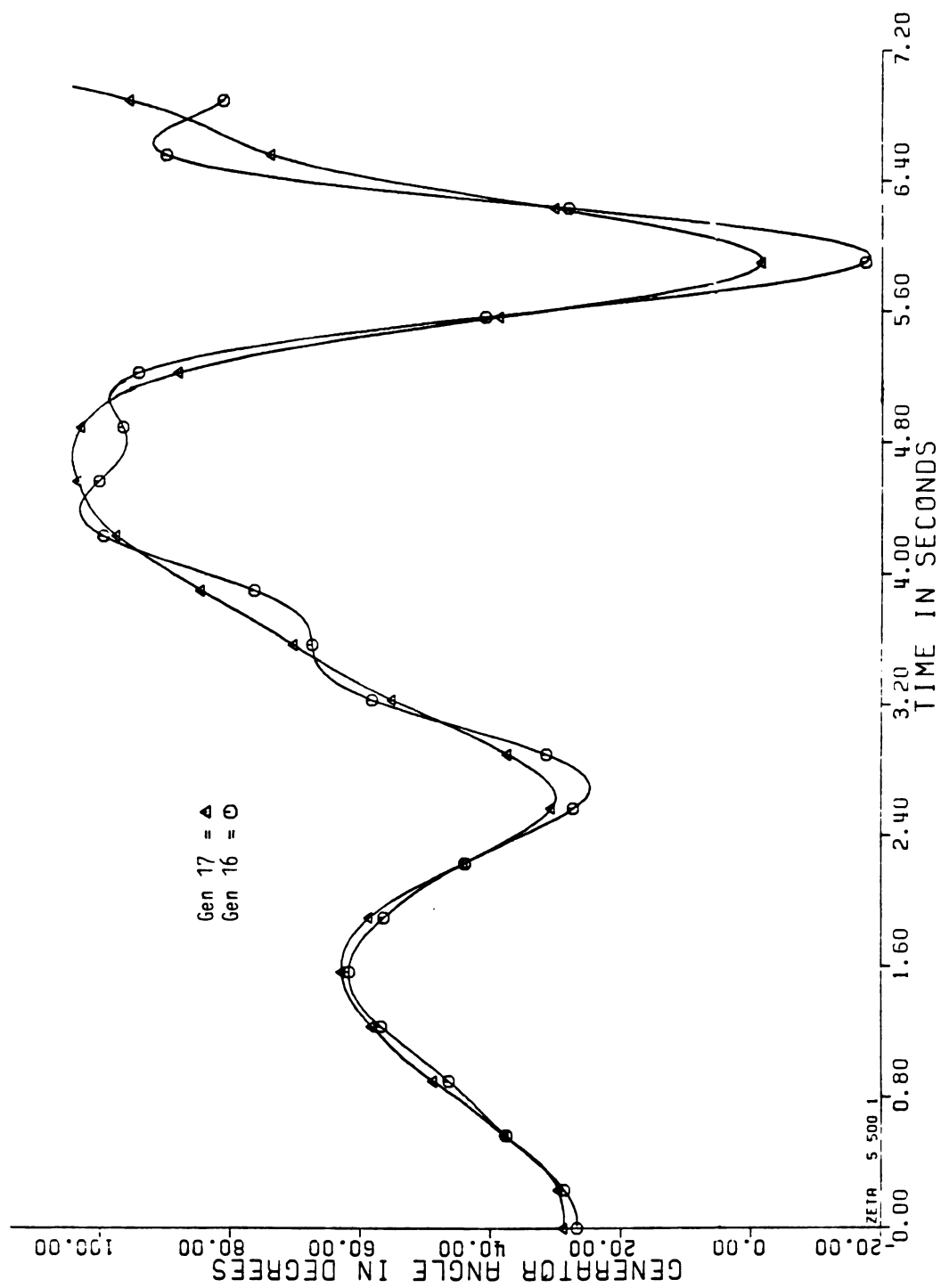
Figure 3.12. Generator Angles After 790 MW Loss of Generation.

associated with inertial and governor load flow can be very severe and lead to system collapse.

The reasons why the governor load flow led to the loss of stability of lines connecting the internal and external system are now given.

The three lines (40, 41), (43, 44), and (23, 24) were importing power to the external system with ample additional capacity. Lines (40, 41), (43, 44), and (23, 24) were importing 7.6 PU, 6.7 PU, and .11 PU with capacity of 11 PU, 20.16 PU, and 8 PU, respectively. The line (40, 41) was initially more heavily loaded than the others. The loss of 790 MW (7.9 PU) generation in the external system near the boundary caused the internal units to respond by governor action much more than by inertia since $(\frac{\beta_{internal}}{\beta_{system}} = .833 > \frac{M_{internal}}{M_{system}} = .336)$. A significant percentage of this internal system response $(\frac{\beta_{internal}}{\beta_{system}})$ x 7.9 PU came over the weakest line (40, 41), causing the loss of stability over this line as can be seen when the power over the line reached 11 PU. Then the boundary lines exceed their stability limit one after another, causing separation of the external and internal system.

The inertial response of the internal generators was not as severe as the governor response and did not cause stability limit violations over the boundary lines, but the inertial flow stressed these lines severely, which is an indication of vulnerability of this boundary to inertial power flow. A very large loss of generation, 20 p.u. at

generator 18 in the external system, showed a loss of sta-
bility at .62 second across this boundary. The loss of
stability occurred due to inertial response but would also
have occurred due to governor response. It is clear that
due to the differences in governor and inertial response
loss of stability can occur due to only inertial, only gov-
ernor, or both inertial and governor responses. When a loss
of stability could occur due to both inertial or governor
response, the actual loss of stability occurs in the iner-
tial time frame since it comes first.

3.3. Simulation of 790 MW Loss of Generation at Bus 12 Using Conventional Load Flow Program

The 790 MW loss of generation at the external bus
number 12 by the governor load flow and the midterm stabil-
ity simulation was shown to cause loss of stability for
governor distribution of this mismatch. This loss of gen-
eration contingency was simulated on the system using a
regular load flow program to study whether the regular load
flow programs could predict an overload or a loss of stabil-
ity across the external and internal boundary. In this
load flow program, the loss of generation was made up on
the large swing generator at bus number 40, which is also
in the external system.

The program does not report any violation of either
line overload of bus voltage limits. This is expected
since a shift of generation in the external system would

not significantly affect the boundary between the external and internal system because it does not require the internal generators to respond to this generation shift.

3.4. Line Outage Contingency of Line (40, 41)

To determine whether the stability problem observed for governor load flow could be assessed by line outage studies, line (40, 41) was outaged using a DC load flow program. The result given in Table 3.6 indicates that the system is operating with no violations of the limits. The angles across the boundary lines (43, 44) and (23, 24) are not even close to the critical angle (90 degrees). This is due to ample capacity of the remaining lines connecting the external and internal system that can handle both the inadvertant flow due to outage of line (40, 41) plus the scheduled power flows.

The results obtained from the simulation below ran on the 40 bus system and are now summarized. These results are extremely important because:

(1) The inertial and governor load flows did predict the dynamic changes in power distribution in this system for loss of generation contingencies. This allows the direct assessment of system and boundary weaknesses to inertial and governor power flows with the methods introduced in Chapter 2.

(2) The loss of stability caused by governor power flow after the first swing contradicts the generally held

Table 3.6.   Angles Across the Transmission Lines After
             Outage of Line (40, 41).

Line from Bus to Bus	Angle (Degree)	Line from Bus to Bus	Angle (Degree)
30, 19	6.90	10, 34	8.80
15, 19	2.50	35, 46	.01
16, 19	2.3	14, 35	.20
22, 21	1.43	35, 48	.21
21, 46	.82	36, 46	.20
45, 22	3.33	49, 36	3.68
24, 23	5.84	11, 37	9.40
23, 43	14.04	12, 37	9.40
38, 24	.70	37, 43	1.19
49, 25	4.19	37, 40	28.35
48, 25	.1	45, 38	4.64
26, 39	7.51	39, 49	3.26
47, 26	9.41	41, 42	24.15
47, 27	32.35	41, 44	13.39
27, 28	1.48	6, 41	6.70
30, 29	2.36	7, 41	6.70
38, 29	1.80	8, 41	6.70
45, 30	4.07	42, 44	10.76
31, 44	6.79	42, 45	2.91
31, 47	1.99	44, 43	28.14
5, 31	8.50	45, 49	1.71
33, 32	3.29	4, 47	7.30
32, 34	1.88	49, 48	4.09
9, 32	2.91	17, 20	2.60
33, 47	1.21	13, 18	4.30
1, 33	5.40	18, 48	.11
2, 33	5.50	20, 40	1.2
3, 33	6.80	48, 28	9.55
34, 39	12.97	43, 40	27.16

understanding of stability that a system that survives the first swing is stable. Moreover, this stability problem is difficult to classify using present power system stability definitions. It would be classified as a transient stability problem due to the fact that it is caused by a large disturbance and requires a nonlinear rather than a linearized model for simulation or analysis. It also could be classified as a "steady state" stability problem because the loss of stability is dictated where line flows or angle differences exceed the steady state stability limit. These results suggest that some modification of power system stability definitions may be appropriate.

(3) The loss of stability caused by governor load flow was not observed in a regular load flow study of the loss of generation contingency where the loss of generation was made up on the large swing generator also lying in the external system.

(4) In the investigation of the 790 MW loss of generation, the loss of stability was caused by governor power flow distribution. The Midterm Stability Program and Long Term Stability Program are the only methods of analyzing the governor power flow distribution effects until now. However, these programs are very expensive to run for the governor time frame and are not able to handle very large data bases.

(5) The vulnerability of the boundary connecting the internal and external system could not be seen by a single contingency line outage on the boundary of line (40, 41). Thus, the stability problem associated with inertial and governor distribution of loss of generation cannot be assessed by line outage studies.

The effects of inertial and governor load flow on very large networks was not investigated in this thesis due in part to the lack of data bases. This task has been proposed to EPRI, which also includes a method for modeling of governor frequency response characteristics of generators for large networks.

CHAPTER 4

SECURITY MEASURES AND SECURITY ASSESSMENT

The objective of this chapter is to propose and theoretically justify a security assessment methodology for inertial and governor generation response to loss of generation contingencies. This security assessment methodology is unique in that:

(1) It is a transient security assessment methodology based on the classical transient stability model.

(2) The vulnerabilities of the system for inertial (and governor) generation response to loss of generation contingencies are associated with the strict synchronizing coherency loss of controllability condition on this classical transient stability model.

(3) The security measures are developed, can be shown to detect the loss of controllability condition, and thus detect the boundaries and lines between groups of generators that are vulnerable to a loss of stability due to the inertial or governor response to loss of generation contingencies. These intertial and governor security measures are probabilistic rather than deterministic, as are all previous security measures [15]. These security measures can be evaluated

by summing the results of DC inertial and DC governor load flows for all single loss of generation contingencies.

(4) The vulnerable boundaries between generator groups are determined by clustering generators into larger and larger groups with successively weaker boundaries. Security measures have not generally been defined over individual network elements and thus have not generally permitted identification of vulnerable boundaries and lines.

The justification that: (1) a specific loss of controllability conditions on the classical transient stability model causes vulnerability to loss of stability for inertial response to loss of generation contingencies, and (2) this loss of controllability condition is detected from the probabilistic security measures (defined from DC inertial and governor load flows) and the boundary identification procedure is given in this chapter. This justification is based on results derived in justifying the modal coherent technique for producing dynamic equivalents for transient stability studies.

This chapter is divided into three sections. The first section develops the linearized classical transient stability model, the probabilistic disturbance model, and the r.m.s. coherency measure. The inertial security measure is defined and related to the r.m.s. coherency by showing that the security measure, evaluated for all single loss of

generation contingencies, is identical to the r.m.s. coher-
ency measure for the modal probabilistic disturbance when
the base case condition is neglected. In the second sec-
tion, the vulnerabilities of boundaries and lines to loss
of stability for inertial generation response to loss of
generation contingencies is related to the strict synchro-
nyzing coherency loss of controllability condition and then
shown to be detected by this security measure and a bound-
ary identification procedure. In section three, the gover-
nor response security measure is defined and shown to be
computed by summing the results of the DC governor load
flow for all single loss of generation contingencies. The
governor security measure and boundary identification pro-
cedure is shown to detect a loss of controllability condi-
tion that causes the vulnerable boundaries and lines to the
loss of stability for governor response to loss of genera-
tion contingencies.

4.1. Security Measure Derivation and Justification

The security assessment or contingency analysis method
depends on the security measure defined in this section that
is evaluated based on a DC inertial load flow simulation of
loss of generation contingencies. The security measure is
justified by showing that it is identical to the square of
the r.m.s. coherency measure evaluated for the linearized clas-
sical transient stability model with a probabilistic dis-
turbance model. The security measure is further justified

in the next section by showing that the strict synchroniz-
ing loss of controllability conditions of this linearized
classical transient stability model will cause the vulnera-
ble boundaries in the transmission network and that these
boundaries can be detected from this security measure using
the boundary identification procedure. Thus, this section
first develops the linearized classical transient stability
model utilized to drive the r.m.s. coherency measure in
this section and to define and discuss the loss of control-
lability conditions for this model in the next section.
The probabilistic disturbance model and the r.m.s. coher-
ency measure are then defined. The security measure is
then defined and shown to be evaluated as the summations of
d.c. inertial load flow for all loss of generation contin-
gencies and to be identical to the r.m.s. coherency measure
for the probabilistic disturbance.

4.1.1. The Linear Power System Model

To obtain a linearized model of power system, the
synchronous machine is presented as:

$$M_i \frac{d}{dt} \Delta\omega_i(t) = \Delta PM_i(t) - \Delta PG_i(t) - D_i \Delta\omega_i(t) \tag{4-1a}$$

$$i = 1, 2, \ldots, N$$

$$\frac{d}{dt} \Delta\delta_i(t) = \Delta\omega_i(t) \quad , \quad i = 1, 2, \ldots, N \tag{4-1b}$$

where:

    i is the subscript for generator i

    Δ indicates that the variable is a small deviation about some specified (pre-calculated) steady-state operating point

    M_i is the inertia constant of generator i in p.u.

    $\Delta\omega_i$ is the speed deviation of generator i

    $\Delta\delta_i$ is the rotor angle deviation of generator i (in radians)

    D_i is the damping constant of generator i (in p.u.)

    ΔPM_i is the change in mechanical input power at generator i in p.u.

    ΔPG_i is the change in electrical output power at generator i in p.u.

The real power flow equations with real and reactive power decoupled are represented in polar form as:

$$\begin{bmatrix} \Delta PG \\ \Delta PL \end{bmatrix} = \begin{bmatrix} \partial \underline{PG}/\partial \underline{\delta} & \partial \underline{PG}/\partial \underline{\theta} \\ \partial \underline{PL}/\partial \underline{\delta} & \partial \underline{PL}/\partial \underline{\theta} \end{bmatrix} \begin{bmatrix} \Delta \underline{\delta} \\ \Delta \underline{\theta} \end{bmatrix} \qquad (4\text{-}2)$$

where:

$\underline{PG} = (PG_1, PG_2, \ldots, PG_N)^T$

$\underline{PL} = (PL_1, PL_2, \ldots, PL_K)^T$

$\underline{\delta} = (\delta_1, \delta_2, \ldots, \delta_N)^T$

$\underline{\theta} = (\theta_1, \theta_2, \ldots, \theta_K)^T$

    K is the number of load buses

    ΔPL_j deviation in power injection at load bus j

    $\Delta\theta_j$ deviation in voltage angle at load bus j

The decoupling of real and reactive power is justified based on the strong dependence of real power on voltage angle and high X/R ratios (loss less network) for the transmission system.

To solve the network equations (4-2), one of the angles must be specified as a reference bus since the power angle Jacobian matrix in the network equation (4-2) is symmetric and singular. This allows a unique solution for $\underline{\Delta\delta}$ and $\underline{\Delta\theta}$, given $\Delta\underline{PG}$ and $\Delta\underline{PL}$. The generator angle of the Nth machine may by chosen as the reference angle; therefore, equations (4-1) and (4-2) may be written in the uniform machine N reference frame [30] as:

$$\frac{d}{dt}\Delta\omega_i = \frac{1}{M_i}(\Delta PM_i - \Delta PG_i) - \frac{1}{M_N}(\Delta PM_N - \Delta PG_N) - \sigma\Delta\hat{\omega}_i$$

$$i = 1,2,\ldots,N-1 \tag{4-3a}$$

where: $\quad \sigma = \dfrac{D_i}{M_i} \quad , \quad i = 1,2,\ldots,N.$

$$\frac{d}{dt}\Delta\hat{\delta}_i = \Delta\hat{\omega}, \quad , \quad i = 1,2,\ldots,N-1 \tag{4-3b}$$

$$\begin{bmatrix} \Delta\underline{PG} \\ \Delta\underline{PL} \end{bmatrix} = \begin{bmatrix} \partial\underline{PG}/\partial\underline{\hat{\delta}} & \partial\underline{PG}/\partial\underline{\hat{\theta}} \\ \partial\underline{PL}/\partial\underline{\hat{\delta}} & \partial\underline{PL}/\partial\underline{\hat{\theta}} \end{bmatrix} \begin{bmatrix} \Delta\underline{\hat{\delta}} \\ \Delta\underline{\hat{\theta}} \end{bmatrix} \tag{4-4}$$

where: $\quad \hat{\delta}_i = \hat{\delta}_i - \hat{\delta}_N \quad , \quad i = 1,2,\ldots,N-1$

$\qquad\qquad \hat{\theta}_j = \hat{\theta}_j - \hat{\theta}_N \quad , \quad j = 1,2,\ldots,K$

$\qquad\qquad \hat{\omega}_i = \hat{\omega}_i - \hat{\omega}_N \quad , \quad i = 1,2,\ldots,N-1$

and:
$$\underline{\hat{\delta}} = [\hat{\delta}_1, \hat{\delta}_2, \ldots, \hat{\delta}_{N-1}]^T$$
$$\underline{\hat{\theta}} = [\hat{\theta}_1, \hat{\theta}_2, \ldots, \hat{\theta}_K]^T$$

To express the model in state space form, equations (4-3) are written in vector form, and network equations (4-4) are used to eliminate $\Delta\underline{PG}$ from the expression. $\Delta\underline{PG}$ in terms of $\Delta\underline{\hat{\delta}}$ and $\Delta\underline{PL}$ is:

$$\Delta\underline{PG} = \underline{T}\Delta\underline{\hat{\delta}} - \underline{L}\Delta\underline{PL} \qquad (4\text{-}5)$$

where:

$$\underline{T} = \partial\underline{PG}/\partial\underline{\hat{\delta}} - (\partial\underline{PG}/\partial\underline{\hat{\theta}}) [\partial\underline{PL}/\partial\underline{\hat{\theta}}]^{-1} (\partial\underline{PL}/\partial\underline{\hat{\delta}}) \qquad (4\text{-}6)$$

is the synchronizing torque coefficient matrix and:

$$\underline{L} = -(\partial\underline{PG}/\partial\underline{\hat{\theta}}) [\partial\underline{PL}/\partial\underline{\hat{\theta}}]^{-1} \qquad (4\text{-}7)$$

is referred to as the load reflection matrix.

The resulting state model may be written as:

$$\underline{\dot{x}}(t) = \underline{A}\,\underline{x}(t) + \underline{B}\,\underline{u}(t) \qquad (4\text{-}8)$$

where:

$$\underline{x} = \begin{bmatrix} \Delta\underline{\hat{\delta}} \\ \Delta\underline{\hat{\omega}} \end{bmatrix} \quad , \quad \underline{u} = \begin{bmatrix} \Delta\underline{PM} \\ \Delta\underline{PL} \end{bmatrix}$$

$$\underline{A} = \begin{bmatrix} \underline{0} & \underline{I} \\ -\underline{M}\,\underline{T} & -\sigma\underline{I} \end{bmatrix} \quad , \quad \underline{B} = \begin{bmatrix} \underline{0} & \underline{0} \\ \underline{M} & \underline{M}\,\underline{L} \end{bmatrix} \qquad (4\text{-}9)$$

and:

$$
\underline{M} = \begin{bmatrix} M_1^{-1} & & & & & -M_N^{-1} \\ & M_2^{-1} & & & & -M_N^{-1} \\ & & \cdot & & & \cdot \\ & & & \cdot & & \cdot \\ & & & & M_{N-1}^{-1} & -M_N^{-1} \end{bmatrix} \qquad (4\text{-}10)
$$

$\underline{M}$ is a $(N-1)N$ dimensional matrix; $\underline{x}$ is a $2N-2$ dimensional state vector.

4.1.2. Disturbance Model

The disturbance model presented in this subsection was developed by Schlueter [22]. The purpose of the disturbance model is to allow modeling of deterministic as well as probabilistic system disturbances.

The initial condition of linear model (4-8) is assumed random with:

$$E\{\underline{x}(0)\} = \underline{0}$$
$$E\{\underline{x}(0)\ \underline{x}^T(0)\} = \underline{V}_x(0)$$

since expected deviation from any operating state is zero, but the variance of such deviation is non zero. The initial conditions are included not to reflect any specific type of disturbance but rather the effects on the state from some hypothetical disturbance whose statistic may be inferred from internal and external operating conditions.

The input composed of deviations in load power, ΔPL, and the deviations in the mechanical input power, ΔPM, can be used to model:

i) loss of generation due to generator dropping

ii) loss of load due to load shedding

iii) line switching

These contingencies can be modeled by an input disturbance $\underline{u}(t)$ where:

$$\underline{u}(t) = \begin{cases} \underline{u} \text{ for } t \geq 0 \\ 0 \text{ for } t < 0 \end{cases} \qquad (4\text{-}11)$$

that is, $\underline{u}(t)$ is a vector step function initiated at time t=0. Non-zero entries in $\underline{u}(t)$ will model loss of generation, loss of load, and line switching type contingencies described above.

The modeling of these three disturbances requires determination of $\underline{u}$ and possible modification of the network before determination of matrices $\underline{A}$ and $\underline{B}$. The procedure for generator dropping and load shedding that is used in this study is discussed below:

generator dropping - the transient reactance of the genera-
    tor dropped is omitted from the network, and the gen-
    erator output ΔPM_i of generator dropped is set equal to
    the loss of generation.

load shedding - the load deviation ΔPL_k for all buses k
    where load is shed should be set equal to the change
    in load caused by the load shedding operations.

To represent the random occurrence of generator drop-
ping, line switching, and load shedding, it is necessary to
define:

$$E\{\underline{u}(t)\} = \begin{bmatrix} \underline{m}_1 \\ \underline{m}_2 \end{bmatrix} = \underline{m} \tag{4-12}$$

$$E\{[\underline{u}(t) - \underline{m}][\underline{u}(t) - \underline{m}]^T\} = \begin{bmatrix} \underline{R}_{11} & \underline{0} \\ \underline{0} & \underline{R}_{22} \end{bmatrix} = R \tag{4-13}$$

The matrices $\underline{m}_1$ and $\underline{R}_{11}$ describe the uncertainty in
the location and magnitude of generation changes $\Delta\underline{PM}$. The
matrices $\underline{m}_2$ and $\underline{R}_{22}$ describe the uncertainty in locations
and magnitude of power injections on buses due to either
load being shed or line being switched.

It should be noted that $\Delta\underline{PM}$ and $\Delta\underline{PL}$ are assumed uncor-
related because this model is to represent only one speci-
fic type of contingency at a time. For the same reason, $\underline{u}$
is assumed uncorrelated with initial condition:

$$E\{\underline{x}(0)\,\underline{u}^T\} = 0 \tag{4-14}$$

The uncertain model of $\underline{u}$ can handle the case of
specific deterministic disturbance by setting $\underline{R}=\underline{0}$ and $\underline{m}=\underline{u}$
for the particular disturbance.

4.1.3. The r.m.s. Coherency Measure

The r.m.s. coherency, $C_{k\ell}$, between generators k and ℓ of a power system is defined as:

$$C_{k\ell} = [\frac{1}{T} E\{\int_0^T [\Delta\delta_k(t) - \Delta\delta_\ell(t)]^2 \, dt\}]^{1/2} \qquad (4\text{-}15)$$

where E is expectation operator.

This coherency measure first was used by Schlueter [22] to determine coherent groups of generators which could be aggregated into a single generators to form a reduced order power system model. It has been shown [23, 24, 25] the resulting equivalent by the r.m.s. coherency measure reflects the overall dynamics of the system better than other coherency measures [26]. The expectation operator E appears, because as shown in [17], the disturbance for detecting coherent groups that depend on the power system structure is probabilistic, and there is no single deterministic disturbance that adequately detects structural coherency. The results of [22-26] for the linear model of subsection 4.1.1 using a probabilistic step disturbance $\underline{u}(t)$ is now given.

To facilitate the computation of r.m.s. coherency measure, the intermediate quantity, $\underline{S}_x(T)$, is defined in terms of the state vector of the linear model as:

$$\underline{S}_x(T) = \frac{1}{T} \int_0^T E\{\underline{x}(t) \, \underline{x}^T(t)\} \, dt \qquad (4\text{-}16)$$

which is a (2N-2)x(2N-2) symmetric matrix where $\underline{x}(t)$ is the state vector.

Thus, the $C_{k\ell}$ can be written as:

$$C_{k\ell} = [\underline{e}_{k\ell}^T \; \underline{S}_x(t) \; \underline{e}_{k\ell}]^{1/2} \qquad (4\text{-}17)$$

with $\underline{e}_{k\ell}$ a 2N-2 vector whose jth entry is defined by:

$$
\{\underline{e}_{k\ell}\}_j \equiv
\begin{cases}
\begin{array}{lll}
1 & j = k \\
-1 & j = \ell \;\} & \text{for } k \neq N, \ell = N \\
0 & j \neq k
\end{array} \\[2ex]
\begin{array}{lll}
1 & j = k \;\} & \text{for } k \neq N, \ell = N \\
0 & j \neq k
\end{array} \\[2ex]
\begin{array}{lll}
1 & j = \ell \;\} & \text{for } k = N, \ell \neq N \\
0 & j \neq \ell
\end{array}
\end{cases}
\qquad (4\text{-}18)
$$

For input function $\underline{u}(t)$, $\underline{x}(t)$ has the form:

$$\underline{x}(t) = e^{AT} \, \underline{x}(0) + \int_0^t e^{\underline{AV}} \, \underline{B} \, \underline{u} \, dV \qquad (4\text{-}19)$$

Substituting this expression for $\underline{x}(t)$ into (4-16) and taking the expectation term by term and utilizing the assumption that $\underline{x}(0)$ is zero leads to the expression:

$$\underline{S}_x(T) = \frac{1}{T} \int_0^T [\int_0^t e^{AV} dV \underline{B}][\underline{R} + \underline{mm}^T][\int_0^t e^{AV} \, dV \underline{B}]^T \, dt \qquad (4\text{-}20)$$

As shown in [17], $\underline{S}_x(T)$ can be written in a closed form by letting $T \to \infty$, that is:

$$\underline{S}_x(\infty) = [\underline{A}^{-1}\underline{B}] \, [\underline{R} + \underline{m}\underline{m}^T] \, [\underline{A}^{-1}\underline{B}]^T \qquad (4\text{-}21)$$

for $\underline{A}$ and $\underline{B}$ given by (4-9), thus,

$$\underline{A}^{-1}\underline{B} = \begin{bmatrix} -(\underline{MT})^{-1} \, \underline{M} & -(MT)^{-1} \, ML \\ \underline{0} & \underline{0} \end{bmatrix} \qquad (4\text{-}22)$$

For step disturbance in mechanical input power, $\underline{m}$ and $\underline{R}$, as defined by (4-12) and 4_13) become:

$$\underline{m} = \begin{bmatrix} \underline{m}_1 \\ \underline{0} \end{bmatrix} \quad , \quad \underline{R} = \begin{bmatrix} \underline{R}_{11} & \underline{0} \\ \underline{0} & \underline{0} \end{bmatrix} \qquad (4\text{-}23)$$

Substituting (4-22) and (4-23) into (4-21) leads to the expression:

$$\underline{S}_x(\infty) = \begin{bmatrix} [(\underline{MT})^{-1}\underline{M}][\underline{R}_{11}+\underline{m}_1\underline{m}_1^T][(\underline{MT})^{-1}\underline{M}]^T & \underline{0} \\ \underline{0} & \underline{0} \end{bmatrix} \qquad (4\text{-}24)$$

Thus the coherency measure for any pair of generators is defined by:

$$\underline{\hat{S}}_x(\infty) = [(\underline{MT})^{-1}][\underline{R}_{11} + \underline{m}_1\underline{m}_1^T][(MT)^{-1}M]^T \qquad (4\text{-}25)$$

A disturbance which causes:

$$\underline{M}(\underline{R}_{11} + \underline{m}_1\underline{m}_1^T) \, \underline{M}^T = \underline{I} \qquad (4\text{-}26)$$

shows that the r.m.s. coherency measure is a function of system structure only, and $\underline{\hat{\delta}}_x(\infty)$ can be written as:

$$\underline{\hat{\delta}}_x(\infty) = [(\underline{MT})^{-1}] \, [(\underline{MT})^{-1}]^T \qquad (4\text{-}27)$$

The disturbance which satisfies (4-26) is:

$$\underline{m}_1 = \underline{0} \quad , \quad \underline{R}_{11} = \text{DIAG } (M_1^2, M_2^2, \ldots, M_{N-1}^2, 0) \quad (4-28)$$

This disturbance is dependent on choice of reference generators. It has been shown [17] a reference independent result can be obtained by allowing the covariance of the disturbance in $\Delta \underline{PM}$ to be:

$$\underline{R}_{11} = \text{DIAG } (M_1^2, M_2^2, \ldots, M_N^2) \quad (4-29)$$

The disburtance defined by (4-29) is called "the modal disturbance," and $\underline{\hat{\delta}}_x(\infty)$ produced by this disturbance is:

$$\hat{S}_x(\infty) = [(\underline{MT})^{-1}] \underline{K} [(\underline{MT})^{-1}]^T \quad (4-30)$$

where $\underline{K}$ is a constant matrix whose ij entry is defined as:

$$\{K\}_{ij} = \begin{cases} 2 & i = j \\ 1 & i \neq j \end{cases} \quad (4-31)$$

4.1.4.   Inertial Security Measure and Its Relation to r.m.s. Coherency Measure.

The ability to transfer power from point A to point B is dictated largely by the angle across equivalent transmission lines between A and B. This angle can reflect the loading of the line and its closeness to the stability limit of the line. Thus, a set of these angles, if appropriately compared and grouped, may be used to identify

weaknesses in the transmission system. Hence, in this sub-section, a security measure is defined based on these angles for inertial power flows.

The inertial security measure for a single loss of generation contingency on generator i is defined as:

$$S_M^i(k,\ell) = [\delta_M(k,i) - \delta_M(\ell,i)]^2 \qquad (4\text{-}32)$$

where $\delta_M(k,i)$ is the phase angle of the inertial load flow at bus k for loss of generation contingency, and:

$$PM_i = PG_i(0) - \Delta PM_i \qquad (4\text{-}33)$$

where ΔPM_i is the lost mechanical power into generator i. ΔPM_i is equal to $PG_i(0)$ for a tripped generator. The angle $\underline{\delta}_M(k,i)$ is obtained by inserting (4-33) into (2-11) to obtain $\{PG_j(1)\}_{i=1}^N$, which is in turn inserted in (2-9) or (2-10) to obtain $\{\delta_M(k,i)\}_{k=1}^{N+M}$.

To account for the effects of all single loss of generation contingencies, a contingency independent security measure (CISM) for inertial load flow is defined as the sum of the inertial security measures for a set of single contingencies:

$$S_M(k,\ell) = \sum_{i=1}^N S_M^i(k,\ell) \qquad (4\text{-}34)$$

where i is summed over all possible loss of generation con-tingencies or some subset. Since CISM considers the

effects of all contingencies, it is used to detect boundary vulnerabilities for inertial load flow in this research.

It is shown in Chapter 2 that inertial distributions of mismatch power due to loss of generation is complete when the acceleration at all generators in the system is equal to the mean acceleration of the system. Knowing this fact, the linear relationship between the security measures and inertial load flow is now given:

$$\dot{\omega}_p = \dot{\omega}_0 \quad , \quad p = 1,2,\ldots,N \tag{4-35}$$

and for the system loss of generation mismatches $\sum_{j=1}^{N}(PM_j^i - PG_j(0))$ are:

$$\dot{\omega}_p = \frac{PM_p^i - PG_p^i(1)}{M_p} \quad , \quad i = 1,2,\ldots,N \tag{4-36}$$

and:

$$\dot{\omega}_0 = \frac{\sum_{j=1}^{N}(PM_j^i - PG_j(0))}{\sum_{j=1}^{N} M_j} \quad , \quad i = 1,2,\ldots,N \tag{4-37}$$

Thus, from (4-36):

$$PG_p^i(1) = PM_p^i - \frac{M_p \sum_{j=1}^{N}(PM_j^i - PG_j(0))}{\sum_{j=1}^{N} M_j} \tag{4-38}$$

$$i = 1,2,\ldots N$$

It is also known:

$$PG_p^i(1) = PG_p(0) + \Delta PG_p^i(1) \quad , \quad p = 1,2,\ldots,N \quad (4\text{-}39)$$

$$PM_p^i = PG_p(0) - \Delta PM_p^i \quad\quad\quad\quad (4\text{-}40)$$

and for loss of generation from (4-5), it is given:

$$\Delta \underline{PG}^i(1) = \underline{T} \, \Delta \underline{\delta}_M^i \quad\quad\quad\quad (4\text{-}41)$$

where:

$$\Delta \underline{\delta}_M^i = [\Delta \delta_{M_1}^i, \Delta \delta_{M_2}^i, \ldots, \Delta \delta_{M_{N-1}}^i]^T$$

are the inertial angle deviations at internal generator buses for loss of generation ΔPM.

Substituted for $\Delta \underline{PG}^i(1)$ from (4-41) into (4-39) and written in vector form:

$$\underline{PG}^i(1) = \underline{PG}(0) + \underline{T}\Delta\underline{\delta}_M^i \quad\quad\quad\quad (4\text{-}42)$$

Inserting $\underline{PM}^i$ from (4-40) in vector form and $\underline{PG}^k(1)$ from (4-42) into (4-38), the term $\Delta\underline{PG}(0)$ is then eliminated from both sides of equation (4-38) to obtain in vector form:

$$\underline{T}\Delta\underline{\delta}_M^i = - \left\{ \underline{I} - \begin{bmatrix} \dfrac{M_1}{M_0} & \dfrac{M_1}{M_0} & . & . & \dfrac{M_1}{M_0} \\ \dfrac{M_2}{M_0} & \dfrac{M_2}{M_0} & . & . & \dfrac{M_2}{M_0} \\ . & & & & \\ . & & & & \\ \dfrac{M_N}{M_0} & . & . & . & . & \dfrac{M_N}{M_o} \end{bmatrix} \right\} \Delta\underline{PM}^i \qquad (4-43)$$

where $\displaystyle\sum_{j=1}^{N} M_j = M_0$. Multiplying both sides of equation (4-43) from the left by $\underline{M}$, where:

$$\underline{M} = \begin{bmatrix} \dfrac{1}{M_1} & & & & -\dfrac{1}{M_N} \\ & . & & & . \\ & & . & & . \\ & & & \dfrac{1}{M_{N-1}} & -\dfrac{1}{M_N} \end{bmatrix}$$

and noting that:

$$\begin{bmatrix} \dfrac{1}{M_1} & & & & -\dfrac{1}{M_N} \\ & . & & & . \\ & & . & & . \\ & & & \dfrac{1}{M_{N-1}} & -\dfrac{1}{M_N} \end{bmatrix} \begin{bmatrix} \dfrac{M_1}{M_0} & \dfrac{M_1}{M_0} & . & . & \dfrac{M_1}{M_0} \\ \dfrac{M_2}{M_0} & . & . & . & . & \dfrac{M_2}{M_0} \\ . & & . & & & \\ \dfrac{M_N}{M_0} & . & . & . & . & \dfrac{M_N}{M_0} \end{bmatrix} = \underline{0}$$

then (4-43) may be written as:

$$-\underline{M} \; \Delta \underline{PM}^i = \underline{MT} \; \Delta \underline{\delta}^i_M$$

Thus, the inertial angle changes for loss of generation i and generator buses are:

$$\Delta \underline{\delta}^i_M = -[\underline{MT}]^{-1} \; \underline{M} \; \Delta \underline{PM}^i \tag{4-44}$$

where $\Delta \underline{PM}^i$ is a N dimensional column vector whose pth entry is defined by:

$$\{\Delta PM^k\}_p = \begin{cases} 0 & p \neq i \\ \Delta PM_p & p = i \end{cases} , \quad i,p = 1,2,\ldots,N \tag{4-45}$$

The inertial angles for loss of generation i for base case angle $\underline{\delta}_0$ are:

$$\underline{\delta}^i_M = \underline{\delta}_0 + \Delta \underline{\delta}^i_M \tag{4-46}$$

Defining:

$$\underline{W}^i_M = \underline{\delta}^i_M \; \dot{\underline{\delta}}^i_M \tag{4-47}$$

the inertial line security measure may be expressed as:

$$S^i_M(k,\ell) = [\underline{e}^T_{k\ell} \; \underline{W}^i_M \; \underline{e}_{k\ell}] \tag{4-48}$$

Then the security for all possible loss of generation contingencies is given by:

$$S_M^i(k,\ell) = \underline{e}_{k\ell}^T \ \underline{W}_M \ \underline{e}_{k\ell} \tag{4-49}$$

where $\underline{e}_{k\ell}$ is defined by (4-18), and:

$$W_M = \sum_{i=1}^{N} W^i = \sum_{i=1}^{N} \underline{\delta}_M^i \ \underline{\delta}_M^{iT} \tag{4-50}$$

Using (4-44), $\underline{W}_M$ can be written as:

$$W_M = \sum_{i=1}^{N} [(\underline{MT})^{-1}\underline{M}] \ [\Delta\underline{PM}^i \ \Delta\underline{PM}^{iT}] \ [(\underline{MT})^{-1}\underline{M}]^T$$

$$+ \sum_{i=1}^{N} 2 \ (\underline{MT})^{-1}\underline{M} \ \Delta\underline{PM}^i \ \underline{\delta}_0^T + N\underline{\delta}_0\underline{\delta}_0^T \tag{4-51}$$

Assuming $\delta_0 \simeq 0$, the expression for $\underline{W}_M$ becomes:

$$W_M = [(MT)^{-1}M] \ \sum_{i=1}^{N} [\Delta\underline{PM} \ \Delta\underline{PM}^T] \ [(MT)^{-1}M]^T \tag{4-52}$$

where:

$$\sum_{i=1}^{N} [\ \underline{PM}^i \ \ \underline{PM}^{iT}] = \begin{bmatrix} \Delta PM_1^2 & & & & \\ & \Delta PM_2^2 & & & \\ & & \cdot & & \\ & & & \cdot & \\ & & & & \Delta PM_N^2 \end{bmatrix} \tag{4-53}$$

The matrix $\underline{W}_M$ is identical to the expression $\hat{\underline{S}}_x$ for the r.m.s. coherency measures if:

$$\sum_{i=1}^{N} \Delta \underline{PM}^i \, \Delta \underline{PM}^{iT} = \underline{R}_{11} + \underline{m}_1 \underline{m}_1^T \tag{4-54}$$

which requires the statistic of disturbance to be represented as a summation of N deterministic disturbances.

Now, assume the loss of generation such that:

$$\frac{\Delta PM_i}{M_i} = C \tag{4-55}$$

where C is a constant, and substitute for ΔPM_i from (4-55) into (4-53), then the expression (4-52) may be written as:

$$W_M = [(\underline{MT})^{-1} \underline{M}] \begin{bmatrix} c^2 M_1^2 & & & & \\ & c^2 M_2^2 & & & \\ & & \cdot & & \\ & & & \cdot & \\ & & & & c^2 M_N^2 \end{bmatrix} [(\underline{MT})^{-1} \underline{M}]^T$$

$$= c^2 (\underline{MT})^{-1} \underline{K} (\underline{MT})^{-T} \tag{4-56}$$

where
$$\{\underline{K}\}_{ij} = \begin{cases} 2 \text{ for } i = j \\ 1 \text{ for } i \neq j \end{cases} \tag{4-57}$$

Equation (4-56) shows that the contingency independent line security measure depends only on the matrix $[\underline{MT}]^{-1}$ (inertially weighted synchronizing torque coefficients) which determines the modal and coherent structure of the

power system. It is clear that the contingency independent security measure can be computed with the probabilistic disturbance (4-29). Using this disturbance, all the boundaries between generation groups for inertial distribution of every loss of generation contingency are equally tested, and modal and coherent properties of the systems are captured by the security measure. A grouping and ranking algorithm, which is described in the next section, can identify the weakest boundary when it uses the security measures produced by this probabilistic disturbance. The next section also discusses the strict synchronizing loss of controllability condition, strict geometric coherency condition, and strict strong linear decoupling condition, and then shows the (CILSM) and boundary identification procedure only detects the strict synchronizing loss of controllability conditions.

4.2. Transmission Boundary Vulnerability Justifications Based on Loss of Controllability Conditions for the Classical Transient Stability Model and the Inertial Security Measure.

The present literature has defined [27, 18] different conditions for which a group of generators behave as a single generator after specific disturbances.

These conditions are based on controllability and obesrvability properties of the transient stability model (4-8)-(4-10) of the systems. The conditions, if satisfied, have been shown [18] to cause coherency [26] and modal [28]

analysis dynamic equivalents to be identical and also [18]
to cause decoupling of fast and slow eigenvalues of the
systems. These conditions are now given.

4.2.1. Observability and Controllability Conditions

To discuss the controllability and observability con-
ditions requires a linearized model of the power system.
The power system model used is a modified version of the
linear model (4-8). This model is divided into an external
and internal system and is expressed in second order form
as:

$$
\begin{bmatrix} \Delta\ddot{\delta}_m \\ \hline \Delta\ddot{\delta}_{n-1} \end{bmatrix}
=
\begin{bmatrix} (-\underline{MT})_{11} & (-\underline{MT})_{12} \\ \hline (-\underline{MT})_{21} & (-\underline{MT})_{22} \end{bmatrix}
\begin{bmatrix} \Delta\delta_m \\ \hline \Delta\delta_{n-1} \end{bmatrix}
-
\begin{bmatrix} \sigma I_m & \underline{0} \\ \hline 0 & \sigma I_{n-1} \end{bmatrix}
\begin{bmatrix} \Delta\dot{\delta}_m \\ \hline \Delta\dot{\delta}_{n-1} \end{bmatrix}
+
$$

$$
\begin{bmatrix} \underline{M}_1 & (\underline{ML})_1 \\ \hline \underline{M}_2 & (\underline{ML})_2 \end{bmatrix}
\begin{bmatrix} \Delta PM \\ \hline \Delta PL \end{bmatrix}
\qquad
\begin{array}{l} (4\text{-}58a) \\ (4\text{-}58b) \end{array}
$$

where:

δ_{n_i} , i = 1,2,...,n, are the internal generator angles of
the external group.

δ_{m_k} , k = 1,2,...,m, are the internal generator angles of
the m generators of the internal group.

$$
\begin{bmatrix} \underline{M}_{11} & \vdots & \underline{M}_{12} \\ \cdots & \cdots & \cdots \\ \underline{0} & \vdots & \underline{M}_{22} \end{bmatrix} =
\left[
\begin{array}{cccc:cccc}
\frac{1}{M_1} & & & & & & & -\frac{1}{M_N} \\
& \frac{1}{M_2} & & & & & & -\frac{1}{M_N} \\
& & \ddots & & & & & -\frac{1}{M_N} \\
& & & & & & & \ddots \\
& & & \frac{1}{M_m} & & & & \\
\hdashline
& & & & \frac{1}{M_{m+1}} & & & \\
& & \underline{0} & & & \ddots & & \\
& & & & & & & \\
& & & & & & \frac{1}{M_{m+n-1}} & -\frac{1}{M_N}
\end{array}
\right]
$$

$$(4\text{-}59)$$

$$
\underline{L} = \begin{bmatrix} \underline{L}_{11} & \underline{L}_{22} \\ \hdashline \underline{L}_{21} & \underline{L}_{22} \end{bmatrix} = -\frac{\partial PG}{\partial \hat{\underline{\theta}}} \left[\frac{\partial PL}{\partial \hat{\underline{\theta}}} \right]^{-1} \qquad (4\text{-}60)
$$

where:

$\underline{I}_m$ and $\underline{I}_{n-1}$ are identity matrices of dimensions m and n-1, respectively.

$\underline{T}$ = N x N-1 matrix of synchronizing power coefficients.

$\underline{M}_1 = [\underline{M}_{11}\underline{M}_{12}]$ is a m x N and consists of the first m rows of $\underline{M}$.

$(\underline{ML})_1 = [\underline{M}_{11}\underline{L}_{11} + \underline{M}_{12}\underline{L}_{12} \ \ \underline{M}_{11}\underline{L}_{12} + \underline{M}_{12}\underline{L}_{22}]$ is m x K and consists of the first rows of $\underline{ML}$.

$(\underline{ML})_2 = [\underline{M}_{22}\underline{L}_{21} \ \underline{M}_{22}\underline{L}_{22}]$ is n-1 x K and consists of the last

n-1 = N-m-1 rows of $\underline{ML}$.

At present, there are five conditions based on controllability and observability concepts. Any of these conditions has been shown [18] to represent modal and coherent properties, and these conditions, if satisfied, have produced identical modal and coherent equivalents. Two of the conditions only hold for the linearized transient stability model (4-58) and are observability conditions. Thus, the three remaining conditions that are applicable to both linear and nonlinear models and are controllability conditions are presented here.

(1) Strict synchornizing coherency (SSC) which requires that there exist (n-1) stiff equivalent lines connecting internal generator buses and that these (n-1) lines form a tree for each n generator coherent group. These (n-1) equivalent lines are very stiff compared to the inertias in the group and cause a decoupling of the eigenvalues that describe oscillation of generators against each other within coherent groups and those eigenvalues that describe the oscillation of one group against another. The eigenvalue association with oscillations within coherent groups would have large imaginary parts compared to the eigenvalues that describe group against group behavior. SSC causes $(-\underline{MT})_{22}^{-1} \rightarrow \underline{0}$ in the limit as the interconnections between generators are progressively stiffened

compared to their inertias. This type of condition
has been shown [18] to be detected by the r.m.s.
coherency measure evaluated for the modal probabilis-
tic disturbance (4-55, 4-29) or by singular perturba-
tion methods described in [29].

(2) Strict geometric coherency (SGC) which requires that
the ratio of synchronizing torque coefficient of
equivalent lines connecting the disturbed bus and an
internal generator bus over the inertia of that gen-
erator to be identical for all generators in the
coherent group. This property causes uniform acceler-
ation of the group over several seconds before gover-
nor control takes over. SGC depends on the connection
to the group and not the connections between members
of the group as does SSC. SGC causes $(-\underline{MT})_{21} = 0$.

(3) Strict strong linear decoupling (SSLD) which is a
group formed by a combination of SSC and SGC which is
different than either of these properties alone. A
portion of the group satisfying SSLD will satisfy SSC,
but the synchronizing torque coefficients of the lines
connected to all members of the group must cause uni-
form acceleration in the group. This property holds
in the nonlinear model since SGC and SSC hold in the
nonlinear models, but the condition was derived based
on the linear model and thus its name. SSLD causes
$(\underline{MT})_{22}^{-1} (\underline{MT})_{21} \rightarrow 0$.

In the next subsection, the SSC loss of controllability condition is discussed in more detail, and it is shown that SSC causes the submatrix $(\underline{MT})_{22}^{-1}$ to go to zero in the limit. This results in a decoupling of the equations for the external group from the equations for the internal systems and that this decoupling is detected in the contingency independent security measure (4-51).

4.2.3. SSC Loss of Controllability Condition

The definition given below for strict synchronizing coherency is:

> A specified group of n-generators within a power system exhibits strict synchronizing coherency if there is at least one infinitely still connection joining each generator of the group (for a minimum total of n-1). [18]

If the SSC condition holds for a group of n generators, this group can be replaced by a single equivalent generator, and the response of the remainder of the system to a disturbance outside the group of n generators is preserved. The proof for this claim is now given. Consider a group of n generators within a power system and let y_{ij} be the admittance between generators i and j of the group. Suppose $y_{ij} \to \infty$, then the voltage magnitude and phase angle must be the same at buses i and j or otherwise there will be an infinite flow of power between the two buses. Thus, generators i, j can be replaced by a single composite generator of inertia $M_i + M_j$ as long as the power flow from the combined generator to the rest of the system is preserved.

Next, let $y_{i+j,k}$ be the admittance between the composite generator and the generator k of the group, and let $y_{i+j,k} \rightarrow \infty$. By repeating the argument above, generator k and the composite of generators i and j can be replaced by a new composite of inertia $M_i + M_j + M_k$. Continuing from n-1 steps produces a single generator equivalent for the original group of n generators. This simply means that the internal behavior of the group of n generators is not controllable by disturbances inside or outside this group. The group formed by SSC conditions is thus called a strongly bound coherent group. Any generator connected to a strongly bound coherent group, but not part of it, has relatively weak connection with the group or otherwise it should be a member of the group.

It is now shown for the model (4-21) that when there are n-1 stiff connections between n generators of external groups (SSC holds), the submatrix $-(MT)_{22}^{-1} \rightarrow 0$ in the limit as the interconnections between generators are progressively stiffened.

Suppose that the conditions for SSC are satisfied and that $(-\underline{MT})_{22}^{-1}$ exists. The inverse of $(-\underline{MT})_{22}$ can be written:

$$-(\underline{MT})^{-1}_{22} = \frac{1}{\text{Det}(-\underline{MT})_{22}} \begin{bmatrix} C_{11} & C_{12} & C_{13} & \cdot & \cdot & C_{1n} \\ C_{21} & C_{22} & \cdot & \cdot & \cdot & C_{2n} \\ \cdot & & & & & \\ \cdot & & & & & \\ C_{n1} & C_{n2} & \cdot & \cdot & \cdot & C_{nn} \end{bmatrix} \qquad (4\text{-}61)$$

where C_{ij} is the ijth cofactor of $(-\underline{MT})_{22}$.

Assume that n-1 of the interconnections that link all n generators of the external group are made infinitely stiff. In the linear model, the corresponding n-1 elements of $(-\underline{MT})_{22}$ become infinitely large. Now $(-MT)_{22}$ is (n-1) x (n-1) so that Det $(-MT)_{22}$ is the summation of (n-1) terms where each term is the product of (n-1) elements of $(-MT)_{22}$ One of these terms is the product of all n-1 elements that are being allowed to become infinitely large. Now each cofactor C_{ij} is, in turn, the summation of (n-1)! terms where each term is the product of (n-2) elements of $(-\underline{MT})_{22}$. Thus, each cofactor C_{ij} can be the product of no more than n-2 of the elements that are becoming infinitely large. As a result, Det$(-\underline{MT})_{22}$ dominates every term in the summation of C_{ij}, i,j=1,2,...,n-1. Thus in the limit, all terms of $(-\underline{MT})^{-1}_{22}$ tend to be zero.

Now assume that $(-MT)_{22}$ is finite and rewrite equation (4-58b) as:

$$(-\underline{MT})_{22}^{-1} \ \Delta\ddot{\underline{\delta}}_{n-1} = -(\underline{MT})_{22}^{-1} \ (-\underline{MT})_{21}\Delta\underline{\delta}_m + \Delta\underline{\delta}_{n-1}$$

$$-\sigma(MT)_{22}^{-1} \ \Delta\underline{\delta}_{n-1} + (-\underline{MT})_{22}^{-1} \ [\underline{M}_2 \ \Delta\underline{PM} + (\underline{ML})_2 \ \Delta\underline{PL}]$$

Letting n-1 elements of $(-MT)_{22}$ become infinitely large results in:

$$\Delta\underline{\delta}_{n-1} = 0 \text{ for all } t > 0 \tag{4-62}$$

This result in turn reduces equation (4-58a) to the form:

$$\Delta\ddot{\underline{\delta}}_m = -(MT)_{11} \ \Delta\underline{\delta}_m - \sigma\Delta\dot{\underline{\delta}}_m + [\underline{M}_1 \ \Delta\underline{PM} + (\underline{ML})_1 \ \Delta\underline{PL}] \tag{4-63}$$

Thus, assuming zero initial conditions, the external groups of n generators behave, from the point of view of the remainder of the system, like a single equivalent generator.

The contingency independent security measure (4-56) will now be shown to depend on submatrix $(\underline{MT})_{22}^{-1}$ of the strongly bound generators of the external system. This security measure detects the SSC loss of controllability of external systems and can be used to capture all the strongly bound groups in the power system model which have weak boundaries.

Assume, as in (4-58), a power system with N = m+n generators, where n is the number of generators in the external system and m is the number of internal generators. Partition matrices $(\underline{MT})$ and $\underline{K}$.

$$[\underline{MT}] = \begin{bmatrix} (\underline{MT})_{11} & (\underline{MT})_{12} \\ (\underline{MT})_{21} & (\underline{MT})_{22} \end{bmatrix}$$

$$\underline{K} = \begin{bmatrix} \underline{K}_{11} & \underline{K}_{12} \\ \underline{K}_{21} & \underline{K}_{22} \end{bmatrix}$$

where $\underline{K}$ is defined by (4-56).

Assuming $(\underline{MT})_{11}$ and $(\underline{MT})_{22}$ are nonsingular, the inverse of $(\underline{MT})$ can be written as:

$$[\underline{MT}]^{-1} = \begin{bmatrix} \underline{Q}^{-1} & -(\underline{MT})_{11}^{-1}(\underline{MT})_{12}\underline{P}^{-1} \\ -(\underline{MT})_{22}^{-1}(\underline{MT})_{21}\underline{Q}^{-1} & \underline{P}^{-1} \end{bmatrix}$$

where:

$$\underline{Q} = (\underline{MT})_{11} - (\underline{MT})_{12}(\underline{MT})_{22}^{-1}(\underline{MT})_{21}$$

$$\underline{P} = (\underline{MT})_{22} - (\underline{MT})_{21}(\underline{MT})_{11}^{-1}(\underline{MT})_{12}$$

Then the security measure (4-56) $\underline{W}_M$ can be written:

$$\underline{W}_M = c^2 [\underline{MT}]^{-1} \underline{K} [\underline{MT}]^{-T}$$

$$= c^2 \begin{bmatrix} \underline{Q}^{-1} & -(\underline{MT})_{11}^{-1}(\underline{MT})_{12}P^{-1} \\ -(\underline{MT})_{22}^{-1}(\underline{MT})_{21}Q^{-1} & \underline{P}^{-1} \end{bmatrix} \begin{bmatrix} \underline{K}_{11} & \underline{K}_{12} \\ \underline{K}_{21} & K_{22} \end{bmatrix}$$

$$\times \begin{bmatrix} \underline{Q}^{-T} & -Q^{-T}(\underline{MT})_{21}(\underline{MT})_{22}^{-T} \\ -\underline{P}^{-T}(\underline{MT})_{12}^{T}(\underline{MT})_{11}^{-T} & \underline{P}^{-T} \end{bmatrix}$$

$$= \begin{bmatrix} \underline{W}_{M_{11}} & \underline{W}_{M_{12}} \\ \underline{W}_{M_{21}} & \underline{W}_{22} \end{bmatrix}$$

where:

$$\underline{W}_{M_{11}} = \underline{Q}^{-1}\underline{K}_{11}\underline{Q}^{-T} - \underline{Q}^{-1}\underline{K}_{12}\underline{P}^{-T}(\underline{MT})_{12}(\underline{MT})_{11}^{-T} - [(\underline{MT})_{11}^{-1}(\underline{MT})_{12}$$
$$\underline{P}^{-1}\underline{K}_{21}\underline{Q}^{-T}] + (\underline{MT})_{11}^{-1}(MT)_{12}P^{-1}K_{22}P^{-T}(\underline{MT})_{12}^{T}(MT)_{11}^{-T}$$

$$\underline{W}_{M_{12}} = \underline{Q}^{-1}\underline{K}_{11}\underline{Q}^{-T}(\underline{MT})_{21}{}^{T}(\underline{MT})_{22}^{-T} + \underline{Q}^{-1}\underline{K}_{12}\underline{P}^{-T} + [(\underline{MT})_{11}^{-1}(\underline{MT})_{12}$$
$$\underline{P}^{-1}\underline{K}_{21}Q^{-T}(\underline{MT})^{T}(\underline{MT})_{22}^{-T}] - (\underline{MT})_{11}^{-1}(\underline{MT})_{12}\underline{P}^{-1}(\underline{K})_{22}P^{-T}$$

$$\underline{W}_{M_{21}} = (\underline{MT})_{22}^{-1}(\underline{MT})_{21}\underline{Q}^{-1}\underline{K}_{11}\underline{Q}^{-T} + [(\underline{MT})_{22}^{-1}(\underline{MT})_{21}\underline{Q}^{-1}\underline{K}_{12}\underline{P}^{-T}(\underline{MT})_{12}^{T}$$
$$(\underline{MT})_{11}^{-T} + \underline{P}^{-1}\underline{K}_{21}\underline{Q}^{-T}] - \underline{P}^{-1}\underline{K}_{22}\underline{P}^{-T}(\underline{MT})_{12}^{T}(\underline{MT})_{11}^{-T}$$

$$\underline{W}_{M_{22}} = (\underline{MT})_{22}^{-1}(\underline{MT})_{21}\underline{Q}^{-1}\underline{K}_{11}\underline{Q}^{-T}(\underline{MT})_{21}^{T}(\underline{MT})_{21}^{-T} + \underline{P}^{-1}\underline{K}_{22}\underline{P}^{-T}$$
$$- (\underline{MT})_{22}^{-1}(\underline{MT})_{21}\underline{Q}^{-1}\underline{K}_{12}\underline{P}^{-T} - \underline{P}^{-1}\underline{K}_{21}\underline{Q}^{-T}(\underline{MT})_{21}^{T}(\underline{MT})_{22}^{-T}$$

The submatrix $\underline{W}_{M22}$ contains the information on the behavior of the n generators of the external group. In the linear model, either condition of strict synchronizing coherency (SSC), $[\underline{MT}]_{22}^{-1} \to \underline{0}$; strict geometric coherency,

$[MT]_{21} = 0$; or strict strong linear decoupling, $[\underline{MT}]_{22}^{-1}[\underline{MT}]_{21} \to 0$ will make:

$$\underline{W}_{M_{22}} = \underline{P}^{-1}\underline{K}_{22}\underline{P}^{-T}$$

Applying the matrix identity on $\underline{P}$, $\underline{P}^{-1}$ can be written:

$$\underline{P}^{-1} = (\underline{MT})_{22}^{-1} + (\underline{MT})_{22}^{-1}(\underline{MT})_{21} \left[(\underline{MT})_{11} - (\underline{MT})_{12}(\underline{MT})_{22}^{-1}\right.$$
$$\left.(\underline{MT})_{21}\right]^{-1}(MT)_{12}(MT)_{22}^{-1}$$

Thus:

$$\underline{P}^{-1} \to \underline{0}$$

$$\underline{W}_{M_{22}} \to \underline{0}$$

if and only if $[MT]_{22}^{-1} \to 0$ given $\underline{K}_{22}$ is positive definite so that $W_{M_{22}}$ only depends on the structure of the strongly bound external group of n generators for a disturbance either in the internal group or within the external group. This is a loss of controllability condition which is detected by the security measure.

The next subsection introduces a boundary identification procedure based on a commutative grouping algorithm. The commutative rule requires that the groups formed have at least n-1 stiff connection in a n generator group.

4.2.4. Grouping Algorithm

The grouping method is based on the cummutative rule [17]. This rule for forming a group requires that a group

is formed if all the generators are coherent with respect to each other; that is, if the group G_1 is a group containing generators A and B, then generator C is added to this group if and only if generator C is coherent with A, and C is coherent with B. This method has been used [17, 18] for clustering generators in coherent groups for producing dynamic equivalents of the system for transient stability studies.

The values of the security measures are ranked from smallest to the largest forming a ranking table; then the groups are formed based on the following algorithm:

(a) Form the first group (a pair) from the smallest security measure at rank 1, r=1.

(b) Decide which of the following possibilities apply to generator k,ℓ at the rank r=r+1.

(c) If r=Nx(N-1)/2, stop. N = number of generators

   (i) If neither k nor ℓ has been previously identified as belonging to a group, then this pair becomes a new group.

   (ii) If generator k(ℓ) belongs to a group but generator ℓ(k) does not, then:

      (1) if ℓ(k) has been previously recognized as coherent with all members of the group to which k(ℓ) belongs except for k(ℓ), then add ℓ(k) to the group containing k(ℓ).

      (2) if ℓ(k) has not been found previously to be coherent with all other members of the

group to which k(ℓ) belongs, then recognize that k and ℓ are coherent but do not add ℓ(k) to the coherent group containing k(ℓ). Return to (b).

(iii) If generators k and ℓ belong to different groups, then:

(1) if all possible generator pairs which can be selected from the members of the two groups except k and ℓ have been previously recognized as being coherent, then merge the two groups to form a single group containing all members of the separate group.

(2) if at least one pair of generators which can be selected from the two groups other than k and ℓ has not yet been recognized as a coherent pair but do not merge the groups. Return to (b).

The algorithm continues the procedure to the bottom of the ranking table, and when every generator pair is checked, it terminates. As one proceeds down the ranking table, individual generators are included to groups and later groups are merged to form larger groups. As groups are merged, the boundaries between groups should be continuously weaker since a coherency measure between generator pairs indicates stiff connection of the generators compared to the inertia of the generators, and the security measures

are ranked from the smallest to the largest in this ranking table. Thus, the boundaries may be ranked from the weakest to strongest based on the reverse order of the group formation; that is, the last two groups to be lumped into a single group have the weakest boundary between them, and the second weakest belongs to the second to last group aggregated, etc.

The commutative grouping rules assure that all the generators in a group formed have stiff connection by requiring a generator to join the group if and only if it is coherent with all the generators in the group, and groups are merged if and only if all the generators in group one are coherent with every generator in group two. This ensures at least n-1 stiff connections between generators in an n generator group.

Now to sum up the procedure for identifying vulnerable boundaries, the following steps are given:

(1) Compute the security measure $S_M(k,\ell)$ for all generator bus pairs.

(2) Rank the security measures from smallest to largest and form a ranking table.

(3) Form groups by the commutative grouping rules and set a group formation table.

(4) Rank the boundaries from the weakest to the strongest based on the reverse order in the group formation table.

4.2.5. Identifying Vulnerable Boundaries by the Security Measure and Grouping Procedure.

It was discussed in Chapter 2 that inertial load flow effects all the generators in the interconnection and therefore is a global phenomenon. The strict synchronizing coherency (SSC) indicates the vulnerable boundaries in the inertial load flow model independent of the location of a contingency and thus identifies vulnerable boundaries in the model in a global manner.

The contingency independent security measure defined in (4-20) and the boundary identification procedure described in subsection 4.2.3 can detect vulnerable boundaries for inertial load flow because of the following reasons:

i) $S_M(k,\ell)$ (4-34) is defined from $S_M^i(k,\ell)$ (4-32), which calculates the effect of inertial load flow for a single loss of generation on the boundaries and lines.

ii) Inertial distribution of a single loss of generation contingency significantly effects the boundary close to the contingency since the inertial flows would all flow through this boundary to cope with the lost generation. The summation of security measures for all possible losses of generation contingencies assures that every boundary is equally tested for inertial flow of all loss of generation contingencies; thus, the weakest among all boundaries is identified.

iii) The security measures are related to the r.m.s. coher-
ency measure. It was shown that the CISM is identical
to the r.m.s. coherency measure for the probabilistic
modal disturbance. This confirms that the security
measure can capture the coherent properties of the
system which causes groups of generators to swing
together and behave like a single generator.

iv) The SCC loss of controllability property that forms
strongly bound coherent groups is detected by the
security measure $S_M(k,\ell)$ summed over all loss of gen-
eration contingencies. Thus, the boundaries between
the strongly bound groups which have n-1 stiff inter-
connections in an n generator group are composed of
relatively weak interconnections for the inertia of
the group they connect, or otherwise the generators
they connect would be in the same strongly bound
group. These security measures would have large
values for generator pairs that belong to the differ-
ent groups but small values for generator pairs in the
same strongly bound group.

v) The commutative grouping rules require at least n-1
stiff interconnection in an n generator group. Hence,
the group formed by this method is a strongly bound
coherent group.

vi) The fast eigenvalues (high frequency) which represent
the stiff interconnection between generators [29] and
slow eigenvalues (low frequency) which represent less

stiff connections between generators are a property similar to SSC [18] that is detected by the security measure and grouping algorithm. The fast eigenvalues are associated with intermachine oscillations within strongly bound coherent groups, and the slow eigenvalues are associated with group against group oscillations.

4.3. <u>Governor State Model, Coherency Measure for Governor Response, Governor Security Measure, SSC Property for Governor Load Flow.</u>

This section develops a state model for governor response, a coherency measure to capture the behavior of coherent groups of generators, a governor security measure based on governor load flow results, and then discusses the SSC condition for governor load flow detected by both the coherency measure and governor security measure.

4.3.1. <u>Governor State Model</u>

To represent the state model of the system during the governor response, the algebraic equation for the power flows among the generator and load buses are the same as equation (4-2). The linear differential equations for the generators are:

$$\Delta \dot{\hat{\delta}}_i = \frac{1}{\beta_i}(\Delta PM_i - \Delta PG_i) - \frac{1}{\beta_N}(\Delta PM_N - \Delta PG_N) \qquad (4-64)$$

$$i = 1, 2, \ldots, N-1$$

where:

$$\Delta\hat{\delta}_i = \Delta\delta_i - \Delta\delta_N$$

$\Delta\delta_i$ is the rotor angel deviation of generator i

β_i is the frequency response characteristic of genera-
tor i

ΔPM_i is the change in mechanical input power at generator
i

ΔPG_i is the change in electrical output power at genera-
tor i

The $\Delta\underline{PG}$ in (4-5) is expressed in terms of $\Delta\underline{\hat{\delta}}$ and $\Delta\underline{PL}$
as:

$$\Delta\underline{PG} = \underline{T}\Delta\underline{\hat{\delta}} - \underline{L}\Delta\underline{PL} \qquad (4\text{-}65)$$

where $\underline{T}$ and $\underline{L}$ are defined by equations (4-6) and (4-7),
respectively.

A state model may be derived by writing the equations
in (4-64) in vector form and (4-65) to eliminate $\underline{PG}$ from
the expression. The state model follows as:

$$\Delta\underline{\dot{\hat{\delta}}} = [-\underline{\beta}\underline{T}]\,\Delta\underline{\hat{\delta}} + [\underline{\beta}][\Delta\underline{PM} + \underline{L}\Delta\underline{PL}] \qquad (4\text{-}66)$$

where:

$$\underline{\beta} = \begin{bmatrix} \frac{1}{\beta_1} & & & & & -\frac{1}{\beta_N} \\ & \frac{1}{\beta_2} & & & & -\frac{1}{\beta_N} \\ & & \cdot & & & \cdot \\ & & & \cdot & & \cdot \\ & & & & \frac{1}{\beta_{N-1}} & -\frac{1}{\beta_N} \end{bmatrix} \qquad (4\text{-}67)$$

$$\Delta\underline{\delta} = [\Delta\hat{\delta}_1, \Delta\hat{\delta}_2, \ldots, \Delta\hat{\delta}_{N-1}]^T$$

$$\Delta\underline{PM} = [\Delta PM_1, \Delta PM_2, \ldots, \Delta PM_N]^T$$

$$\Delta\underline{PL} = [\Delta PL_1, \Delta PL_2, \ldots, \Delta PL_K]^T$$

4.3.2. r.m.s. Coherency Measure for Governor Load Flow

The purpose of this subsection is to show that an r.m.s. coherency measure can be obtained for the linearized model of (4-66). This measure could be used to determine coherent groups of generators during the governor response for producing a dynamic equivalent of a power system.

For the linear model (4-66), the r.m.s. coherency measure $C_{k,\ell}$ between generator k, ℓ is defined as:

$$C_{k\ell} = [\frac{1}{T} E\{\int_0^T [\Delta\delta_k(t) - \Delta\delta_\ell(t)]^2 \, dt\}]^{1/2}$$

$$= [\frac{1}{T} E\{\int_0^T [(\Delta\delta_k(t) - \Delta\delta_N(t)) - (\Delta\delta_\ell(t) - \Delta\delta_N(t))]^2 \, dt\}]^{1/2}$$

$$= [\frac{1}{T} E\{\int_0^T [\Delta\hat{\delta}_k(t) - \Delta\hat{\delta}_\ell(t)]^2 dt]^{\frac{1}{2}}$$

$$= [\underline{e}_{k\ell}^T \underline{S}_x (T) \underline{e}_{k\ell}]^{\frac{1}{2}} \qquad (4\text{-}68)$$

where:

$$\underline{S}_x(t) = \frac{1}{T} \int_0^T E \{\Delta\underline{\hat{\delta}}(t) \quad \Delta\underline{\hat{\delta}}^T(t)\} dt \qquad (4\text{-}69)$$

and $\underline{e}_{k\ell}$ is defined in (4-18).

Let us assume disturbances in mechanical input power $\Delta\underline{PM}$, where:

$$E \{\Delta\underline{PM}\} = \underline{m}_1 \qquad (4\text{-}70)$$

and:

$$E \{(\Delta\underline{PM} - \underline{m}_1)(\Delta\underline{PM} - \underline{m}_1)^T\} = \underline{R}_{11} \qquad (4\text{-}71)$$

For the input $\Delta\underline{PM}$, $\Delta\underline{\hat{\delta}}(t)$ has the form:

$$\Delta\underline{\delta}(t) = e^{[-\underline{\beta T}]t}\Delta\underline{\delta}(0) + \int_0^t e^{[-\underline{\beta T}]v} \underline{\beta}\Delta\underline{PM} \, dv \qquad (4\text{-}72)$$

Substituting this expression for $\Delta\delta(t)$ in (4-69) and carrying out the expectation operation term by term and utilizing the assumption $\Delta\underline{\delta}(0)$ is zero leads to the expression:

$$\underline{S}_x(T) = \frac{1}{T} \int_0^T [\int_0^t e^{(-\underline{\beta T}]v} dv\underline{\beta}] [\underline{R}_{11} + \underline{m}_1\underline{m}_1^T]$$

$$[\int_0^t e^{[-\underline{\beta T}]v} dv\underline{\beta}]^T dt \qquad (4\text{-}73)$$

given:

$$\int_0^t e^{[-\underline{\beta T}]v} \, dv = [-\underline{\beta T}]^{-1} [e^{[-\underline{\beta T}]t} - \underline{I}] \tag{4-74}$$

and defining:

$$\underline{P} = \underline{\beta} \, [\underline{R}_{11} + \underline{m}_1 m_1]^T \, \underline{\beta}^T \tag{4-75}$$

expression (4-73) becomes:

$$S_x(T) = \frac{1}{T}[-\underline{\beta T}]^{-1} \int_0^T [e^{[-\underline{\beta T}]t} \underline{P} e^{[-\underline{\beta T}]^T t} - e^{[-\underline{\beta T}]t} \underline{P}$$

$$- \underline{P} e^{[-\underline{\beta T}]^T t} + \underline{P}] \, dt \, [-\underline{\beta T}]^{-1T} \tag{4-76}$$

Letting $T \to \infty$, the first three terms in the integral (4-76) vanish, that is:

$$\underline{S}_x(\infty) = [(\underline{\beta T})^{-1}\underline{\beta}] \, [\underline{R}_{11} + \underline{m}_1 \underline{m}_1^T] \, [(\underline{\beta T})^{-1}\underline{\beta}]^T$$

$$= [(\underline{\beta T})^{-1}] \, \underline{\beta} \, (\underline{R}_{11} + \underline{m}_1 \underline{m}_1^T] \, \underline{\beta}^T \, [(\underline{\beta T})^{-1}]^T \tag{4-77}$$

A disturbance:

$$\underline{\beta}(\underline{R}_{11} + \underline{m}_1 \underline{m}_1^T) \, \underline{\beta}^T = \underline{I} \tag{4-78}$$

causes the r.m.s. coherency measure:

$$\underline{S}_x(\infty) = [(\underline{\beta T})^{-1}][(\underline{\beta T})^{-1}]^T \tag{4-79}$$

to depend solely on system structure and is determined by governor frequency response characteristics and

synchronizing torque coefficients. Moreover, the coherent groups identified for aggregation using the coherency measure evaluated from (4-79) are determined by line stiffness weighted by the governor frequency response characteristic of generators at the end of each equivalent line. The disturbance which satisfies (4-78) has the statistics:

$$E \{\Delta \underline{PM}\} = \underline{m}_1 = 0 \tag{4-80}$$

$$E \{\Delta \underline{PM} \Delta \underline{PM}^T\} = DIAG \ (\beta_1^2, \beta_2^2, \ldots, \beta_{N-1}^2 \ , \ 0)$$

Another disturbance with:

$$\underline{m}_1 = 0 \ and \ \underline{R}_{11} = DIAG \ (\beta_1^2, \beta_2^2, \ldots, \beta_N^2) \tag{4-81}$$

results in:

$$\underline{B}(\underline{m}_1 \underline{m}_1^T + \underline{R}_{11})\underline{B}^T = \underline{K} \tag{4-82}$$

and:

$$\underline{S}_x(\infty) = [(\underline{B}\underline{T})^{-1}] \ \underline{K}[(\underline{B}\underline{T})^{-1}]^T \tag{4-83}$$

where:

$$\{K\}_{ij} = \begin{cases} 2 & i = j \\ 1 & i \neq j \end{cases}$$

This disburbance is over all the generators of the system and is reference independent.

4.3.3. Governor Time Frame Security Measure

The difference between distribution of power mismatch for inertial response and governor response of generating units requires the investigation of the significant effect and difference of governor load flow in contrast to inertial load flow on the transmission network and assessment of security and stability problems associated with this governor power flow.

Like the inertial security measures, the governor security measures are defined based on angles across the transmission lines at the governor time frame discussed in Chapter 2.

Governor response security measure for a single loss of generation is defined as:

$$S_{\beta}^{i}(k,\ell) = [\delta_{\beta}(k,i) - \delta_{\beta}(\ell,i)]^2 \qquad (4\text{-}84)$$

where $\delta_{\beta}(k,i)$ is the phase angle of governor load flow at bus k for a loss of generation contingency:

$$PM_{i} = PG_{i}(0) - \Delta PM_{i} \qquad (4\text{-}85)$$

where PM_{i} is the lost mechanical power into the generator i. The angle $\delta_{\beta}(k,i)$ for loss of generation i is obtained by inserting (4-85) into (2-12) to obtain $\{PG_{i}(2)\}_{i=1}^{N}$ which is in turn inserted into (2-9) or (2-10) to obtain $\delta_{\beta}(k,i)$.

Similar to inertial contingency independent security measure, the governor response contingency independent

security measure is defined as:

$$S_\beta(k,\ell) = \sum_i S_\beta^i(k,\ell) \qquad (4\text{-}86)$$

where i is summed over all possible loss of generation contingencies.

Now the linear relationship between the security measures and governor load flows is derived, and the governor security measure is then shown to be identical to the square of the governor coherency measure when the base case load flow condition is neglected.

After inertial distribution of mismatch power due to loss of generation contingency, governor frequency regulation begins to arrest the change in frequency. When the governor regulation is complete, frequency is constant throughout the interconnection, and the rate of change in frequency is arrested. It can be written:

$$\omega_i = \omega_0$$

where:

$$\omega_p = \frac{PM_p^i - PG_p(2)}{\beta_p} \qquad (4\text{-}87)$$

$$\omega_0 = \frac{\sum_j (PM_j^i - PG_j(9))}{\sum_j \beta_j} \qquad (4\text{-}88)$$

then:
$$\frac{PM_p^i}{\beta_p} - \frac{PG_p^i}{\beta_p} = \frac{\sum_j (PM_j^i - PG_j(0))}{\sum_j \beta_j} \qquad (4\text{-}89)$$

The above expression can be written as:

$$PG_p^i(2) = PM_p^i - \frac{\beta_p}{\sum_j \beta_j} \sum_j (PM_j^i - PG_j(0)) \tag{4-90}$$

where:

$PG_p^i(2)$ = the electrical power delivered to the network when governor frequency regulation is complete.

$$PM_p^i = PG_p(0) - \Delta PM_p^i \tag{4-91}$$

is mechanical power input at generator p after loss of generation ΔPM_p^i.

The electrical power delivered to the network after governor load flow response is related to the power delivered to the network before the loss of generation by the following equation:

$$\underline{PG}^i(2) = \underline{PG}(0) + \Delta \underline{PG}^i(2) \tag{4-92}$$

and from (4-5):

$$\Delta \underline{PG}^i(2) = \underline{T} \Delta \underline{\delta}_\beta^i \tag{4-93}$$

where:

$$\Delta \underline{\delta}_\beta^i = [\Delta \delta_{M,1}^i, \Delta \delta_{M,2}^i, \ldots, \Delta \delta_{M,N-1}^i]^T$$

are the derivation bus phase angles for governor load flow due to loss of generation $\{\Delta PM_p^i\}_{p=1}^N$.

Write the equation (4-90) in matrix form and substitute for $\underline{PG}^k(2)$ from (4-92) and (4-93) and represent:

$$\underline{PM}^i - \underline{PG}(0) - \Delta\underline{PM}^i$$

then the equation (4-90) becomes:

$$\underline{PG}(0)+\underline{T\Delta\delta}^i=\underline{PG}(0)-\Delta\underline{PM}^i+\begin{bmatrix} \dfrac{\beta_1}{\beta_0} & \dfrac{\beta_1}{\beta_0} & \cdot\cdot & \dfrac{\beta_1}{\beta_0} \\[2mm] \dfrac{\beta_2}{\beta_0} & \dfrac{\beta_2}{\beta_0} & \cdot\cdot & \dfrac{\beta_2}{\beta_0} \\[2mm] \cdot & \cdot & & \\ \cdot & \cdot & & \\ \dfrac{\beta_N}{\beta_0} & \dfrac{\beta_2}{\beta_0} & \cdot\cdot & \dfrac{\beta_N}{\beta_0} \end{bmatrix}\Delta\underline{PM}^i$$

Eliminating $\underline{PG}(0)$, the above equation becomes:

$$\underline{T\Delta\delta}_\beta^i = -\left\{ I - \frac{1}{\beta_0}\begin{bmatrix} \beta_1 & \beta_1 & \cdot\cdot & \beta_1 \\ \beta_2 & \beta_2 & \cdot\cdot & \beta_2 \\ \cdot & & & \cdot \\ \cdot & & & \cdot \\ \beta_N & \beta_N & \cdot\cdot & \beta_N \end{bmatrix}\right\}\Delta\underline{PM}^i \qquad (4\text{-}94)$$

Define:

$$
\underline{\beta} = \begin{bmatrix}
\frac{1}{\beta_1} & & & & & -\frac{1}{\beta_N} \\
& \frac{1}{\beta_2} & & & & \cdot \\
& & \cdot & & & \cdot \\
& & & \cdot & & \cdot \\
& & & & \frac{1}{\beta_{N-1}} & -\frac{1}{\beta_N}
\end{bmatrix}
\tag{4-95}
$$

and multiply both sides of (4-94) by $\underline{\beta}$:

$$\underline{\beta T} \Delta \underline{\delta}^i = -\underline{\beta} \Delta \underline{PM}^i$$

where:

$$
\begin{bmatrix}
\frac{1}{\beta_1} & & & & & -\frac{1}{\beta_N} \\
& \frac{1}{\beta_2} & & & & \cdot \\
& & \cdot & & & \cdot \\
& & & \cdot & & \cdot \\
& & & & \frac{1}{\beta_{N-1}} & -\frac{1}{\beta_N}
\end{bmatrix}
\begin{bmatrix}
\beta_1 & \cdot\cdot & \beta_1 \\
\beta_2 & \cdot\cdot & \beta_2 \\
\cdot & & \cdot \\
\cdot & & \cdot \\
\beta_N & \cdot\cdot & \beta_N
\end{bmatrix}
= \underline{0}
$$

Therefore, the vector $\Delta \underline{\delta}^i_\beta$ has the form:

$$\Delta \underline{\delta}^i = -[\underline{\beta T}]^{-1} \underline{\beta}\, \Delta \underline{PM}^i \tag{4-96}$$

where $\Delta \underline{PM}^i$ is defined by equation (4-44).

$\underline{\beta}$ coefficient matrix acts the same way as the coefficient matrix $\underline{M}$ in inertial load flow. To obtain the security measures, define:

$$\underline{W}_\beta^i = \underline{\delta}_\beta^i \underline{\delta}_\beta^{iT} \tag{4-97}$$

where $\underline{\delta}_\beta = \underline{\delta}_0 + \Delta\underline{\delta}_\beta^i$ is a vector of phase angles at buses for governor load flow, and $\underline{\delta}_0$ is an operating point before loss of generation. Hence:

$$S_\beta^i(k,\ell) = [\underline{e}_{k\ell}^T \underline{W}_\beta^i \underline{e}_{k\ell}] \tag{4-98}$$

where $\underline{e}_{k\ell}$ is defined by equation (4-18), and for all possible loss of generation contingencies:

$$S_\beta(k,\ell) = \underline{e}_{k\ell}^T \underline{W}_\beta \underline{e}_{k\ell} \tag{4-99}$$

where:

$$\underline{W}_\beta = \sum_{i=1}^{N} W_\beta^i = \sum_{i=1}^{N} \underline{\delta}_\beta^i \underline{\delta}_\beta^{iT} \tag{4-100}$$

Using (4-96) and substituting for $\underline{\delta}_\beta$ into (4-100) leads to:

$$W_\beta = \sum_{i=1}^{N} [(\underline{\beta T})^{-1}\underline{\beta}][\Delta\underline{PM}^i \Delta PM^{iT}][(\underline{\beta T})^{-1}\underline{\beta}]^T$$

$$+ \sum_{i=1}^{N} 2[(\underline{\beta T})^{-1}\underline{\beta}] \Delta\underline{PM}^i \underline{\delta}_0^T + N\underline{\delta}_0\underline{\delta}_0^T \tag{4-101}$$

Assuming $\underline{\delta}_0 = \underline{0}$, $\underline{W}_\beta$ may be written as:

$$\underline{W}_\beta = [(\underline{\beta T})^{-1}\underline{\beta}][\sum_{i=1}^{N}\Delta\underline{PM}^i\Delta\underline{PM}^{iT}][(\underline{\beta T})^{-1}\underline{\beta}]^T \tag{4-102}$$

which has the same form as $\underline{S}_x(\infty)$ for the r.m.s. coherency measure for governor load flow.

$\sum_{i=1}^{N}\underline{PM}^i\ \underline{PM}^{iT}$ is the summation of a single loss of generation contingency and can be written as:

$$\sum_{i=1}^{N}\Delta\underline{PM}^i\Delta\underline{PM}^{iT} = \begin{bmatrix} \Delta PM_1^2 & & & & \\ & \Delta PM_2^2 & & & \\ & & \cdot & & \\ & & & \cdot & \\ & & & & \Delta PM_N^2 \end{bmatrix} \tag{4-103}$$

This disturbance can be presented by a probabilistic disturbance with the covariance equal to (4-103). With a disturbance proportional to β_i for each generator, (4-102) can now be expressed as:

$$W_\beta = [(\underline{\beta T})^{-1}\underline{\beta}] \begin{bmatrix} \beta_1^2 & & & & \\ & \beta_2^2 & & & \\ & & \cdot & & \\ & & & \cdot & \\ & & & & \beta_N^2 \end{bmatrix} [(\underline{\beta T})^{-1}\underline{\beta}]^T \tag{4-104}$$

Rearranging the β and β^T and carrying out the multiplication:

$$W_\beta = [(\underline{\beta T})^{-1}] \; \underline{K} \; [(\underline{\beta T})^{-1}]^T \qquad\qquad (4\text{-}105)$$

which is identical to the $S_x(\infty)$ for the r.m.s. coherency measure given by equation (4-83). Thus, the security measure evaluated when $\underline{\delta}_0 = \underline{0}$ is the square of the r.m.s. coherency measure.

The security measure with the disturbance described above depends on synchronizing torque coefficients weighted by the governor frequency characteristic of the generators. This disturbance equally tests all the boundaries between generation groups for the governor distribution of power mismatch due to every single loss of generation contingency since β_i is proportional to the capacity of generator i. The governor security measure (4-99) with the boundary identification procedure detects the cumulative effects of governor load flow on the boundaries, and the weak boundaries for governor load flow loss of generation mismatch can be identified.

The justification of boundary detection by the security measures based on an SSC loss of controllability property for governor laod flow is given in the next subsection.

4.3.4. SSC Condition in Governor Load Flow.

The SSC loss of controllability condition, which was discussed for the classical transient stability model, is applicable for the linear model (4-66). It was shown that

governor coherency measure for a probabilistic disturbance depends only on matrix $(\underline{\beta}T)^{-1}$ which reflects the structure of the system when the generators of the power system respond based on their governor frequency characteristics.

The definition of SSC condition for governor response of generators is now given:

> If there is at least one stiff connection joining each generator compared to the governor frequency characteristic of generator in an n generator group, then this group of n generators exhibits SSC.

If SSC condition is satisfied for n generators of external systems, there results a decoupling of the equation of the external group from the remaining internal system due to the fact that submatrix $(\underline{\beta}T)^{-1}_{22}$, which represents the structure of the external group, goes to zero in the limit as the interconnection between n generators of the external group are progressively stiffened compared to their frequency response characteristic. This is now shown.

The linear model of (4-66) is divided into two groups as the internal system and the external system. Thus, the power system model (4-66) may now be written as:

$$\begin{bmatrix} \Delta\hat{\underline{\delta}}_1 \\ \Delta\hat{\delta}_2 \end{bmatrix} = \begin{bmatrix} (-\underline{\beta}T)_{11} & (-\underline{\beta}T)_{12} \\ (-\underline{\beta}T)_{21} & (-\underline{\beta}T)_{22} \end{bmatrix} \begin{bmatrix} \Delta\hat{\underline{\delta}}_1 \\ \Delta\hat{\underline{\delta}}_2 \end{bmatrix} \qquad (4\text{-}106a)$$

$$+ \begin{bmatrix} \underline{\beta}_{11} & \underline{\beta}_{12} \\ \underline{0} & \underline{\beta}_{22} \end{bmatrix} \begin{bmatrix} \Delta\underline{PM} + \underline{L}_{11}\Delta PL_1 \\ \Delta\underline{PM}_2 + \underline{L}_{22}\Delta PL_2 \end{bmatrix} \qquad (4\text{-}106b)$$

where $\Delta\hat{\underline{\delta}}_1 = [\Delta\hat{\delta}_1,\Delta\hat{\delta}_2,\ldots,\Delta\hat{\delta}_m]^T$ are the generator angles of the internal group, and $\Delta\hat{\underline{\delta}}_1 = [\Delta\hat{\delta}_{m+1},\Delta\hat{\delta}_{m+2},\ldots,\Delta\hat{\delta}_{m+n-1}]$ are the generator angles of the external group. The generator N in the external group is chosen as the reference genera- tor and:

$$
\begin{bmatrix} \underline{B}_{11} & \underline{B}_{12} \\ \underline{0} & \underline{B}_{22} \end{bmatrix} =
\begin{bmatrix}
\frac{1}{\beta_1} & & & & & & & -\frac{1}{\beta_N} \\
& \frac{1}{\beta_2} & & & & & & -\frac{1}{\beta_N} \\
& & \ddots & & & & & \\
& & & \ddots & & & & \vdots \\
& & & & \frac{1}{\beta_m} & & & \\
& & & & & \frac{1}{\beta_{n+1}} & & \\
& & & & & & \ddots & \vdots \\
& & & & & & \frac{1}{\beta_{m+n-1}} & -\frac{1}{\beta_N}
\end{bmatrix}
$$

where:

$N = m+n$

$\underline{L} = [\underline{L}_{11} , L_{22}] = -\dfrac{\partial \underline{PG}}{\partial\hat{\theta}} [\dfrac{\partial \underline{PL}}{\partial\hat{\theta}}]^{-1}$

$\Delta\underline{PL} = [\Delta\underline{PL}_1 , \Delta\underline{PL}_2]^T$

$\Delta\underline{PM} = [\Delta\underline{PM}_1 , \Delta\underline{PM}_2]^T$

It is assumed $(-\underline{BT})^{-1}_{22}$ exists and there are $(n-1)$ stiff interconnections between n generators of the external system. Then $(-\underline{BT})^{-1}_{22} \rightarrow 0$ in the limit for the governor load flow if $(n-1)$ equivalent lines between n

generators are progressively stiffened compared to the governor frequency characteristic of generators. The proof is as simple as before for inertial load flow given in section 4.2.3. The proof argues that the cofactors of matrix $(-\underline{\beta T})_{22}$ are small, compared to the Det $(-\underline{\beta T})_{22}$ which causes the $(-\underline{\beta T})_{22}^{-1}$ to go to zero.

Equation (4-106b) can be written as:

$$(-\underline{\beta T})_{22}^{-1} \Delta\hat{\underline{\delta}}_2 = (\underline{\beta T})_{22}^{-1}(\underline{\beta T})_{21}\Delta\hat{\underline{\delta}}_1 + \Delta\hat{\underline{\delta}}_2$$

$$+ (-\beta T)_{22}^{-1}\underline{\beta}_{22}[\Delta\underline{PM}_2 + L_{22} \Delta PL_2]$$

If SSC is satisfied for the external groups, then:

$$(-\beta T)_{22}^{-1} \to 0$$

and $\Delta\hat{\underline{\delta}}_2 = 0$ for all $t > 0$.

Thus, assuming zero initial conditions, the external group of n generators behaves, from the point of view of the rest of the system, as a single generator. Hence, this group can be replaced by a ficticious generator with capacity of the n generators it represents.

The SSC condition is captured by the contingency independent governor security measure (4-105). That is, if $(\underline{\beta T})_{22}^{-1}$ goes to zero, then the security measure (4-105) $\underline{W}_{\beta 22}$ also goes to zero. The proof is similar to the inertial load flow security measure given in 4.2.3 where $\underline{W}_\beta$ and $\underline{K}$ are partitioned and written as:

$$\underline{W}_\beta = \begin{bmatrix} \underline{W}_{\beta 11} & \underline{W}_{\beta 12} \\ \underline{W}_{\beta 21} & \underline{W}_{\beta 22} \end{bmatrix} \quad \text{and} \quad \underline{K} = \begin{bmatrix} \underline{K}_{11} & \underline{K}_{12} \\ \underline{K}_{21} & \underline{K}_{22} \end{bmatrix}$$

Then equation (4-105) can be written as:

$$\begin{bmatrix} \underline{W}_{\beta 11} & \underline{W}_{\beta 12} \\ \underline{W}_{\beta 21} & \underline{W}_{\beta 22} \end{bmatrix} = \begin{bmatrix} (\underline{\beta T})_{11} & (\underline{\beta T})_{12} \\ (\underline{\beta T})_{21} & (\underline{\beta T})_{22} \end{bmatrix}^{-1} \begin{bmatrix} \underline{K}_{11} & \underline{K}_{12} \\ \underline{K}_{21} & \underline{K}_{22} \end{bmatrix} \begin{bmatrix} (\underline{\beta T})_{11} & (\underline{\beta T})_{12} \\ (\underline{\beta T})_{21} & (\underline{\beta T})_{22} \end{bmatrix}^{-T}$$

in a manner similar to subsection 4.2.3. $\underline{W}_{\beta 22}$ can be written as:

$$\underline{W}_{\beta 22} = (\underline{\beta T})_{22}^{-1}(\underline{\beta T})_{21}\underline{Q}^{-1}\underline{K}_{11}Q^{-T}(\underline{\beta T})_{21}^{T}(\underline{\beta T})_{22}^{-T} + \underline{P}^{-1}\underline{K}_{22}\underline{P}^{-T}$$

$$- (\underline{\beta T})_{22}^{-1}(\underline{\beta T})_{21}\underline{Q}^{-1}\underline{K}_{12}\underline{P}^{-T} - \underline{P}^{-1}\underline{K}_{21}\underline{Q}^{-T}(\underline{\beta T})_{21}^{T}(\underline{\beta T})_{22}^{-T}$$

where:

$$\underline{Q} = (\underline{\beta T})_{11} - (\underline{\beta T})_{12}(\underline{\beta T})_{22}(\underline{\beta T})_{21}$$

$$\underline{P} = (\underline{\beta T})_{22} - (\underline{\beta T})_{21}(\beta T)_{11}^{-1}(\underline{\beta T})_{12}$$

Applying the matrix identity:

$$\underline{P}^{-1} = (\underline{\beta T})_{22}^{-1} + (\underline{\beta T})_{22}^{-1}(\underline{\beta T})_{21}[(\underline{\beta T})_{11} - (\underline{\beta T})_{12}(\underline{\beta T})_{22}^{-1}(\underline{\beta T})_{21}]^{-1}(\underline{\beta T}_{12})(\underline{\beta T})_{22}^{-1}$$

The SSC for the n strongly bound generators of external systems causes $(\underline{\beta T})_{22}^{-1} \rightarrow \underline{0}$. This leads to:

$$\underline{W}_{\beta 22} = \underline{P}^{-1}\underline{K}_{22}\underline{P}^{-T}$$

and:

$$\underline{P}^{-1} \rightarrow \underline{0}$$

Thus,

$$\underline{W}_{\beta_{22}} \rightarrow \underline{0}$$

The submatrix $\underline{W}_{\beta_{22}}$ contains the information on the behavior of the n generator of the external group at governor time frame. Hence, the loss of controllability conditions of the strongly bound group of external system is detected by the governor security measure. It could be shown that if K_{22} is positive definite, only $(\beta T)_{22}^{-1} \rightarrow 0$ could cause $\underline{W}_{\beta_{22}} \rightarrow 0$.

Governor load flow is a global phenomenon in the interconnected power system in a manner similar to inertial load flow and also depends on the synchronizing power coefficient matrix $\underline{T}$, which represents the degree of stiffness of the lines connecting the generators of the system. Instead of generator inertias in inertial load flow, governor frequency response characteristics of generators dictate the distribution of power mismatch in the governor load flow, and its effects are represented by the matrix $\underline{\beta}$. In a more general form, $(\underline{\beta T})^{-1}$ represents the effects of governor load flow on the power system.

The governor security measure (4-99) was shown to be a function of $(\underline{\beta T})^{-1}$, and for a strongly connected n

generator group of the external system, a function of $(\beta T)_{22}^{-1}$. This submatrix reflects the structure of the strongly bound group of n generators for governor load flow and will make the security measure reflect strongly bound groups and the relative strengths or weaknesses of the boundaries that surround them.

The governor coherency measure for a probabilistic disturbance (4-81) was shown to be solely dependent on $(\beta T)^{-1}$. Thus, this coherency measure captures the SSC loss of controllability condition, which causes a group of generators to swing together. The governor security measure is related to the governor coherency measure, and it was shown for the probabilistic disturbance that this security measure is identical to the square of the coherency measure when the base case voltage angles are ignored. Hence, the security measure also captures the SSC property for the governor load flow.

The governor security measure summed over all the security measures for single loss of generation disturbances tests all the boundaries equally. Each boundary is affected by the loss of generation contingencies close to this boundary, and the effect of every loss of generation contingency on all boundaries is captured by the summation of the effects (which is presented by the governor coherency measure for a probabilistic disturbance of form (4-81)). Every β_i is proportional to the capacity of generators by the relationship of $\beta_i \simeq \dfrac{Cap_i}{R}$; thus, the

disturbance is an appropriate disturbance which propor-
tionately affects all the boundaries in the system accord-
ing to the capacity of generators it connects.

The commutative grouping rules require the SSC prop-
erty to hold before forming a group. Hence, only strongly
bound groups which have n_i-1 stiff interconnections com-
pared to their governor frequency characteristic in an n_i
generator group are formed. The boundaries between these
groups are vulnerable to governor load flow and are possi-
ble candidates for causing stability and security problems.

Thus, the security measure (4-99) and boundary identi-
fication procedure can detect and identify the weak bound-
aries. The procedure for ranking the boundaries is
identical to the one described for inertial load flow.

In the next section, the boundary identification pro-
cedure is carried on the 49 bus test system, and the weak-
est boundary for inertial and governor load flow is
identified. This boundary is shown to be the boundary
between the external and the internal system where each
group is a strongly bound group of generators.

CHAPTER 5

TESTING THE BOUNDARY IDENTIFICATION METHOD
ON THE 49 BUS (EPRI) TEST SYSTEM

In this chapter, the method developed in Chapter 4 for identifying and ranking vulnerable boundaries to inertial and governor load flow is applied to the 40 bus test system.

First, the inertial DC load flow and governor DC load flow are run for contingencies:

$$\{\Delta \underline{PM}^i\}_j = \begin{cases} M_i & i = j \\ 0 & i \neq j \end{cases} \tag{5-1}$$

to produce inertial angle changes $\Delta \underline{\delta}_M^i$ for $i = 1, 2, \ldots, 22$ and:

$$\{\Delta \underline{PM}^i\}_j = \begin{cases} \beta_i = \dfrac{CAP_i}{R} & i = j \\ 0 & i \neq j \end{cases} \tag{5-2}$$

to produce $\Delta \underline{\delta}_\beta^i$ for $i = 1, 2, \ldots, 22$ where 22 is the number of generators in this system. CAP_i and M_i are megawatt capacity and inertia of the generator i with the regulation coefficient R. The angles are then used to compute the $S_M(k, \ell)$ and $S_\beta(k, \ell)$ from equations (4-34) and (4-86), respectively.

This procedure for computing the inertial and governor security measures is equal to applying the probabilistic modal disturbance to the system for both inertial and governor load flows and computing the r.m.s. coherency measures. These security measures are ranked for each pair of generators from the smallest to the largest for both the inertial response and the governor response load flows to form ranking tables of the security measures. The group formation tables, which specify strongly bound groups of generators for inertial and governor load flows, are determined by applying the commutative rule to these ranking tables. These groups are merged to form larger groups at each level of group formation. Moving down to the bottom of the ranking table results in a single large system group containing all the generators. The result of this group formation is tabulated in a group formation table. The ranking of the boundaries from the weakest to the strongest is based on the reverse order of the group formation table. That is, the weakest boundary is between the last two groups to be combined together to form a single system group containing all the generators.

The above procedure was carried out for the inertial angles obtained from inertial load flow results to the disturbance (5-1). Table 5.1 is the ranking table for the $S_M(k,\ell)$ security measure for generator bus pairs. In this table, pairs are specified by generator numbers.

Table 5.1. Ranking Table of the Inertial Security Measures.

Rank	Generator Pair	Security Measure	Rank	Generator Pair	Security Measure
1.	S (18, 22)	.8628	46.	S (1, 10)	2.4341
2.	S (7, 8)	1.3336	47.	S (9, 13)	2.4500
3.	S (6, 7)	1.3330	48.	S (2, 7)	2.4549
4.	S (6, 8)	1.3335	49.	S (1, 7)	2.4550
5.	S (1, 2)	1.4813	50.	S (2, 8)	2.4551
6.	S (13, 14)	1.5508	51.	S (2, 6)	2.4551
7.	S (2, 17)	1.6118	52.	S (1, 8)	2.4552
8.	S (1, 17)	1.6118	53.	S (1, 6)	2.4552
9.	S (2, 3)	1.6844	54.	S (9, 14)	2.4725
10.	S (1, 3)	1.6844	55.	S (3, 13)	2.5106
11.	S (9, 17)	1.8093	56.	S (13, 15)	2.5176
12.	S (2, 4)	1.8276	57.	S (3, 14)	2.5340
13.	S (1, 4)	1.8276	58.	S (14, 15)	2.5499
14.	S (9, 10)	1.8581	59.	S (5, 9)	2.5634
15.	S (3, 17)	1.8649	60.	S (10, 15)	2.5674
16.	S (15, 17)	1.9084	61.	S (3, 10)	2.5834
17.	S (3, 4)	2.0115	62.	S (4, 15)	2.6283
18.	S (2, 5)	2.0188	63.	S (3, 7)	2.6964
19.	S (1, 5)	2.0189	64.	S (3, 8)	2.6965
20.	S (2, 9)	2.0189	65.	S (3, 6)	2.6965
21.	S (1, 9)	2.0190	66.	S (5, 15)	2.7408
22.	S (13, 17)	2.0541	67.	S (7, 13)	2.7681
23.	S (14, 17)	2.0680	68.	S (8, 13)	2.7683
24.	S (7, 17)	2.1032	69.	S (6, 13)	2.7683
25.	S (6, 17)	2.1034	70.	S (7, 14)	2.7708
26.	S (8, 17)	2.1034	71.	S (8, 14)	2.7710
27.	S (4, 17)	2.1473	72.	S (6, 14)	2.7710
28.	S (11, 12)	2.1843	73.	S (4, 13)	2.7778
29.	S (10, 17)	2.1855	74.	S (10, 13)	2.7809
30.	S (12, 21)	2.1879	75.	S (4, 10)	2.7958
31.	S (11, 21)	2.1879	76.	S (4, 14)	2.7977
32.	S (3, 9)	2,1936	77.	S (10, 14)	2.8007
33.	S (5, 17)	2.2111	78.	S (7, 9)	2.8276
34.	S (3, 5)	2.2115	79.	S (8, 9)	1.8277
35.	S (2, 15)	2.2211	80.	S (6, 9)	2.8277
36.	S (1, 15)	2.2211	81.	S (5, 13)	2.8307
37.	S (9, 15)	2.2642	82.	S (5, 14)	2.8480
38.	S (2, 13)	2.3362	83.	S (5, 7)	2.8673
39.	S (1, 13)	2.3362	84.	S (5, 8)	2.8675
40.	S (4, 5)	2.3497	85.	S (5, 6)	2.8675
41.	S (2, 14)	2.3592	86.	S (7, 15)	2.9267
42.	S (1, 14)	2.3592	87.	S (8, 15)	2.9268
43.	S (3, 15)	2.3844	88.	S (6, 15)	2.9268
44.	S (4, 9)	2.4241	89.	S (5, 10)	2.9415
45.	S (2, 10)	2.4341	90.	S (4, 7)	2.9983

Table 5.1. (Continued)

Rank	Generator Pair	Security Measure	Rank	Generator Pair	Security Measure
91.	S (4, 8)	2.9985	136.	S (10, 16)	4.3331
92.	S (4, 6)	2.9985	137.	S (13, 16)	4.3578
93.	S (17, 19)	3.0306	138.	S (14, 16)	4.3812
94.	S (18, 21)	3.0791	139.	S (19, 20)	4.4045
95.	S (2, 19)	3.1949	140.	S (4, 16)	4.4540
96.	S (1, 19)	3.1949	141.	S (7, 20)	4.5121
97.	S (21, 22)	3.1992	142.	S (8, 20)	4.5121
98.	S (15, 19)	3.2187	143.	S (6, 20)	4.5121
99.	S (7, 10)	3.2305	144.	S (5, 16)	4.5749
100.	S (8, 10)	3.2306	145.	S (16, 19)	4.6789
101.	S (6, 10)	3.2306	146.	S (7, 12)	4.7210
102.	S (9, 19)	3.2606	147.	S (7, 11)	4.7210
103.	S (12, 18)	3.2743	148.	S (8, 12)	4.7215
104.	S (11, 18)	3.2743	149.	S (8, 11)	4.7215
105.	S (3, 19)	3.2971	150.	S (6, 12)	4.7215
106.	S (12, 22)	3.3723	151.	S (6, 11)	4.7215
107.	S (11, 22)	3.3723	152.	S (7, 16)	4.9300
108.	S (4, 19)	3.4422	153.	S (8, 16)	4.9300
109.	S (10, 19)	3.4991	154.	S (6, 16)	4.9300
110.	S (15, 16)	3.5161	155.	S (16, 20)	4.9912
111.	S (13, 19)	3.5464	156.	S (17, 21)	5.1597
112.	S (14, 19)	3.5671	157.	S (2, 21)	5.4864
113.	S (5, 19)	3.6248	158.	S (1, 21)	5.4864
114.	S (17, 20)	3.6883	159.	S (14, 21)	5.5907
115.	S (15, 10)	3.7847	160.	S (13, 21)	5.6051
116.	S (9, 20)	3.8221	161.	S (12, 17)	5.6643
117.	S (2, 10)	3.8594	162.	S (11, 17)	5.6643
118.	S (1, 20)	3.8594	163.	S (3, 21)	5.6775
119.	S (3, 20)	3.9384	164.	S (5, 21)	5.7219
120.	S (10, 20)	4.0074	165.	S (9, 21)	5.8295
121.	S (13, 20)	4.0160	166.	S (15, 21)	5.8881
122.	S (14, 20)	4.0376	167.	S (4, 21)	5.9293
123.	S (16, 17)	4.0699	168.	S (2, 12)	5.9810
124.	S (7, 19)	4.0898	169.	S (2, 11)	5.9810
125.	S (8, 19)	4.0899	170.	S (1, 12)	5.9811
126.	S (6, 19)	4.0899	171.	S (1, 11)	5.9811
127.	S (4, 20)	4.1060	172.	S (12, 14)	6.0673
128.	S (9, 16)	4.1631	173.	S (11, 14)	6.0673
129.	S (7, 21)	4.1782	174.	S (12, 13)	6.0810
130.	S (8, 21)	4.1787	175.	S (11, 13)	6.0810
131.	S (6, 21)	4.1787	176.	S (10, 21)	6.1334
132.	S (5, 20)	4.2168	177.	S (3, 12)	6.1640
133.	S (2, 16)	4.2284	178.	S (3, 11)	6.1640
134.	S (1, 16)	4.2284	179.	S (5, 12)	6.2114
135.	S (3, 16)	4.2924	180.	S (5, 11)	6.2114

Table 5.1. (Continued)

Rank	Generator Pair	Security Measure	Rank	Generator Pair	Security Measure
181.	S (5, 11)	6.2114	206.	S (14, 18)	7.9041
182.	S (9, 12)	6.3104	207.	S (13, 18)	7.9249
183.	S (9, 11)	6.3104	208.	S (12, 16)	7.9329
184.	S (12, 15)	6.3622	209.	S (11, 16)	7.9329
185.	S (11, 15)	6.3622	210.	S (5, 18)	8.0092
186.	S (4, 12)	6.4150	211.	S (3, 18)	8.0195
187.	S (4, 11)	6.4150	212.	S (2, 22)	8.0263
188.	S (7, 18)	6.4472	213.	S (1, 22)	8.0263
189.	S (6, 18)	6.4477	214.	S (14, 22)	8.0869
190.	S (8, 18)	6.4477	215.	S (13, 22)	8.1088
191.	S (10, 11)	6.6059	216.	S (9, 18)	8.1735
192.	S (7, 22)	6.6182	217.	S (5, 22)	8.1824
193.	S (6, 22)	6.6187	218.	S (3, 22)	8.2014
194.	S (8, 22)	6.6187	219.	S (15, 18)	8.2278
195.	S (19, 21)	6.8692	220.	S (4, 18)	8.2314
196.	S (20, 21)	7.1077	221.	S (9, 22)	8.3569
197.	S (12, 19)	7.3194	222.	S (4, 22)	8.4064
198.	S (11, 19)	7.3194	223.	S (15, 22)	8.4128
199.	S (16, 21)	7.5230	224.	S (10, 18)	8.4310
200.	S (17, 18)	7.5278	225.	S (10, 22)	8.6094
201.	S (12, 20)	7.5280	226.	S (18, 19)	9.1063
202.	S (11, 20)	7.5280	227.	S (19, 22)	9.2806
203.	S (17, 22)	7.7109	228.	S (18, 20)	9.3111
204.	S (2, 18)	7.8439	229.	S (20, 22)	9.4917
205.	S (1, 18)	7.8439	230.	S (16, 18)	9.7169
			231.	S (16, 22)	9.8983

The commutative rule was applied to this ranking table. The group containing generators 18 and 22 (18, 22) is the first group of strongly bound generators. At rank 2 of the ranking table, group (7, 8) is formed as the second group. At rank 3, generators 6 and 7 do not form a group since 7 is already a member of group (7, 8), and generator 6 cannot join this group because at this rank generator 6 has not been shown to have a tight connection to 8 with respect to its inertia. At rank 4, generator 6 is combined with the group (7, 8), forming a new group of (7, 8, 6) since generator 6 is now tightly bound with both generators 7 and 8. Moving down to the bottom of the ranking table results in larger and larger groups which later are merged and finally form a single generator. This is shown in group formation Table 5.2, which also shows the ranks of ranking table at which groups are merged or a new pair group is formed.

Level 20 of Table 5.2 shows the last two groups. Group No. 1 identifies the external system generator, and group No. 2 contains all the generators in the internal system. Hence, for this system, the boundary which connects the external and the internal system is the weakest boundary to inertial power flow due to loss of generation contingencies. This was shown in Chapter 3 to be true, since this boundary was shown to have the largest angle across the lines forming the boundary for several loss of generation contingencies.

Table 5.2.   Group Formation Table Based on Inertial
            Security Measure of Ranking Table.

Level	Rank	Group	
1	1	1	(18, 22)
2	2	1	(18, 22)
		2	(7, 8)
3	4	1	(18, 22)
		2	(7, 8, 6)
4	5	1	(18, 22)
		2	(7, 8, 6)
		3	(1, 2)
5	6	1	(18, 22)
		2	(7, 8, 6)
		3	(1, 2)
		4	(13, 14)
6	8	1	(18, 22)
		2	(7, 8, 6)
		3	(1, 2, 17)
		4	(13, 14)
7	14	1	(18, 22)
		2	(7, 8, 6)
		3	(1, 2, 17)
		4	(13, 14)
		5	(9, 10)
8	15	1	(18, 22)
		2	(7, 8, 6)
		3	(1, 2, 17, 3)
		4	(13, 14)
		5	(9, 10)
9	27	1	(18, 22)
		2	(7, 8, 6)
		3	(1, 2, 17, 3)
		4	(13, 14)
		5	(9, 10)
10	28	1	(18, 22)
		2	(7, 8, 6)
		3	(1, 2, 17, 3, 4)
		4	(13, 14)
		5	(9, 10)
		6	(11, 12)
11	31	1	(18, 22)
		2	(7, 8, 6)
		3	(1, 2, 17, 3, 4)

Table 5.2. (Continued)

Level	Rank	Group	
11 (cont)	31	4	(13, 14)
		5	(9, 10)
		6	(11, 12, 21)
12	40	1	(18, 22)
		2	(7, 8, 6)
		3	(1, 2, 17, 3, 4, 5)
		4	(13, 14)
		5	(9, 10)
		6	(11, 12, 21)
13	58	1	(18, 22)
		2	(7, 8, 6)
		3	(1, 2, 17, 3, 4, 5)
		4	(13, 14, 15)
		5	(9, 10)
		6	(11, 12, 21)
14	77	1	(18, 22)
		2	(7, 8, 6)
		3	(1, 2, 17, 3, 4, 5)
		4	(13, 14, 15, 9, 10)
		6	(11, 12, 21)
15	89	1	(18, 22)
		2	(7, 8, 6)
		3	(1, 2, 17, 3, 4, 5, 13, 14, 15, 9, 10)
16	101	1	(18, 22)
		2	(7, 8, 6, 1, 2, 17, 3, 4, 5, 13, 14, 15, 9, 10)
		6	(11, 12, 21)
17	107	1	(18, 22, 11, 12, 21)
		2	(7, 8, 6, 1, 2, 17, 3, 4, 5, 13, 14, 15, 9, 10)
18	126	1	(18, 22, 11, 12, 21)
		2	(7, 8, 6, 1, 2, 17, 3, 4, 5, 13, 14, 15, 9, 10, 19)
19	143	1	(18, 22, 11, 12, 21)
		2	(7, 8, 6, 1, 2, 17, 3, 4, 5, 13, 14, 15, 9, 10, 19, 20)
20	155	1	(18, 22, 11, 12, 21)
		2	(7, 8, 6, 1, 2, 17, 3, 4, 5, 13, 14, 15, 9, 10, 19, 20, 16)
21	231	1	(18, 22, 11, 12, 21, 7, 8, 6, 1, 2, 17, 3, 4, 5, 13, 14, 15, 9, 10, 19, 20, 16)

In a manner similar to that for the inertial security measure, the governor security measure $S_\beta (k,\ell)$ was computed for disturbance given in equation (5-2) using the DC governor load flow. The ranking table for the governor security measure was formed. The commutative rule was applied to the governor security measure ranking table from the top to the bottom. The final result is presented in Table 5.3. This table contains the strongly bound groups of generators at different levels of group formation for governor response of each generating unit.

Groups formed based on the governor security measure shown in Table 5.3 are somewhat different from those given in Table 5.2. However, the last two groups in Tables 5.2 and 5.3 are identical. This indicates that the weakest boundary for governor power flow in this system is also between the internal and external system. This is also true since the loss of stability across this boundary was shown to occur for governor power flow due to loss of generation contingencies in the external system.

The results of Chapter 3 showed that the inertial and the governor security measures with commutative grouping procedure accurately detected the weakest boundary for inertial and governor power flow in this system. The investigation of the second and third weakest boundaries was not performed in this and is a subject of future research.

Table 5.3. Group Formation Based on Governor Security
           Measure.

Level	Rank	Group	
1	1	1	(18, 22)
2	2	1	(18, 22)
		2	(15, 16)
3	3	1	(18, 22)
		2	(15, 16)
		3	(13, 14)
4	5	1	(18, 22)
		2	(15, 16)
		3	(13, 14)
		4	(17, 20)
5	6	1	(18, 22)
		2	(15, 16)
		3	(13, 14)
		4	(17, 20)
		5	(7, 8)
6	8	1	(18, 22)
		2	(15, 16)
		3	(13, 14)
		4	(17, 20)
		5	(7, 8, 6)
7	9	1	(18, 22)
		2	(15, 16)
		3	(13, 14)
		4	(17, 20)
		5	(7, 8, 6)
		6	(2, 3)
8	13	1	(18, 22)
		2	(15, 16)
		3	(13, 14)
		4	(17, 20)
		5	(7, 8, 6)
		6	(2, 3, 1)
9	19	1	(18, 22)
		2	(15, 16)
		3	(13, 14)
		4	(17, 20)
		5	(7, 8, 6)
		6	(2, 3, 1, 4)
10	25	1	(18, 22)
		2	(!5, 16)
		3	(13, 14)

Table 5.3.   (Continued)

Level	Rank	Group	
10 (cont)	25	4	(17, 20)
		5	(7, 8, 6)
		6	(2, 3, 1, 4)
		7	(11, 12)
11	28	1	(18, 22)
		2	(15, 16, 17, 20)
		3	(13, 14)
		5	(7, 8, 6)
		6	(2, 3, 1, 4)
		7	(11, 12)
12	38	1	(18, 22)
		2	(15, 16, 17, 20)
		3	(13, 14)
		5	(7, 8, 6)
		6	(2, 3, 1, 4, 5)
		7	(11, 12)
13	58	1	(18, 22)
		2	(15, 16, 17, 20)
		3	(13, 14)
		5	(7, 8, 6)
		6	(2, 3, 1, 4, 5)
		7	(11, 12, 21)
14	60	1	(18, 22)
		2	(15, 16, 17, 20, 13, 14)
		5	(7, 8, 6)
		6	(2, 3, 1, 4, 5)
		7	(11, 12, 21)
15	82	1	(18, 22)
		2	(15, 16, 17, 20, 13, 14, 2, 3, 1, 4, 5)
		5	(7, 8, 6)
		7	(11, 12, 21)
16	91	1	(18, 22)
		2	(15, 16, 17, 20, 13, 14, 2, 3, 1, 4, 5)
		5	(7, 8, 6)
		7	(11, 12, 21)
		8	(9, 10)
17	103	1	(18, 22)
		2	(15, 16, 17, 20, 13, 14, 1, 2, 1, 4, 5, 7, 8, 6)
		7	(11, 12, 21)
		8	(9, 10)

Table 5.3. (Continued)

Level	Rank	Group	
18	131	1	(18, 22, 11, 12, 21)
		2	(15, 16, 17, 20, 13, 14, 2, 3, 1, 4, 5, 7, 8, 6)
		8	(9, 10)
19	140	1	(18, 22, 11, 12, 21)
		2	(15, 16, 17, 20, 13, 14, 2, 3, 1, 4, 5, 7, 8, 6)
		8	(9, 10, 19)
20	146	1	(18, 22, 11, 12, 21)
		2	(15, 16, 17, 20, 13, 14, 2, 3, 1, 4, 5, 7, 8, 6, 9, 10, 19)
21	231	1	(18, 22, 11, 12, 21, 15, 16, 17, 20, 13, 14, 2, 3, 1, 4, 5, 7, 8, 6, 9)

CHAPTER 6

CONCLUSIONS AND FUTURE INVESTIGATION

6.1. Overview of Thesis

A review of present planning methods was presented, and the lack of detailed planning procedures for the possible stability and security violation caused by inertial and governor response to loss of generation contingencies was pointed out.

The presently available simulation methods for governor and inertial response to loss of generation contingencies were also reviewed. The lack of simulation techniques that can handle the large data base required to simulate the inertial and governor response on large interconnected systems was pointed out. The need to develop simulation methods and contingency assessment methods for these inertial and governor transient responses to loss of generation contingencies was noted.

In the second chapter, the dynamic distribution of power mismatch to loss of generation contingencies was discussed in detail, and it was shown that the generating units respond to the mismatch: first, proportional to synchronizing power coefficient of equivalent lines connecting the generation to the disturbed bus; second, proportional

to their inertia; third, by governor action proportional to governor frequency response characteristics; and finally, by automatic generation control participation factors or the operator. Chapter 3 also developed a simulation method for governor load flow to complement the inertial load flow. These governor and inertial load flows allow direct assessment of stability and security problems due to generation response to loss of generation contingencies on large networks that is presently not possible. The inertial and governor power flows were indicated to be different and cause different stability problems. The reasons given are:

(a) M_i is not proportional to CAP_i for generators of different size and type.

(b) The effective β_i is reduced on generation far from the disturbed bus due to governor deadband and value set point nonlinearities.

(c) Some types of units may not have governor regulation or sharply reduced regulation participation.

(d) Some utilities' automatic generation controls dispatch in proportion to area control error as well as the integral of area control error. When AGC has proportional control, the effective β_i on generators under AGC is increased.

Chapter 3 demonstrated the performance of the DC inertial and governor load flow on a 49 bus test system. The results of DC inertial and governor load flow for a 490 MW loss of generation at the external system, when compared

with the Midterm Stability Program results for this contingency, showed that the inertial and governor power flow angle changes were captured reasonably accurately by the DC load flow methods. The results also indicated that the power flow for inertial response of generating units is different from the governor power flows.

The 790 MW loss of generation at the external system caused a line stability limit violation over the boundary between the external and internal system since the governor response of generating units in the internal system was much greater than the inertial response. This further justified the difference between inertial and governor power flows and their uniqueness in causing different stability and security problems. This 790 MW loss of generation, when simulated on the 49 bus test system using regular load flow, did not cause any stability limit violation. The line outage study of line (40, 41), which exceeded its stability limit due to governor power flow, also did not indicate any problem across the internal and external system. These two simulation runs showed that the stability and security problem associated with inertial and governor power flow cannot be assessed by present load flow and line outage studies. The use of the Midterm Stability Program for assessing inertial and governor power flow stability problems is prohibited because of its cost and inability to handle large data bases. Thus, the inertial and governor

load flow method is a significant contribution to power system planning and security assessment studies.

In Chapter 4, a set of security measures was proposed for the inertial and governor time frame. The inertial security measure was shown to be identical to the square of the r.m.s. coherency measure evaluated for the linearized classical transient stability model for a probabilistic disturbance when the base case was ignored. This security measure was further justified by showing that the strict synchronizing loss of controllability condition of this linearized classical stability model, which causes the vulnerable boundaries in the transmission network, is detected by this security measure.

It was argued that the inertial security and stability problem depends on SSC loss of controllability condition since the groups formed by this property have weak boundaries. The cummutative grouping algorithm was chosen to guarantee that the groups formed are strongly bound groups. Thus, the inertial security measure and commutative grouping algorithm were used to identify the vulnerable boundaries to inertial power flows.

In Chapter 4, the governor security measure was also defined. It was shown that the governor power flow security problem depends on the state model for this time frame and SSC condition for this model. It was also argued that the governor security measure and the commutative

governor power flows due to loss of generation contingen-
cies.

In both the inertial and governor boundary identifica-
tion methods, the weakest boundaries lie between the last
two groups of strongly bound groups to be combined
together to form a single group. The results of testing
the vulnerable boundary identification method on the 49 bus
EPRI system were summarized in Chapter 5 and indicated that
the method worked very well since the weakest boundary
identified was the boundary which caused stability limit
violation shown in Chapter 3.

Knowing weak boundaries gives planners and operators
the insight needed for transfer limit studies. The bound-
ary vulnerability ranking can assist operation planners in
adjusting unit commitment, economic dispatch, and line
maintenance schedules to minimize or eliminate the most
significant boundary and line vulnerabilities. It can also
assist expansion transmission planners to assess security
of various alternate expansion configurations and their
effect on present network vulnerabilities and new vulnera-
bilities produced by each expansion alternative.

6.2. Future Research

The results obtained for inertial and governor
response of generators to loss of generation contingencies
in Chapter 3 are based on a linearized DC load flow. A
useful investigation would be the comparison of the

performance of inertial and governor decoupled load flow with the midterm stability simulation in an effort to obtain more accurate results than achieved with the DC load flow used in this research. The Consumer Power Company's decoupled load flow could be a prime candidate for this study. This program, at present, can handle 3,000 buses, 5,500 lines, 750 generators, and 750 transformers and can be made, with proper input data, to compute inertial and governor load flow. This program is almost the size needed to handle the large data base required for analyzing the power transfers to the Northeast United States. Thus, this program is an excellent candidate for performing the inertial and governor load flows for large interconnected networks.

Another useful investigation would be the development of a better governor model for simulating loss of generation contingencies on large interconnected networks where the average frequency deviation would be below governor deadband (.036 hz). The loss of generation must be above 1.2% of total system capacity to exceed governor deadband. If the loss of generation were not above governor deadband for all generators, no generators in the system could respond to this generation loss. The transient after the loss of generation affects generators electrically close much more than those further away and will cause these generators that are electrically close to exceed governor deadband. An algorithm for determining which generators

participate in governor generation response in large inter-
connected systems is thus another subject of future
research.

The line power flow measurement for the recent Ontario
Hydro Nanticocke 2000 MW loss of generation is available.
Thus, the post mortem on this Nanticocke 2000 MW loss of
generation is a valuable investigation using the inertial
and governor load flow. An investigation of this actual
contingency with the inertial and governor load flow can:

(1) determine the principal transmission network for
     those regions that participate in governor regulation
     and can lead to proper modeling of governor load flow
     for large networks;

(2) give an insight on how to determine a proper base case
     load flow and an equivalent for inertial load flow.
     This can be based on knowledge of generation availa-
     ble, generation loading, transfers, and network con-
     figurations.

A new security analysis procedure that utilizes the
information developed by identifying the weak base case
boundaries in the system could be developed. This secur-
ity analysis procedure involves:

(1) determining the groups of generators that are sepa-
     rated by the weakest transmission boundaries;

(2) determining the network elements that comprise these
     base case transmission boundaries;

(3) identifying network elements that are vulnerable to
     stability or security violations for all loss of gen-
     eration contingencies, all line outage contingencies,
     and all loss of generation/line outage combination
     contingencies. The security or stability vulnerabil-
     ity of a network element could be assessed based on
     an r.m.s. average over all contingencies as well as
     the enumeration and ranking of specific contingencies
     that caused overload or stability constraint viola-
     tions for this element. Vulnerable elements that lie
     in weak boundaries and that do not lie in the weak
     base case boundary could be enumerated. The assess-
     ment of network element security by an r.m.s. average
     over all contingencies of a particular type deter-
     mines elements and ranking that are continually vul-
     nerable, and the enumeration of contingencies that
     cause overload indicates elements that are vulnerable
     for a very specific contingency or contingencies;

(4) a contingency security analysis procedure that could
     determine the effects of a specific loss of genera-
     tion, line outage, or loss of generation/line outage
     combination contingency on stability or security by
     r.m.s. average of the effects on all vulnerable net-
     work elements for that contingency type as well as
     enumerating and ranking the overloaded elements for a
     specific contingency. The r.m.s. average over vulner-
     able network elements pick out contingencies that have

a rather pronounced widespread effect on network
security and the enumeration of overloads indicates
the effects of contingency on a specific element or
elements. The loss of generation line outage or loss
of generation/line outage combination contingencies
that affect and do not affect the base case boundary
network could be identified.

The identification of vulnerable network elements
based on a security measure based average over all contin-
gencies of a particular type and the identification of
whether these elements belong to the weak base case bound-
aries will determine whether these weak base case bound-
aries dictate the security problems a utility experiences
as the transmission network is weakened by line outages or
is stressed by line outage/loss of generation combinations.
This information would be helpful to operation and expan-
sion planners. The security measure based average overall
contingencies of a particular type will indicate how vul-
nerable a network element is on the average, which is not
possible to assess if only overload or stability limit vio-
lations for specific contingencies are enumerated. Using
sums of the security measures for vulnerable network ele-
ments as a system security measure would allow planners or
operators to assess specific operation or expansion alter-
natives and even perform such an evaluation using optimiza-
tion procedures. Thus, the investigation of network

element security measures and procedures for operation
and expansion planning is a topic for further research.

The identification of contingencies that cause loss of
security or stability based on a security measure average
over all network elements or all weak base case boundary
network elements for a specific contingency indicates the
effect of that contingency on network security better than
just enumerating overloads or stability limit violations
for that contingency alone without the contingency security
measure evaluation. The restriction of the contingency
security measure to average only over vulnerable network
elements or vulnerable base case boundary network elements
provides a better picture of how a specific contingency
affects security. Present contingency security assessment
methods [20] only utilize a contingency security measure
evaluated over all network elements. Thus, the investiga-
tion of contingency security measures restricted to vulner-
able elements or vulnerable elements in the weak base case
boundaries is a subject for further research.

BIBLIOGRAPHY

BIBLIOGRAPHY

1. C. W. Taylor, F. R. Nassief, T. L. Cresap, "Northwest Power Pool Transient Stability and Load Shedding Control for Generation Load Imbalances," IEEE Transaction on Power Apparatus and Systems, PAS-100, July 81, pp. 3486-3495.

2. R. Rudenberg, Transient Performance of Electric Power Systems, McGraw-Hill, New York, 1950 (MIT Press, Cambridge, Mass., 1967).

3. R. A. Hore, Advanced Studies in Electrical Power Systems Design, Chapman and Hall, London, 1966.

4. "Regional Power System Planning; A State of the Art Assessment," Final Report to US Department of Energy under Contract AS05-77ET29144, October 1980.

5. C. A. Macarthur, "Transmission Limitations Computed by Superposition," AIEE Transactions, Part III, PAS-80, August 1961, pp. 824-831.

6. B. Stott, "Decoupled Newton Load Flow," IEEE Transaction on Power Apparatus and Systems, PAS-100, September/October 1972, pp. 1955-1959.

7. C. Young, R. Webler, "A New Stability Program for Predicting the Dynamic Performance of Electric Power Systems," Proc. Am. Power Conf. 29, 1967.

8. "Mid Term Simulation of Electric Power Systems," Final Report on EPRI Project 745, June 1979.

9. M. Falvo, "System Incident at Nanticok TGS," Ontario Hydro System Control Report, August 21, 1981.

10. "Long-Term Power System Dynamics," Final Report of EPRI Research Project 90-70-0, April 1974.

11. "Long-Term Power System Dynamics, Phase II," Final Report of EPRI Research Project 764-1, October 1976.

12. "Long-Term Power System Dynamics, Phase III," Final Report of EPRI Research Project 764-2, May 1982.

13. L. H. Fink, K. Carlsen, "Operating Under Stress and Strain," IEEE Spectrum, March 1978, pp. 48-53.

14. C. B. Somuah, F. C. Schweppe, "On-Line Computer Control of a Power System During an Emergency," presented at the IEEE PES summer meeting, Minneapolis, Minnesota, July 13-18, 1980.

15. IBM Research Division, San Jose, California, "Bulk Power Security Assessment," Research Project RP90-3, November 1970.

16. A. S. Debs, A. R. Benson, "Security Assessment of Power Systems," presented at the Engineering Foundation Conference on Systems Engineering for Power, New England College, Henniker, N.H., August 17-22, 1975.

17. J. Lawler, "Modal-Coherent Equivalents Derived from an RMS Coherency Measure." Ph.D. dissertation, Michigan State University, August 1980.

18. J. Dorsey, "The Determination of Reduced Order Models for Local and Global Analysis of Power Systems." Ph.D. dissertation, Michigan State University, July 1980.

19. J. G. Blaschak, G. T. Heydt, J. M. Bright, "A Generation Dispatch Strategy for Power Systems Operation Under Alert Status," presented at the IEEE PES Summer Meeting, Vancouver, British Columbia, Canada, July 15-20, 1979. (Abstract A-79-4748), IEEE Transaction on Power Apparatus and Systems, PAS 99, January/February 1980, pp. 1-10.

20. T. A. Mikolinnas, B. F. Wollenberg, "An Advanced Contingency Selection Algorithm," IEEE Transaction on Power Apparatus and Systems, PAS-100, February 1981, pp. 608-617.

21. L. M. Smith, "PJM Dynamic Systems Model User's Guide," Energy Conversion Research Section, Philadelphia Electric Co., Philadelphia, PA, July 1974.

22. R. A. Schlueter, H. Akhtar, and H. Modir, "An RMS Coherency Measure, A Basis for Unification of Coherency and Modal Analysis Aggregation Techniques," IEEE 1978 Summer Power Meeting Test of Abstract Papers, IEEE Publication 78, ch. 1361-5.

23. R. A. Schlueter, and U. Ahn, "Modal Analysis Equivalents Derived Based on the RMS Coherency Measure," IEEE 1979 Winter Power Meeting Text of Abstract Papers, IEEE Publication 79, ch. 1418-3.

24. J. Lawler, R. A. Schlueter, P. Rusche, and D. L. Hackett, "Model Coherent Equivalents Derived Based on the RMS Coherency Measure," IEEE Transaction on Power Apparatus and Systems, PAS-99, No. 2, pp. 1415-1425, July/August 1980.

25. J. Lawler and R. A. Schlueter, "Computational Algorithms for Deriving Modal Coherent Equivalents," presented at IEEE 1981 Summer Power Meeting and accepted for IEEE Transaction on Power Apparatus and Systems.

26. R. Podmore and A. Germond, "Development of Dynamic Equivalents for Transient Stability Studies," Final Report on EPRI Research Project 763, April 1977.

27. U. Dicapiro and R. Marconato, "Structural Coherency Conditions for Multi-Machine Power Systems," VII IFAC World Congress, Helsinki, Finland, July 1979.

28. J. M. Undrill and A. E. Turner, "Power System Equivalents," Final Report on ERC Project RP904, January 1971.

29. J. R. Winkelman, J. H. Chow, B. C. Bowler, B. Avramovic, P. V. Kokotovic, "An Analysis of Inerarea Dynamics of Multi-Machine Systems," IEEE Transaction on Power Apparatus and Systems, February 1981, pp. 754-763.

30. J. Meisel, "Reference Frames and Emergency State Control for Bulk Electric Power Systems," Proceedings of the 1977 Joint Automatic Control Conference, Vol. 2, pp. 747-754.